Estudio de los efectos de agentes anticolinérgicos y de inhibidores de fosfodiesterasa-5 sobre la estructura pulmonar en un modelo experimental de enfermedad pulmonar obstructiva crónica inducido por humo de tabaco en el cobayo

David Domínguez Fandos

UNIVERSITAT DE BARCELONA

ESTUDIO DE LOS EFECTOS DE AGENTES ANTICOLINÉRGICOS Y DE INHIBIDORES DE FOSFODIESTERASA-5 SOBRE LA ESTRUCTURA PULMONAR EN UN MODELO EXPERIMENTAL DE ENFERMEDAD PULMONAR OBSTRUCTIVA CRÓNICA INDUCIDO POR HUMO DE TABACO EN EL COBAYO

Tesis presentada por

David Domínguez Fandos

Para obtener el título de doctor por la Universitat de Barcelona

Dirigida por:

Dr. Joan Albert Barberà Mir

Dr. Víctor Ivo Peinado Cabré

Programa de doctorado Medicina

Universitat de Barcelona

2015

HUB^{C} Health Universitat de Barcelona Campus

B:KC Barcelona Knowledge Campus

La presente tesis doctoral ha sido realizada dentro del programa de Doctorado Medicina de la Facultat de Medicina de la Universitat de Barcelona. La Comisión de Doctorado ha evaluado y autorizado la presentación de ésta tesis doctoral como compendio de publicaciones. Siguiendo la normativa vigente esta tesis se presenta como compendio de artículos originales de una misma unidad temática publicados en revistas indexadas. Los artículos son los siguientes:

1) **Pulmonary inflammatory reaction and structural changes induced by cigarette smoke exposure in the Guinea pig.** David Domínguez-Fandos, Víctor Ivo Peinado, Raquel Puig-Pey, Elisabet Ferrer, Melina Mara Musri, Josep Ramírez, Joan Albert Barberà. *COPD. 2012 Aug;9(5):473-84*.

2) **Effects of Aclidinium Bromide in a Cigarette Smoke-Exposed Guinea Pig Model of COPD.** David Domínguez-Fandos, Elisabet Ferrer, Raquel Puig-Pey, Cristina Carreño, Neus Prats, Mònica Aparici, Melina Mara Musri, Amadeu Gavaldà, Víctor Ivo Peinado, Montserrat Miralpeix, Joan Albert Barberà. *Am J Respir Cell Mol Biol. 2014 Feb;50(2):337-46*.

3) **Sildenafil in a cigarette smoke-Induced model of COPD in the guinea pig.** David Domínguez-Fandos, César Valdés, Elisabet Ferrer, Raquel Puig-Pey, Isabel Blanco, Olga Tura-Ceide, Tanja Paul, Víctor I. Peinado, Joan A. Barberà. *Eur Respir J.* (actualmente en segunda revisión).

La estructura de esta tesis incluye una introducción general sobre el tema, seguida de las hipótesis y los objetivos globales y concretos que resaltan los motivos por los que se desarrolló el trabajo. A continuación, se exponen los resultados principales de cada artículo y se hace una discusión conjunta de todos los resultados que fundamenta la tesis doctoral, para finalmente reflejar las conclusiones. Los artículos se adjuntan en el formato electrónico de la revista.

Jo, Dr. Joan Albert Barberà Mir, consultor sènior del servei de pneumologia de l'Hospital Clínic de Barcelona,

FAIG CONSTAR:

Les tres publicacions que formen part de la present tesi doctoral amb el corresponent factor d'impacte de la revista:

1) **Pulmonary inflammatory reaction and structural changes induced by cigarette smoke exposure in the Guinea pig.** COPD. 2012 Aug;9(5):473-84. Factor de impacto: 2.310 (Posición 28 de 50). Tercer cuartil del área de conocimiento "Respiratory system".

2) **Effects of Aclidinium Bromide in a Cigarette Smoke-Exposed Guinea Pig Model of Chronic Obstructive Pulmonary Disease.** Am J Respir Cell Mol Biol. 2014 Feb;50(2):337-46. Factor de impacto: 4.109 (Posición 7 de 53). Primer cuartil del área de conocimiento "Respiratory system".

3) **Sildenafil in a cigarette smoke-Induced model of COPD in the guinea pig.** Eur Respir J. (actualmente en segunda revisión). Factor de impacto: 7.125 (Posición 4 de 54). Primer cuartil del área de conocimiento "Respiratory system".

I DECLARO:

Que aquestes publicacions no han estat utilitzades ni s'utilitzaran en tesis futures.

I signo la present per deixar-ne constància als efectes oportuns.

J. A. Barberà

Dr. Joan Albert Barberà

Jo, Dr. Víctor Ivo Peinado Cabré, investigador sènior del CIBER de Enfermedades Respiratorias (CIBERES) - IDIBAPS,

FAIG CONSTAR:

Les tres publicacions que formen part de la present tesi doctoral amb el corresponent factor d'impacte de la revista:

1) **Pulmonary inflammatory reaction and structural changes induced by cigarette smoke exposure in the Guinea pig.** COPD. 2012 Aug;9(5):473-84. Factor de impacto: 2.310 (Posición 28 de 50). Tercer cuartil del área de conocimiento "Respiratory system".

2) **Effects of Aclidinium Bromide in a Cigarette Smoke-Exposed Guinea Pig Model of Chronic Obstructive Pulmonary Disease.** Am J Respir Cell Mol Biol. 2014 Feb;50(2):337-46. Factor de impacto: 4.109 (Posición 7 de 53). Primer cuartil del área de conocimiento "Respiratory system".

3) **Sildenafil in a cigarette smoke-Induced model of COPD in the guinea pig.** Eur Respir J. (actualmente en segunda revisión). Factor de impacto: 7.125 (Posición 4 de 54). Primer cuartil del área de conocimiento "Respiratory system".

I DECLARO:

Que aquestes publicacions no han estat utilitzades ni s'utilitzaran en tesis futures.

I signo la present per deixar-ne constància als efectes oportuns.

Peinado

Dr. Víctor Ivo Peinado Cabré

A los míos

A mi madre

Agradecimientos

Quiero dar las gracias a todas aquellas personas que de una manera u otra han contribuido a la realización de esta tesis doctoral.

Als meus directors de tesi, pels seus coneixements experts i donar-me l'oportunitat de formar-me en aquest camp de la biomedicina que tant us apassiona.

A totes i tots els companys que he tingut en el laboratori de malalties respiratòries. Per la ciència i d'altres coses molt gratificants compartides.

A les persones del Centre diagnòstic respiratori - Funció pulmonar del Departament de Pneumologia de l'Hospital Clínic.

A d'altres persones de la Fundació Clínic per la Recerca Biomèdica, IDIBAPS, CELLEX, CEK, Facultat de Medicina de la Universitat de Barcelona, Hospital Clínic i d'altres institucions, que he tingut el plaer de conèixer.

A totes les persones amb qui vaig compartir la meva estada al laboratori de genètica humana de la Facultat de Medicina de la Universitat de Barcelona durant la qual vaig fer els cursos del programa de doctorat i vaig obtenir el Diploma d'Estudis Avançats (DEA) - suficiència investigadora. Vaig conèixer persones que aprecio molt i s'han convertit en molt bones amistats.

Al finançament de les entitats públiques i empreses privades i als seus treballadors, i pel mecenatge. Todo y que desearía que se apostara mucho más por investigación, ya que es una buena elección no sólo por el compromiso que supone con el avance científico y la mejora de la calidad de vida de las personas sino porque construye una sociedad de pensamiento más crítico y por lo tanto más libre.

A mis verdaderas amigas y amigos fuera del ámbito laboral, por vuestro apoyo y consejos. Os quiero, sois parte muy importante de mí.

Y para acabar, mi más sentido agradecimiento a mi familia, en especial a mi madre, mi padre, mi pareja, mi hermana, mi hermano, mi cuñada, mi cuñado, y mis sobrinas. A vosotros os dedico especialmente esta tesis doctoral, por vuestro amor y apoyo incondicional en todo. Os quiero muchísimo.

¡Muchísimas gracias!

ÍNDICE

ABREVIACIONES

ACh	Acetilcolina
ADP	Adenosina Difosfato
cGMP	Cyclic Guanosine Monophosphate
CML	Células Musculares Lisas
eNOS	Endothelial Nitric Oxide Synthase
EPOC	Enfermedad Pulmonar Obstructiva Crónica
FR	Frecuencia respiratoria
HC	Humo de cigarrillo
HAP	Hipertensión Arterial Pulmonar
HP	Hipertensión Pulmonar
iNOS	inducible nitric oxide synthase
LAMAs	Long-Acting Muscarinic Antagonists
LBA	Lavado Broncoalveolar
LPS	Lipopolisacárido
MMPs	Metaloproteinasas de la matriz
MLI	Mean Linear Intercept
NO	Nitric Oxide
PAPm	Presión Media de la Arteria Pulmonar
PDE5	Fosfodiesterasa-5
Penh	Enhanced pause
RVP	Resistencia Vascular Pulmonar
sGC	Soluble Guanylate Cyclase

TNF-α	Tumor Necrosis Factor Alpha
V_A/Q	Relación Ventilación-Perfusión
VC	Volumen Corriente
VD	Ventrículo Derecho
VEGF	Vascular Endothelial Growth Factor
VEGFR	Vascular Endothelial Growth Factor Receptor
FEV_1	Volumen Espiratorio Máximo en el primer Segundo
VM	Ventilación minuto
VPH	Vasoconstricción Pulmonar Hipóxica

INTRODUCCIÓN

1.- Enfermedad Pulmonar Obstructiva Crónica

1.1.- Etiología y fisiopatología

La enfermedad pulmonar obstructiva crónica (EPOC) es una patología prevenible caracterizada por una limitación al flujo aéreo progresiva y no completamente reversible, disnea, producción de esputo y tos crónica.

La obstrucción al flujo aéreo se asocia a un proceso inflamatorio crónico en la vía aérea y el parénquima pulmonar en respuesta a partículas nocivas o gases inhalados, en particular al humo de cigarrillo (HC) (Figura 1) (1, 2). Esta respuesta inflamatoria crónica puede inducir la destrucción del parénquima pulmonar o enfisema y alteraciones estructurales de la vía aérea pequeña al alterar los mecanismos de reparación y defensa. De esta manera, se produce limitación progresiva al flujo aéreo debido a la menor retracción elástica y aumento de la distensibilidad pulmonar. La inflamación y el estrechamiento de la vía aérea periférica también contribuyen a la limitación del flujo aéreo produciendo una disminución del volumen de aire espirado en el primer segundo de la espiración forzada (FEV_1) en la espirometría forzada (3, 4). Además, alteraciones en las relaciones ventilación-perfusión (V_A/Q) pueden dar lugar a hipoxemia e hipercapnia en estos pacientes (5). Por otro lado, la inflamación inducida por el HC lleva a la hipersecreción mucosa, que también se asocia con el declive del FEV_1 (6), debida al mayor número de células caliciformes en la epitelio bronquial y al aumento de las glándulas submucosas, resultando en tos productiva que es característica de la bronquitis crónica, entidad clínica independiente (7).

En el curso evolutivo de la EPOC puede desarrollarse hipertensión pulmonar (HP) debida al remodelado vascular caracterizado por la hiperplasia de la capa íntima y la muscularización de arteriolas (8). Estos cambios se han atribuido a la acción directa del HC sobre el endotelio vascular, a la cual puede añadirse la vasoconstricción pulmonar hipóxica (VPH). Por otro lado, se postula que la pérdida de lecho capilar pulmonar debido al enfisema podría contribuir al desarrollo de la HP asociada a la EPOC (9, 10). También se ha demostrado infiltración por células inflamatorias y disfunción endotelial en las arterias pulmonares de pacientes con EPOC (11, 12). Por su parte, la HP sostenida puede promover la hipertrofia del ventrículo derecho (VD) y llevar al desarrollo de *cor pulmonale* e insuficiencia cardíaca derecha. Los pacientes con EPOC también presentan comorbilidades a nivel sistémico, incluyendo enfermedades cardiovasculares, disfunción del músculo esquelético, y cáncer de pulmón (13, 14).

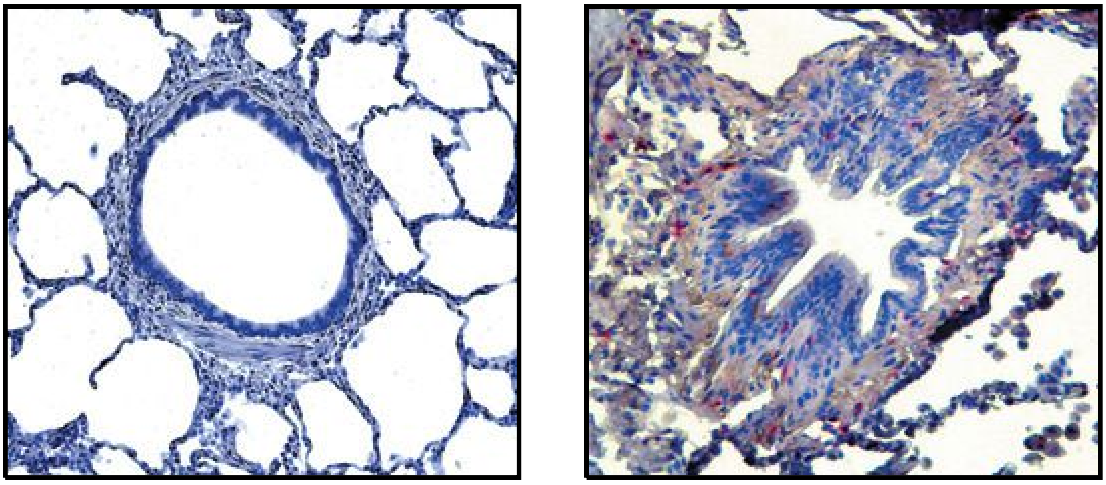

Figura 1. *Bronquiolos membranosos de un individuo no fumador y de un paciente con EPOC.* En el individuo no fumador (izquierda), la pared es delgada, y los alvéolos intactos están unidos a lo largo de su circunferencia. En el bronquiolo del paciente con EPOC (derecha), el diámetro de la vía aérea está estrechado, la pared engrosada, y varios septos alveolares destruidos. Los linfocitos T CD8+ (en rojo) infiltran la pared de la vía aérea en el fumador con EPOC pero no en el no fumador (1).

1.2.- Factores de riesgo y repercusiones

La exposición activa al HC es el factor de riesgo más común y mejor estudiado de EPOC en todo el mundo (15, 16). Otros tipos de tabaco (pipa, cigarro, pipa de agua (17) y la marihuana (18) también son factores de riesgo de EPOC. Se ha demostrado una asociación entre la cantidad de paquetes-año de cigarrillos fumados y la reducción del FEV_1 (19). A pesar de la estrecha relación entre el tabaco y la EPOC, otros factores de riesgo o diferencias genéticas pueden contribuir al desarrollo de la EPOC, como son la exposición pasiva (exposición ambiental) al HC (20) y la ocupacional a polvos orgánicos e inorgánicos y agentes químicos (21). También la contaminación del aire por biomasa quemada para utilizarla como combustible en calefacciones y para cocinar en lugares con poca ventilación es factor de riesgo de EPOC (22). El factor de riesgo genético mejor documentado es el déficit de la enzima α-1-antitripsina, que inhibe proteasas de neutrófilos contribuyendo a que no se degrade la matriz extracelular del parénquima pulmonar (23).

En cuanto a las repercusiones, la EPOC representa un problema de salud pública ya que a nivel mundial ocupará el quinto puesto en cuanto a carga de la enfermedad y el tercero en términos de mortalidad (24, 25) debido principalmente a la epidemia del tabaquismo. A pesar de ello, hay un bajo reconocimiento e infradiagnóstico de la EPOC (26).

1.3.- Alteraciones de la vía aérea y el parénquima pulmonar

Inflamación crónica

El HC induce un proceso inflamatorio en el pulmón que podría subyacer en el desarrollo de la EPOC. Este infiltrado inflamatorio involucra el reclutamiento hacia el pulmón de neutrófilos, macrófagos y linfocitos, y la inducción de estrés oxidativo que provocaría la destrucción del parénquima pulmonar y el remodelado de la vía aérea (1, 3, 27-29). El conocimiento del papel de las diferentes células inflamatorias es complejo porqué en la EPOC se alteran distintas estructuras (patología de la vía aérea, enfisema y alteraciones vasculares) con diferentes patrones de inflamación y diferentes patologías.

Neutrófilos: la acumulación de neutrófilos es uno de los eventos del daño pulmonar en fumadores, particularmente en el desarrollo de enfisema (30), al inducir un desequilibrio proteasa-antiproteasa y/o oxidante-antioxidante. El HC también lesionaría el epitelio respiratorio induciendo el reclutamiento de neutrófilos hacia las vías aéreas (31, 32). Estudios en humanos muestran una distribución no uniforme tanto en fumadores con función pulmonar normal como con EPOC, y una correlación entre el número de neutrófilos y el de paquetes-año fumando (33). Los neutrófilos liberan radicales de oxígeno, elastasa y citocinas que activan la secreción de las glándulas submucosas de la vía aérea (34) induciendo la producción de esputo mediando efectos en las células caliciformes, además de inducir enfisema e inflamación. Los inhibidores de metaloproteinasas mejoran el enfisema y el remodelado de los bronquios pequeños (35), demostrando el rol de las proteasas de neutrófilos en la patología. Por otro lado, el HC disminuye la capacidad fagocítica de los neutrófilos al suprimir la actividad de la caspasa-3 (36).

Macrófagos: los macrófagos también contribuyen en la fisiopatología de la EPOC (37). En humanos, los macrófagos se localizan en zonas de destrucción de la pared alveolar y se relacionan con el enfisema, además, su número en la vía aérea correlaciona con la severidad de la EPOC (38). Esto indica que estas células también pueden inducir una respuesta elastolítica con la exposición al HC (39, 40). De hecho, los macrófagos pueden liberar especies reactivas de oxígeno, citocinas, quimiocinas y metaloproteinasas de la matriz (MMPs) (41). En fumadores, los macrófagos a nivel de la vía aérea distal se asocian a fibrosis peribronquiolar (42) y en EPOC, los macrófagos tienen menor capacidad para fagocitar células epiteliales apoptóticas de la vía aérea contribuyendo a la no resolución del daño a este nivel (43).

Eosinófilos: aunque el papel de los eosinófilos en la patogénesis de la EPOC está poco clarificado, se postula que un número elevado de eosinófilos en las secreciones bronquiales puede representar un fenotipo distinto de la enfermedad ya que éstos pacientes responden al tratamiento con corticosteroides (44, 45). La infiltración de la vía aérea por eosinófilos se considera un rasgo característico del asma, pero se ha demostrado su presencia en la vía aérea, en el 20%-40% de las muestras de esputo inducido en pacientes con EPOC estable y durante las exacerbaciones (46, 47). Esto sugiere que el tabaco tiene un papel potencial en el reclutamiento de eosinófilos hacia el pulmón (48). Además, hay que considerar que algunos pacientes con EPOC tienen rasgos que concuerdan con el asma y en los que el patrón inflamatorio contiene un aumento de eosinófilos (49).

Linfocitos: además de la infiltración ya comentada del pulmón por las células del sistema inmune innato, las células del sistema inmune adaptativo también participarían en el proceso inflamatorio de la EPOC (3). En este sentido, los linfocitos T CD8+ y CD4+ también están implicados en esta respuesta inflamatoria crónica pulmonar en la EPOC. La inflamación mediada por los linfocitos se distribuye difusamente en el pulmón y persiste después de dejar de fumar (50, 51). El número de células T CD8+ está aumentado en el parénquima pulmonar y la vía respiratoria, correlacionándose inversamente con el FEV_1 (52), sugiriendo que estas células causan daño tisular en la EPOC. También se ha relacionado el número de células apoptóticas en el parénquima pulmonar con el de linfocitos T, principalmente células CD8+ citolíticas, como mecanismo en el desarrollo del enfisema (53) y hay mayor número de linfocitos CD4+ en la vía aérea de estos pacientes (28). Además, las células T y B se agregan formando folículos linfoides que se encuentran en mayor número en pacientes con EPOC más severa (3, 27). El incremento de células T y B en los pulmones de pacientes con EPOC podría suponer un rasgo característico de la autoperpetuación del proceso inflamatorio en esta patología y su persistencia crónica en los pacientes (1).

Enfisema pulmonar

En el enfisema hay destrucción de las paredes alveolares (Figura 2), con el consecuente aumento de los espacios aéreos distales que contribuye a la limitación al flujo aéreo debido a la reducción de la elastancia (3, 24). La destrucción de la elastina, componente importante del tejido conectivo del parénquima pulmonar, mediada por elastasas liberadas por macrófagos y neutrófilos que sobrepasaría la actividad antiproteasa fisiológica se cree que es uno de los mecanismos fisiopatogénicos en la inducción de la destrucción del parénquima alveolar. Al desequilibrio destrucción-reparación se le añadiría el efecto inhibitorio del HC sobre la síntesis de colágeno y elastina (54). También se ha de considerar la relación entre la deficiencia genética de la proteína α-1-antitripsina circulante, que inhibe la elastasa de neutrófilos con el enfisema pulmonar (55). Por otro lado, destacar que el número total de bronquiolos terminales y el área transversal que ocupan éstos dentro del pulmón está reducido en los pacientes con EPOC y enfisema. Además, el estrechamiento y la pérdida de bronquiolos terminales precederían a la aparición de la destrucción del parénquima pulmonar. Este proceso explicaría el incremento por un factor de 4 a 40 de la resistencia de la vía aérea pequeña en los pacientes con EPOC (56). También, como ya se ha comentado, la pérdida de lecho capilar y densidad vascular pulmonar asociada al enfisema podría contribuir al desarrollo de la HP asociada a la EPOC (9, 10, 57, 58). Y por otro lado, la desnutrición crónica también se asocia a alteraciones semejantes al enfisema pulmonar, con una menor superficie alveolar y mayor volumen aéreo pero sin disminución del flujo aéreo (59).

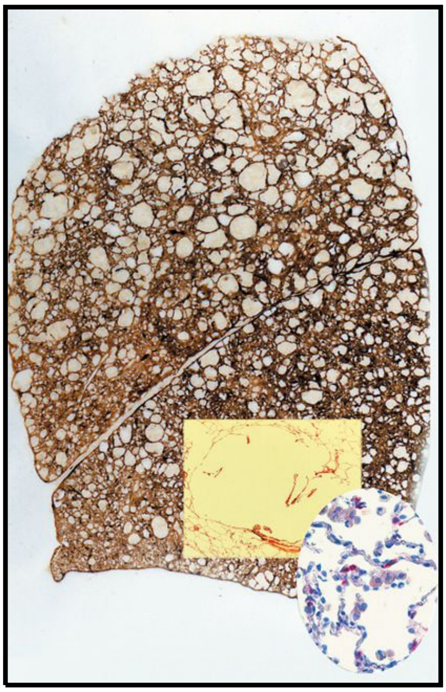

Figura 2. *Enfisema en la EPOC.* Corte de un pulmón completo que muestra enfisema, más prominente en los lóbulos superiores. El recuadro rectangular muestra destrucción centrolobulillar y agrandamiento. El recuadro oval muestra infiltrado inflamatorio consistente en macrófagos, linfocitos T CD8+ (inmunotinción), y otras células, en la pared y los espacios aéreos alveolares (1).

Además, se postula que el enfisema también podría deberse, al menos en parte, a una homeostasis y reparación del parénquima pulmonar alteradas, mediado por la vía de señalización NO-cGMP. Esta vía, que se alteraría con la exposición al HC, tendría una acción importante en la preservación de la arquitectura pulmonar a través de mediadores como VEFGA y FGF10, y enzimas antioxidantes, como SOD1, además de reducir la inflamación (60). Por otra parte, hay evidencia de un papel causativo de la sintasa inducible de NO (iNOS) y peroxinitrito (ONOO-) en el enfisema inducido por HC (61) que podría prevenirse incrementando los niveles de cGMP (60).

Fibrosis

En individuos fumadores, se ha observado cierto grado de fibrosis en la vía aérea (3, 62). Las fibras de colágeno gruesas se asocian con la cicatrización y podrían modular la rigidez de los tejidos (63). Además, la asociación de la fibrosis con el enfisema se considera una entidad específica de pronóstico reservado (64-66). Los mecanismos que llevan a la fibrosis alrededor de las vías aéreas se desconocen, pero podría tratarse de un intento de reparación de la inflamación crónica.

1.4.- Alteraciones de la circulación pulmonar

El HC también se asocia con disfunción del endotelio vascular (67), sobreexpresión de factores de crecimiento (68) e infiltración de células inflamatorias en las arterias pulmonares (11). Estos factores inducen la proliferación de células musculares lisas (CML) en las arterias pulmonares y consecuentemente, el remodelado vascular e incremento de la resistencia vascular pulmonar (RVP).

Remodelado vascular

El remodelado vascular es el conjunto de cambios estructurales vasculares que llevan a la reducción de la luz de las arterias pulmonares, principalmente en los vasos más pequeños y las arterias precapilares (67, 69). Los cambios estructurales consisten en el engrosamiento de la capa íntima debido a la proliferación de CML, sin embargo, el engrosamiento de la capa muscular, de existir, es menos evidente (Figura 3) (70, 71). El remodelado vascular explica el incremento irreversible de la RVP y es la causa principal de HP en la EPOC. El remodelado de la íntima también se debe al depósito de elastina y colágeno (71). Tanto la VPH persistente (72) como los efectos directos de HC (67) explicarían el remodelado vascular pulmonar asociado con la EPOC (71, 72).

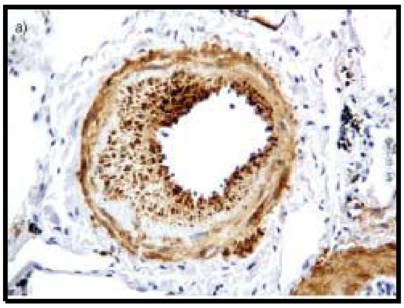

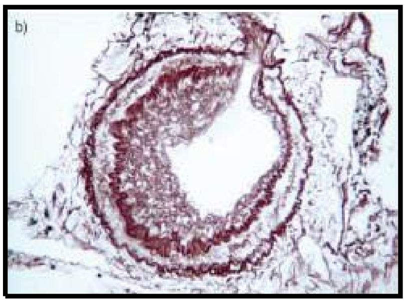

Figura 3. *Arteria muscular pulmonar de un paciente con EPOC.* Nótese el engrosamiento prominente de la íntima y el estrechamiento luminal. a) Inmunotinción con anticuerpo monoclonal contra α-actina de músculo liso, que muestra proliferación de CML en la íntima. b) Tinción de orceína que revela abundante depósito de fibras elásticas en la capa íntima (70).

Disfunción endotelial

El endotelio pulmonar tiene un importante papel en el control de la homeostasis vascular (73) al liberar agentes vasodilatadores como el óxido nítrico (NO) y la prostaciclina, y vasocontrictores como la endotelina-1 o la angiotensina. La disfunción endotelial es entendida como una respuesta vasodilatadora inadecuada debida al desequilibrio en la liberación de estos agentes. En individuos fumadores y pacientes con EPOC, las arterias intrapulmonares muestran disfunción endotelial, que se asocia a una menor expresión de la sintasa endotelial de NO (eNOS) y, consecuentemente, a una menor síntesis de NO por las células endoteliales, principal vasodilatador endógeno y regulador del crecimiento celular. Estas alteraciones se considera que son las que promueven el desarrollo de HP en la EPOC (Figura 4) (8, 67, 74).

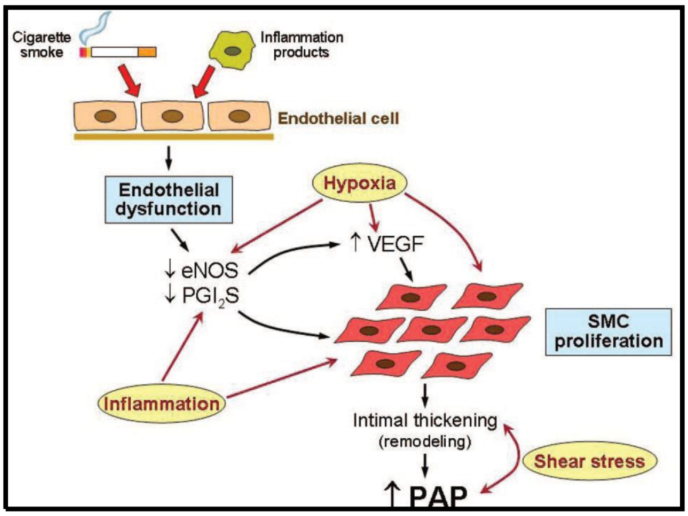

Figura 4. *Fisiopatología de la HP en la EPOC.* El HC y/o los productos de la inflamación pueden iniciar los cambios al dañar las células endoteliales y producir disfunción endotelial. Esto comporta un desequilibrio entre factores vasoactivos y de crecimiento promoviendo la proliferación de CML. La hipoxia, inflamación, y estrés de fricción amplifican y perpetúan los efectos, contribuyendo aún más a la HP (8).

El NO endotelial activa la guanilato ciclasa soluble (sGC) produciendo la formación del segundo mensajero monofosfato de guanosina cíclico (cGMP) (74, 75). El cGMP intracelular disminuye la concentración de calcio intracelular, produciendo una acción vasorelajadora y de inhibición de la proliferación sobre las CML (60, 76). En el pulmón, el cGMP es metabolizado por la acción de la fosfodiesterasa-5 (PDE5). Por otro lado, la prostaglandina (PGI_2), sintetizada tanto por las células endoteliales como CML, estimula la adenilato ciclasa, incrementando la producción de monofosfato de adenosina cíclico (cAMP) que actúa como segundo mensajero relajando las CML e inhibiendo su proliferación. Este mediador está disminuido en pacientes con HP (77, 78). Las arterias pulmonares de pacientes con EPOC y fumadores con función pulmonar normal desarrollan mayor efecto vasoconstrictor y menor vasorelajación en respuesta a vasodilatadores dependientes de la síntesis de NO como acetilcolina (ACh) y adenosina difosfato (ADP) (12, 67), sugiriendo que la exposición al HC podría ser, en parte, el causante de la lesión endotelial.

Hipertensión pulmonar

La HP asociada a la EPOC es una complicación grave presente en más de la mitad de los pacientes en estadio severo y que está desencadenada, en parte, por la exposición al HC (79). Además, constituye un factor de mal pronóstico (80, 81). La HP se clasifica clínicamente en diferentes grupos que comparten características patológicas y hemodinámicas y aproximaciones terapéuticas similares (Tabla 1) (82):

Table 1	**Updated Classification of Pulmonary Hypertension***
	1. Pulmonary arterial hypertension
	1.1 Idiopathic PAH
	1.2 Heritable PAH
	1.2.1 BMPR2
	1.2.2 ALK-1, ENG, **SMAD9, CAV1, KCNK3**
	1.2.3 Unknown
	1.3 Drug and toxin induced
	1.4 Associated with:
	1.4.1 Connective tissue disease
	1.4.2 HIV infection
	1.4.3 Portal hypertension
	1.4.4 Congenital heart diseases
	1.4.5 Schistosomiasis
	1′ Pulmonary veno-occlusive disease and/or pulmonary capillary hemangiomatosis
	1″. Persistent pulmonary hypertension of the newborn (PPHN)
	2. Pulmonary hypertension due to left heart disease
	2.1 Left ventricular systolic dysfunction
	2.2 Left ventricular diastolic dysfunction
	2.3 Valvular disease
	2.4 Congenital/acquired left heart inflow/outflow tract obstruction and congenital cardiomyopathies
	3. Pulmonary hypertension due to lung diseases and/or hypoxia
	3.1 Chronic obstructive pulmonary disease
	3.2 Interstitial lung disease
	3.3 Other pulmonary diseases with mixed restrictive and obstructive pattern
	3.4 Sleep-disordered breathing
	3.5 Alveolar hypoventilation disorders
	3.6 Chronic exposure to high altitude
	3.7 Developmental lung diseases
	4. Chronic thromboembolic pulmonary hypertension (CTEPH)
	5. Pulmonary hypertension with unclear multifactorial mechanisms
	5.1 Hematologic disorders: **chronic hemolytic anemia**, myeloproliferative disorders, splenectomy
	5.2 Systemic disorders: sarcoidosis, pulmonary histiocytosis, lymphangioleiomyomatosis
	5.3 Metabolic disorders: glycogen storage disease, Gaucher disease, thyroid disorders
	5.4 Others: tumoral obstruction, fibrosing mediastinitis, chronic renal failure, **segmental PH**

*5th WSPH Nice 2013. Main modifications to the previous Dana Point classification are in bold.
BMPR = bone morphogenic protein receptor type II; CAV1 = caveolin-1; ENG = endoglin; HIV = human immunodeficiency virus; PAH = pulmonary arterial hypertension.

En la EPOC, la fisiopatología de la HP se caracteriza por disfunción endotelial (67), desequilibrio de factores de crecimiento (68) y una respuesta inflamatoria aumentada (11) en los vasos pulmonares. Estos factores inducen la proliferación de CML en la pared del vaso que lleva al aumento de RVP. La HP se define por valores anormalmente elevados de la presión media de la arteria pulmonar (PAPm) ≥25mmHg y una presión enclavada pulmonar normal (≤15mmHg), medidas mediante cateterismo cardíaco derecho (83). En la EPOC la supervivencia se relaciona inversamente con el valor de PAP (81, 84, 85) (Figura 5).

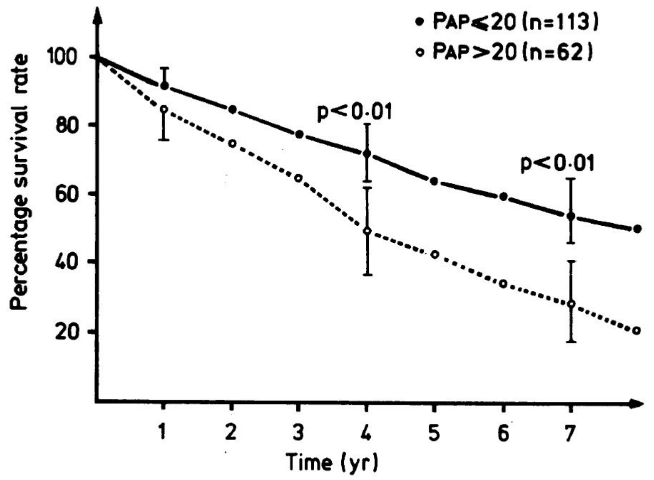

Figura 5. *Índices de supervivencia según el nivel inicial de PAPm (≤20 mmHg o > 20 mmHg).* Los dos subgrupos muestran diferencias significativas tras cuatro y siete años (81).

Entre los factores implicados en la HP asociada a la EPOC se encuentran:

Humo de cigarrillo (HC): además de alquitrán y nicotina contiene otros compuestos tóxicos y carcinógenos como metales pesados, hidrocarburos aromáticos policíclicos, azaarenos, N-nitrosaminas, óxido de nitrógeno y ácido cianhídrico. Se generan radicales libres y oxidantes altamente reactivos (86, 87) que causan daño oxidativo a las membranas celulares, enzimas y ADN (88). La exposición ambiental a HC (fumadores pasivos) también favorece la predisposición a la mayoría de enfermedades respiratorias (89, 90).

Hipoxia alveolar: actúa como estimulador de la VPH (91, 92), produciéndose redistribución del flujo sanguíneo hacia los segmentos mejor ventilados para mantener una relación V_A/Q adecuada (93). La VPH es específica de la circulación pulmonar puesto que a nivel sistémico la hipoxia produce vasodilatación para mantener la oxigenación tisular (94). El NO liberado por las células endoteliales pulmonares, que puede disminuir debido a las alteraciones vasculares de la EPOC, contrarresta la VPH (95, 96). Por otro lado, la hipoxia crónica induce el remodelado de las arterias pulmonares con hipertrofia de la capa muscular (y no de la capa íntima como en la EPOC) y consecuentemente el aumento de la RVP que puede llevar a la hipertrofia del VD e insuficiencia cardíaca derecha.

Disfunción endotelial: la disfunción endotelial en las arterias pulmonares de pacientes con EPOC se asocia con la expresión disminuida de eNOS y la liberación reducida de NO (67, 74). Las arterias pulmonares de los pacientes con EPOC muestran menor vasodilatación dependiente de endotelio. Estudios *in vitro* en baño de órganos con arterias intrapulmonares de estos pacientes muestran la respuesta disminuida a ADP de estas arterias (67). Por lo tanto, la desregulación de mediadores endoteliales como la disminución de NO y el aumento de entotelina-1 tendrían un papel patogénico en el desarrollo de la HP (97, 98). Además, la disfunción endotelial correlaciona con la severidad del remodelado vascular que también llevaría al desarrollo de HP (12).

Inflamación: la infiltración de las arterias pulmonares por células inflamatorias podría favorecer el desarrollo y progresión de la HP asociada a la EPOC (11). Aunque no está claro el papel patogénico de estas células, podrían contribuir a las alteraciones vasculares pulmonares mediante la expresión de citocinas y factores de crecimiento. En este sentido, el incremento de linfocitos correlaciona con la disminución en la relajación dependiente de endotelio y el engrosamiento de la íntima de las arterias (67). El infiltrado inflamatorio también correlaciona con el grosor de la pared arterial e inversamente con la función endotelial (11). Además, la interleuquina-6 (IL-6), la proteína C reactiva (PCR) y el TNF-α se asocian a mayor PAP en la EPOC (99, 100).

2.- Modelo experimental de EPOC

El modelo experimental de EPOC debería reproducir los cambios morfológicos y funcionales que se observan en los pacientes con EPOC. La posibilidad de disponer de modelos experimentales de EPOC permite estudiar los mecanismos patogénicos y los efectos de las intervenciones terapéuticas tanto sobre la estructura como sobre estos mecanismos alterados. En el diseño del modelo animal se han de tener en cuenta las diferencias anatómicas y genéticas entre especies animales que comportan diferente susceptibilidad al desarrollo de las alteraciones de la EPOC. A continuación se resume algunos de los modelos animales disponibles en la literatura que intentan mimetizar los cambios fisiopatológicos más destacados de la EPOC:

2.1.- Inflamación pulmonar

Las enfermedades respiratorias como la bronquitis crónica, asma o EPOC se caracterizan por la limitación al flujo aéreo debida en parte a la inflamación pulmonar crónica que contribuye al remodelado bronquial y vascular y al enfisema. Los modelos animales de inflamación son frecuentes en la investigación de enfermedades respiratorias crónicas (101, 102).

El lipopolisacárido (LPS) es una endotoxina de las bacterias Gram negativas utilizada como factor inductor de la inflamación pulmonar (102, 103). El LPS, administrado intratraquealmente o inhalado, estimula el sistema inmune innato iniciando el influjo de neutrófilos (104, 105), la liberación de TNF-α, IL-1β, MMP-9 y MMP-12 (106, 107), inflamación bronquial, remodelado y obstrucción de la vía aérea, enfisema y alteración de la función pulmonar (108, 109). Sin embargo, la relevancia como modelo de EPOC es cuestionable debido a que induce inflamación que responde a glucocorticoides (110) y tolerancia inmunológica.

También se ha utilizado contaminantes inhalados como polvo orgánico y peptidoglicano para inducir cambios inflamatorios en el parénquima pulmonar y la vía aérea (111). En otros modelos animales se ha intentado reproducir la inflamación crónica del pulmón mediante la colonización bacteriana de la vía aérea por instilación intratraqueal de bacterias vivas (112). De hecho, al ser la inflamación crónica y la bronquitis crónica entidades características de la EPOC, también se ha utilizado la exposición crónica al HC como modelo de inflamación pulmonar (113).

2.2.- Enfisema

La generación del enfisema se podría explicar, en parte, por la teoría proteasa-antiproteasa. La instilación en hámsteres de papaína (proteasa obtenida de la papaya) induce lesiones enfisematosas (114) que apuntaría a las proteasas liberadas por células inflamatorias reclutadas en el tracto respiratorio como mediadoras que participan en la destrucción del parénquima pulmonar y el desarrollo de enfisema en la EPOC (115). En modelos animales la instilación de enzimas elastolíticas como la elastasa pancreática porcina y de neutrófilos humanos induce enfisema (30, 116). Este modelo animal se caracteriza por la degradación de la elastina junto con la infiltración inflamatoria por macrófagos, neutrófilos y linfocitos , la sobreexpresión de mediadores proinflamatorios como TNF-α, IL-1β, IL-6 y IL-8 (117) y la metaplasia de células caliciformes (118) que conlleva el empeoramiento de la función pulmonar.

Debido a que en humanos la desnutrición puede asociarse a la aparición de lesiones enfisematosas (59), algunos autores han utilizado la restricción calórica en modelo animal para reproducir la pérdida alveolar (119). También, según algunos estudios en modelos animales el enfisema podría explicarse por un mantenimiento y reparación deficiente del parénquima pulmonar que podría inducirse por procesos de apoptosis regulados por VEGF (120) y su receptor VEGFR (121) y la activación de caspasa-3 (122).

2.3.- Hipertensión pulmonar

La hipoxia crónica induce HP en modelos animales (123). En ratas produce un aumento de la PAPm que se correlaciona con el desarrollo de hipertrofia del VD. En ratones, la exposición a hipoxia también produce un incremento de la PAPm, pero menor remodelado vascular que en ratas (124, 125). En este modelo también se desarrolla remodelado de los vasos pulmonares con aumento de expresión de α-actina de CML.

En modelos animales, la monocrotalina (MCT), que es un alcaloide de pirrolizidina y constituyente de la planta tóxica *Crotalaria spectabilis*, causa HP, hipertrofia y disfunción del VD y alteraciones en la vasculatura pulmonar. En ratas la MCT causa daño endotelial que lleva al desarrollo de HP (126, 127). En este modelo experimental el aumento de la PAP y el remodelado vascular también podrían deberse al infiltrado inflamatorio vascular inducido por MCT (128). Sin embargo, este modelo se considera más propio de hipertensión arterial pulmonar (HAP) que de HP asociada a la EPOC.

2.4.- Modelo de EPOC por exposición al humo de cigarrillo

Los modelos in vivo de inflamación y daño pulmonar inducido por HC se utilizan para investigar los mecanismos patogénicos de la EPOC. La ventaja más importante sobre otros modelos experimentales es la utilización del principal agente primario causante de la enfermedad en humanos, el HC, para modelar y reproducir las alteraciones fisiopatológicas que caracterizan a la EPOC (129-135). Por consiguiente, los modelos animales de exposición al HC muestran el nexo causal entre la exposición al HC y la inflamación y los cambios vasculares y de la vía aérea asociados con la EPOC. Entre estos modelos animales por exposición al HC, el cobayo desarrolla de manera más próxima que otros modelos animales alteraciones pulmonares morfológicas y funcionales que se asemejan a las observables en pacientes con EPOC (133). En este sentido, los cobayos expuestos al HC desarrollan enfisema, remodelado de la vía aérea con metaplasia de células caliciformes, infiltración inflamatoria y reproducen las alteraciones de los vasos pulmonares en la EPOC al inducir su muscularización, incrementar la PAP y provocar disfunción endotelial (131, 136, 137). Por lo tanto, este modelo experimental desarrolla HP por lo que se pueden investigar los mecanismos implicados (60, 138). Sin embargo, la naturaleza y características del infiltrado inflamatorio celular y su relación con los cambios estructurales que tienen lugar en el pulmón no están completamente caracterizadas en el modelo experimental de EPOC por exposición crónica a HC en cobayos.

3.- Tratamiento farmacológico en la EPOC y la HP

La terapia farmacológica reduce los síntomas de la EPOC, la frecuencia y severidad de las exacerbaciones, mejora la calidad de vida y la tolerancia al ejercicio. El tratamiento actual de la EPOC se fundamenta en el empleo de agentes broncodilatadores de larga duración, agonistas beta-adrenérgicos o anticolinérgicos (24). Por otro lado, con el uso de vasodilatadores se intenta combatir la HP asociada a la EPOC reduciendo la PAP y la sobrecarga del VD, incrementando el gasto cardíaco y mejorando la oxigenación tisular (139). Pero en estos pacientes, los agentes vasodilatadores pueden empeorar el intercambio gaseoso al inhibir la VPH, dando lugar a un mayor desequilibrio ventilación-perfusión (140-143). En la presente tesis doctoral se han evaluado los efectos de dos tipos de compuestos, tanto sobre la estructura como sobre los mecanismos patogénicos en el modelo de EPOC en cobayos por exposición crónica a HC. Estas intervenciones farmacológicas son las que a continuación se detallan:

3.1.- Antagonistas muscarínicos: bromuro de aclidinio

Los antagonistas muscarínicos (anticolinérgicos) de acción prolongada (*Long-Acting Muscarinic Antagonists*, LAMAs) son fármacos de primera elección en el tratamiento de la EPOC estable (24) y entre otros beneficios reducen la frecuencia de exacerbaciones (144) y el nivel de declive en el FEV_1 (145), lo que sugiere que sus efectos podrían ir más allá de la acción broncodilatadora (146), pudiendo tener efectos sobre los cambios histopatológicos pulmonares de la EPOC. En este sentido, la activación de receptores muscarínicos puede inducir la secreción de citocinas y leucotrienos por las células inflamatorias y epiteliales (147-149), la proliferación de fibroblastos (150), aumentar la respuesta de las CML a los factores de crecimiento (151, 152), y modular la expresión de proteína contráctil de CML (150).

Bromuro de aclidinio es un LAMA inhalado que fue aprobado para su comercialización en julio de 2012 por la European Medicines Agency (EMA) y la U.S. Food and Drug Administration (FDA) para el tratamiento de la EPOC. Aclidinio se une a los receptores muscarínicos M1-M5, tiene una mayor selectividad por los receptores M3 que por los M2, y se disocia más lentamente de los M3 que de los M2 (153). En ensayos clínicos con pacientes con EPOC, aclidinio produjo una broncodilatación sostenida durante 24 horas, incrementó la tolerancia al ejercicio (154), mejoró la obstrucción al flujo aéreo, redujo la percepción de disnea, y retrasó la aparición de la primera exacerbación (155-157). En modelos experimentales, bromuro de aclidinio ha demostrado una actividad antagonista potente y de larga duración de los receptores muscarínicos, comparable a bromuro de ipratropio y bromuro de tiotropio (153). Estudios en modelos experimentales de obstrucción al flujo aéreo han demostrado que el tratamiento con LAMAs disminuye el número de células inflamatorias en el lavado broncoalveolar (LBA) (158, 159), reduce la liberación de citocinas inflamatorias por las CML de la vía aérea (147), y contrarresta el proceso de remodelado de la vía aérea (159, 160), evidenciando que además de la acción broncodilatadora la terapia anticolinérgica podría añadir otros beneficios terapéuticos en el manejo de la EPOC (Figura 6) (161).

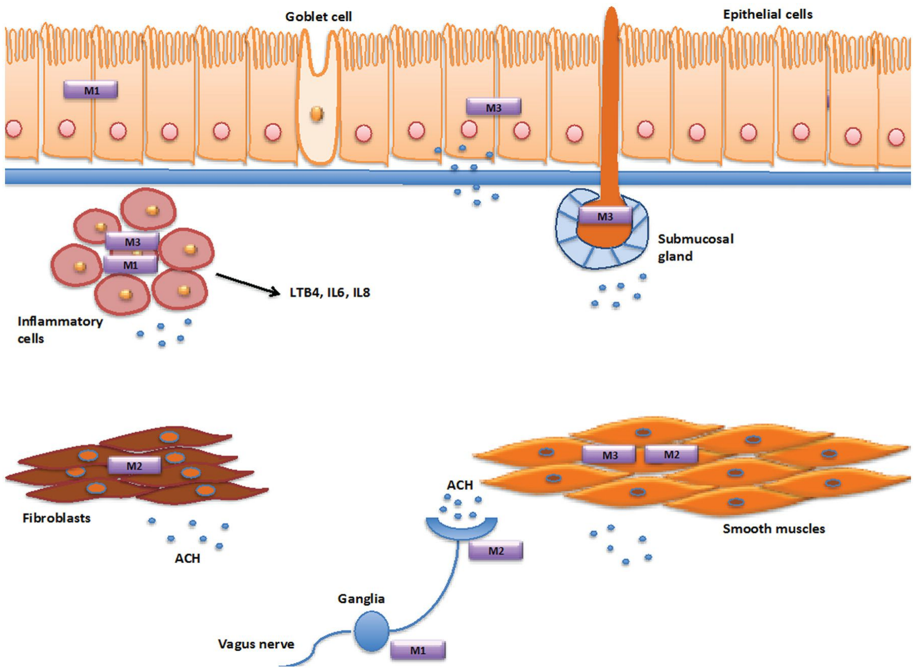

Figura 6. *Receptores muscarínicos*. La distribución de los receptores muscarínicos en el árbol bronquial está principalmente restringida a los receptores M1, M2 y M3 (161).

La mayoría de estudios experimentales con antagonistas muscarínicos se han realizado en modelos de asma alérgico (160, 162, 163), daño pulmonar inducido por instilación de LPS (164) y exposición aguda al HC (158). Sin embargo, se conoce poco de los efectos de los LAMAs en modelos animales de EPOC inducida por la exposición crónica al HC, que además de utilizar el mismo agente causativo reproducen de manera más parecida los cambios morfológicos y funcionales que aparecen en los pacientes con EPOC (133, 135).

3.2.- Inhibidores de la fosfodiesterasa-5: sildenafilo

Como se ha comentado, la disfunción endotelial en arterias pulmonares de pacientes con EPOC se asocia con la expresión reducida de eNOS y una liberación disminuida de NO (67, 74). Éste NO endotelial activa la sGC que lleva a la formación del segundo mensajero cGMP (74, 75). El cGMP intracelular disminuye la concentración de calcio intracelular, y de esta forma, se relajan las CML vasculares (165). El NO endotelial puede también inhibir la proliferación de CML a través de mecanismos dependientes de cGMP (166). En el pulmón, el cGMP se metaboliza principalmente por la acción de la PDE5. Los inhibidores de PDE5, como sildenafilo, mejoran la vía de señalización NO-cGMP y ejercen efectos vasodilatador y antiproliferativo (Figura 5) (167, 168). Estudios en modelos experimentales de HP inducida por hipoxia (169) o MCT (170, 171) han demostrado que sildenafilo reduce la PAP, previene la hipertrofia del VD y ejerce un efecto antirremodelado en los vasos pulmonares. Sin embargo, los efectos de sildenafilo sobre la estructura pulmonar no se han evaluado en modelos experimentales de EPOC por exposición crónica al HC. Sildenafilo se utiliza actualmente en el tratamiento de la HAP (172).

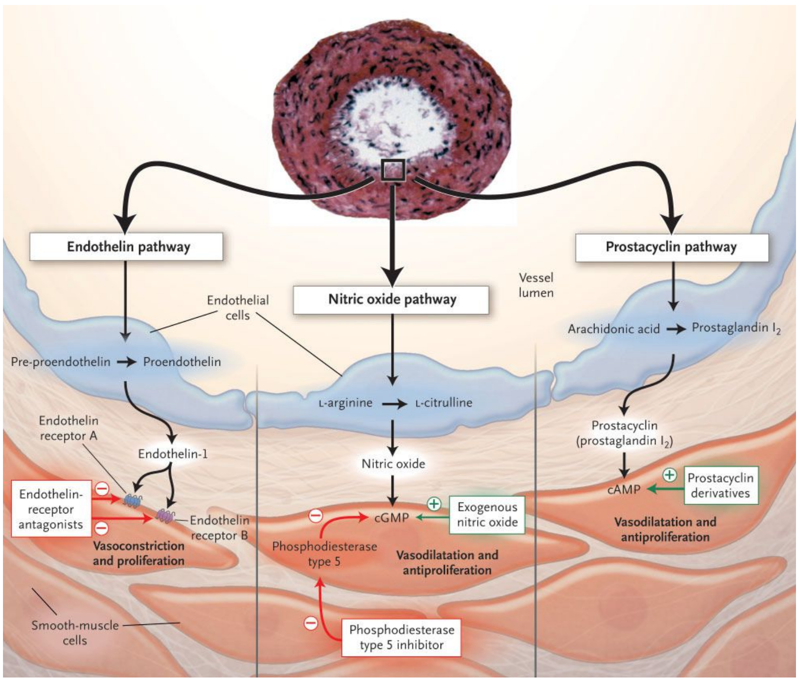

Figura 7. *Dianas terapéuticas en HAP.* Tres vías de señalización involucradas en la proliferación y contracción de CML de la arteria pulmonar en HAP. Las células endoteliales disfuncionales de la arteria pulmonar (azul) disminuyen la producción de prostaciclina y NO endógeno, y aumentan endotelina-1, promoviendo vasoconstricción y proliferación de CML en la arteria pulmonar (rojo) (167).

En pacientes con EPOC y HP asociada, hemos demostrado que sildenafilo disminuye la RVP de manera aguda (142), pero este efecto no se trasladó a una mayor tolerancia al ejercicio al administrarlo durante 3 meses (173). Esta influencia limitada en la tolerancia al ejercicio podría deberse a los cambios concomitantes que tienen lugar en el parénquima pulmonar y vía aérea de los pacientes con EPOC.

HIPÓTESIS

La presente tesis doctoral se plantea en base a las siguientes hipótesis:

1. El modelo experimental de EPOC por exposición al HC en cobayos reproduce la destrucción del parénquima y las alteraciones en la vía aérea y vasos pulmonares características de la EPOC, en los que diferentes mediadores químicos y células inflamatorias tendrían un papel fisiopatológico destacable. Por este motivo, hipotetizamos que la exposición crónica al HC producirá en cobayos un proceso inflamatorio asociado con cambios morfológicos y funcionales en las estructuras pulmonares similares a lo que se observa en los pacientes con EPOC.

2. La adecuada caracterización del modelo experimental de EPOC en cobayos permitiría su uso en la evaluación de los efectos de nuevos fármacos y dianas terapéuticas en el tratamiento de la EPOC. En este sentido, se evalúan los efectos de bromuro de aclidinio, un antagonista muscarínico de acción prolongada, y sildenafilo, un inhibidor selectivo de la PDE5.

    2.1. Basándonos en estudios previos realizados y en que aclidinio tiene una potente afinidad por el receptor muscarínico M3 (153) que media la acción proinflamatoria y proliferativa de la ACh (146, 149, 151), y su efecto inhibitorio en la diferenciación miofibroblástica (174), hipotetizamos que además de su actividad broncodilatadora aclidinio podría tener efectos antirremodelado y antiinflamatorio en el tejido pulmonar en este modelo animal de EPOC por exposición crónica al HC.

    2.2. Por otro lado, el cobayo carece de VPH pero desarrolla HP tras la exposición crónica a HC (134). La falta de VPH permite testar los efectos antirremodelado de vasodilatadores minimizando el potencial efecto perjudicial en el intercambio de gases. En un estudio reciente hemos demostrado que en cobayos expuestos crónicamente al HC la administración de un estimulador de sGC independiente de NO que incrementa los niveles de cGMP, reduce la RVP y previene el remodelado vascular pulmonar, y el desarrollo de enfisema (60). Por lo tanto, hipotetizamos que sildenafilo, que aumenta la actividad de cGMP al impedir su metabolización, podría ejercer efectos favorables sobre la estructura pulmonar además de su acción vasodilatadora.

OBJETIVOS

De acuerdo con las hipótesis y los antecedentes expuestos, los objetivos que se plantearon en los tres artículos que conforman esta tesis doctoral fueron:

1.- Primer artículo. ***Pulmonary inflammatory reaction and structural changes induced by cigarette smoke exposure in the Guinea pig.***

Objetivo general

Evaluar la naturaleza y características de la reacción inflamatoria en el pulmón, y su implicación en los cambios estructurales que tienen lugar a nivel pulmonar en el modelo experimental de EPOC en cobayos expuestos crónicamente al HC.

Objetivos concretos

I. Caracterizar el tipo de células inflamatorias y su distribución en las estructuras pulmonares (vía aérea, vasos y parénquima).
II. Analizar el remodelado de la vía aérea y de los vasos pulmonares.
III. Evaluar la presencia de fibrosis y la aparición de enfisema en el parénquima.
IV. Explorar los mecanismos que interconectan la infiltración de células inflamatorias con las alteraciones estructurales características de la EPOC.
V. Establecer la importancia, el orden secuencial y la dinámica de estas alteraciones en el desarrollo de la EPOC.

2.- Segundo artículo. ***Effects of Aclidinium Bromide in a Cigarette Smoke-Exposed Guinea Pig Model of Chronic Obstructive Pulmonary Disease***.

Objetivo general

Investigar los efectos del broncodilatador bromuro de aclidinio sobre los cambios histopatológicos y el infiltrado de células inflamatorias en los pulmones del modelo de EPOC en cobayos crónicamente expuestos al HC.

Objetivos concretos

I. Evaluar el efecto de aclidinio sobre las alteraciones morfológicas, como potencial agente antirremodelado de la vía aérea.

II. Evaluar el efecto de aclidinio sobre la infiltración de células inflamatorias en las estructuras pulmonares, como potencial agente antiinflamatorio.

III. Evaluar el efecto de aclidinio sobre la función pulmonar y los signos respiratorios característicos de la EPOC, particularmente su efecto broncodilatador.

IV. Evaluar el efecto de aclidinio sobre otras alteraciones típicas de la EPOC como la metaplasia de células caliciformes y el desarrollo de enfisema pulmonar.

V. Explorar posibles mecanismos que interconectan los diferentes cambios observados con la administración de aclidinio.

3.- Tercer artículo. ***Sildenafil in a cigarette smoke-induced model of COPD in the guinea pig.***

Objetivo general

Evaluar los efectos del vasodilatador sildenafilo sobre la hemodinámica pulmonar, función endotelial, y el remodelado vascular y del parénquima, en el modelo de EPOC en cobayos crónicamente expuestos al HC.

Objetivos concretos

I. Evaluar el efecto de sildenafilo sobre la hemodinámica pulmonar, como agente vasodilatador de la circulación pulmonar.

II. Evaluar el efecto de sildenafilo sobre la hipertrofia del VD y la función endotelial de arterias pulmonares.

III. Evaluar el efecto de sildenafilo sobre las alteraciones morfológicas y el remodelado vascular pulmonar, como potencial agente antiproliferativo.

IV. Evaluar el efecto de sildenafilo sobre el funcionalismo respiratorio.

V. Integrar posibles mecanismos que expliquen los cambios producidos con la administración de sildenafilo.

RESULTADOS

Esta tesis doctoral se fundamenta en los siguientes tres artículos originales de los que el doctorando es primer autor:

Primer artículo:

Domínguez-Fandos D, Peinado VI, Puig-Pey R, Ferrer E, Musri MM, Ramírez J, Barberà JA. ***Pulmonary inflammatory reaction and structural changes induced by cigarette smoke exposure in the Guinea pig.*** COPD. 2012 Aug;9(5):473-84.

Factor de impacto: 2.310 (Posición 28 de 50). Tercer cuartil del área de conocimiento "Respiratory system" (ISI Web of Knowledge℠, Journal Citation Reports®,

http://sauwok5.fecyt.es/admin-apps/JCR/JCR?RQ=RECORD&rank=28&journal=COPD

Segundo artículo:

Domínguez-Fandos D, Ferrer E, Puig-Pey R, Carreño C, Prats N, Aparici M, Musri MM, Gavaldà A, Peinado VI, Miralpeix M, Barberà JA. ***Effects of Aclidinium Bromide in a Cigarette Smoke-Exposed Guinea Pig Model of Chronic Obstructive Pulmonary Disease.*** Am J Respir Cell Mol Biol. 2014 Feb;50(2):337-46.

Factor de impacto: 4.109 (Posición 7 de 53). Primer cuartil del área de conocimiento "Respiratory system" (ISI Web of Knowledge℠, Journal Citation Reports®,

http://sauwok5.fecyt.es/admin-apps/JCR/JCR?RQ=RECORD&rank=7&journal=AM+J+RESP+CELL+MOL

Tercer artículo:

Domínguez-Fandos D, Valdés C, Ferrer E, Puig-Pey R, Blanco I, Tura-Ceide O, Paul T, Peinado VI, Barberà JA. Sildenafil in a cigarette smoke-Induced model of COPD in the guinea pig. Eur Respir J. (actualmente en segunda revisión).

Factor de impacto: 7.125 (Posición 4 de 54). Primer cuartel y decil del área de conocimiento “Respiratory system” (ISI Web of Knowledge^{SM}, Journal Citation Reports$^{®}$,

http://sauwok5.fecyt.es/admin-apps/JCR/JCR?RQ=RECORD&rank=16&journal=EUR+RESPIR+J

1.- Primer artículo

Pulmonary inflammatory reaction and structural changes induced by cigarette smoke exposure in the Guinea pig.

David Domínguez-Fandos, Víctor Ivo Peinado, Raquel Puig-Pey, Elisabet Ferrer, Melina Mara Musri, Josep Ramírez, Joan Albert Barberà.

Artículo publicado en COPD-Journal of Chronic Obstructive Pulmonary Disease 2012 Aug;9(5):473-84.

COPD JOURNAL OF CHRONIC OBSTRUCTIVE PULMONARY DISEASE

informa healthcare

COPD, 9:473–484, 2012
ISSN: 1541-2555 print / 1541-2563 online

DOI: 10.3109/15412555.2012.691999

ORIGINAL RESEARCH

Pulmonary Inflammatory Reaction and Structural Changes Induced by Cigarette Smoke Exposure in the Guinea Pig

David Domínguez-Fandos,[1] Víctor I. Peinado,[1,3] Raquel Puig-Pey,[1] Elisabet Ferrer,[1] Melina M. Musri,[1] Josep Ramírez,[2] and Joan A. Barberà[1,3]

1 Department of Pulmonary Medicine, Hospital Clínic-Institut d'Investigacions Biomèdiques August Pi i Sunyer, University of Barcelona, Barcelona, Spain

2 Department of Pathology, Hospital Clínic-Institut d'Investigacions Biomèdiques August Pi i Sunyer, University of Barcelona, Barcelona, Spain

3 Ciber de Enfermedades Respiratorias, Spain

Abstract

Cigarette smoke (CS) induces an inflammatory process in the lung that may underlie the development of chronic obstructive pulmonary disease (COPD). The nature and characteristics of this process have not been fully established in animal models. We aimed to evaluate the pulmonary inflammatory reaction and its involvement in structural changes in guinea pigs chronically exposed to CS. 19 Hartley guinea pigs were exposed to 7 cigarettes/day, during 3 or 6 months. 18 control guinea pigs were sham-exposed. Numbers of neutrophils, macrophages and eosinophils and lymphoid follicles were assessed in different lung structures. Airway and vessel morphometry, alveolar space size and collagen deposition were also quantified. After 6 months of exposure, CS-exposed guinea pigs showed increased numbers of neutrophils, macrophages and eosinophils in the airways, intrapulmonary vessels and alveolar septa, as well as lymphoid follicles. Increased numbers of muscularized intrapulmonary vessels were apparent at 3 months. After 6 months of exposure, the airway wall thickened and the alveolar space size increased. Collagen deposition was also apparent in airway walls and alveolar septa after 6 months' exposure. The magnitude of airway wall-thickening correlated with the number of infiltrating inflammatory cells, and the extension of collagen deposition correlated with alveolar space size. We conclude that in the guinea pig, 6 months of CS exposure induces inflammatory cell infiltrate in lung structures, at an intensity that correlates with airway remodelling. These changes resemble those observed in COPD, thus endorsing the pathogenic role of CS and the usefulness of this animal model for its study.

Introduction

Chronic obstructive pulmonary disease (COPD) is characterized by progressive and not fully reversible airflow limitation, usually associated with a chronic inflammatory process in the airways and lung parenchyma in response to noxious particles or gases, in particular cigarette smoking (1,2).

The pathogenesis of COPD involves the recruitment of neutrophils, macrophages, and lymphocytes to the lung, as well as the induction of oxidative stress, all of which result in lung parenchymal destruction and airway remodelling (3–7). Full understanding of the role of inflammatory cells in COPD is difficult because this disease involves a mixture of processes (airways disease, emphysema and vascular abnormalities) with different patterns of inflammation and different pathologies.

Keywords: Cigarette smoke, Animal models, Lung inflammation, Chronic obstructive pulmonary disease.

The authors thank Montserrat Cerrillo and Ingrid Victoria for their technical assistance.

Correspondence to: Joan A. Barberà, Servei de Pneumologia, Hospital Clínic, Villarroel 170, 08036, Barcelona, Spain. phone: +34-932275540, fax: +34-932275455. email: jbarbera@clinic.ub.es

Over the last 10 years in vivo models of lung inflammation and lung damage induced by cigarette smoke (CS) have been used to investigate mechanisms related to COPD. Their greatest advantage over other experimental models is the ability to use the primary disease-causing agent to model several key features of the disease in small animals. CS-exposure animal models therefore provide the strongest evidence for a causal link between inflammation and the structural changes associated with COPD.

The guinea pig develops, more closely than other animal models (8), morphological and physiological alterations after exposure to CS that resemble those seen in COPD. The nature and characteristics of inflammatory cell infiltrate and its eventual relationship with structural changes occurring in the lung have not been fully characterized.

The present study aimed to investigate the nature and characteristics of the inflammatory cell infiltrate in the lungs of guinea pigs after two periods of CS exposure, and to assess its relationship with structural abnormalities in the airways, lung parenchyma and pulmonary vessels.

Methods

Additional information on methods is provided in the supplementary material.

Animals and experimental model

Thirty-seven male Hartley guinea pigs (~300 g) were randomly divided into four groups. Nineteen guinea pigs were exposed to the smoke of 7 non-filtered research cigarettes (1R3F; Kentucky University Research; Lexington, KY, USA) per day, 5 days a week, using a nose-only system (9) (Protowerx Design Inc; Langley, British Columbia, Canada). One group (n = 6) was exposed to CS for 3 months and the other group (n = 13) for 6 months. The other two groups were 18 control animals, sham-exposed to CS by placing them for the same length of time in the nose-only system over the same periods of time (n = 10 for 3 months and n = 8 for 6 months) without lighting the cigarettes. At the end of the 3- or 6-month period, the animals were sacrificed under anesthesia 24 h after the end of the experiments. The ethical review board for animal research of the University of Barcelona approved all the experimental protocols and the experiments were performed following institutional guidelines that comply with national and international laws and policies.

Lung tissue preparation

The lungs were removed and inflated intratracheally with 4% formaldehyde for 24 h under a constant pressure of 25 cm H_2O. The lung tissue blocks were embedded in paraffin.

Characterization of inflammatory cells

The assessment of inflammatory cell infiltrate was performed on 5 μm serial sections stained with H&E to identify neutrophils and lymphoid follicles. The presence of eosinophils and macrophages was quantified on sections stained with Congo red and PAS, respectively (10;11).

The number of neutrophils, eosinophils and macrophages infiltrating the adventitia was counted in 10 airways (median of internal luminal perimeter (Pil), 971 μm) and in 10 pulmonary arteries (median of internal elastic lamina perimeter (Pim), 324 μm) per animal. Inflammatory cells in alveolar septa were counted in 20 fields, randomly selected at a magnification of x640. The results were expressed as the number of cells per alveolar septal area. The lung tissue sections were examined for the presence or absence of lymphoid follicles. The rate of guinea pigs with lymphoid follicles was calculated.

Morphometric measurements

Serial sections 5 μm thick were immunostained with a mouse monoclonal antibody against human smooth muscle α-actin (M0851; DakoCytomation, Glostrup, Denmark). Sites of primary antibody were revealed with an ABC system kit (PK-6102 kit; Vector Laboratories, Burlingame (CA), US) and DAB+chromogen solution as substrate (DakoCytomation).

Ten non-cartilaginous airways per animal were randomly selected and photographed using a bright field microscope (Leica Microsystems Imaging Solutions Ltd, Cambridge, UK) coupled to a digital camera (Leica). Images were processed using analysis software (Image-Pro Plus, Media Cybernetics, Carlsbad, Calif). For each airway, the outer and inner aspects of the muscular layer (12) and the internal luminal perimeter (Pil) were outlined and the occupied areas were calculated. The thickness of the smooth muscle layer in airways was estimated as the difference in the delimited areas of the outer and inner aspects of the muscular layer normalized by the Pil. Similarly, the perimeter of adventitia was outlined and the area was computed. Pil was used as the internal reference measure (13) to normalize all the airway dimensions. Pulmonary vessels with an external diameter <50 μm were analyzed in lung sections stained with orcein. Vessels with double elastic laminas were counted and expressed as the number per sq. mm of tissue.

Lung sections were assessed by immunohistochemistry with anti-α-actin and anti-desmin antibodies (Dako, Glostrup, Denmark). The immunoreactions to both antibodies were quantified as the number of positive vessels per sq. mm of tissue. The presence of emphysema was evaluated by measuring the mean linear intercept of alveolar septa in 20 randomly selected fields per slice using an image analysis system (Leica Qwin) in H&E-stained lung sections.

Assessment of fibrosis

Total collagen in lung structures was evaluated in paraffin-embedded sections stained with Sirius red. An average of 11 airways and 16 fields of alveolar septa per animal were randomly captured.

The percentage of alveolar septa occupied by collagen fibres and the area of muscular layer in airways occupied by collagen were determined under bright field microscopy. Thick and thin collagen fibres were identified by brightening to orange-red and green, respectively, under polarized light microscopy (14). The areas for each type of fibre were evaluated by an image analysis system (Image-Pro Plus). Areas of fibrosis in the airways were normalized by Pil.

Data analysis

Results of normally distributed variables are shown as mean±standard deviation (SD) in tables and as mean±standard error of the mean (SEM) in figures. Results of non-normally distributed variables are expressed as median and interquartile range (IQR). Results in figures are showed as mean ± SEM.

Comparisons between groups were carried out by using a two-way analysis of variance (ANOVA), considering exposure and time as main factors. When significant, *post-hoc* pairwise comparisons were performed using the unpaired *t*-test or Mann-Whitney rank sum test to identify the source of variation, for normally and non-normally distributed data, respectively.

To investigate whether cell counts may differ according to the size of the airways or pulmonary vessels (15), specific assessments were carried out in airways and vessels with Pil and Pim values, above (larger) or below (smaller) the median value. The occurrence of lymphoid follicles was determined by Fisher exact test, constructing a contingency table for each period of time. Relationships between variables were assessed using the Pearson's correlation test. A p-value lower than 0.05 was considered significant.

Results

Nineteen of the 24 CS-exposed animals and all the 18 non-exposed animals completed the exposure period and were used for the morphological analysis. The cause of death was attributed to severe bronchoconstriction during CS exposure. Animals showed normal behaviour and activity during the experimental procedures and they did not reveal any signs of respiratory infection or major abnormalities in the lungs after sacrifice.

Inflammatory cells

Compared with non-exposed animals, the number of neutrophils increased in airways and vessels after 6 months of CS exposure (Figure 1 and Table 1). This response was observed irrespective of the size of the airways or pulmonary vessels (Table 1). After 3 months of exposure, the number of neutrophils was already

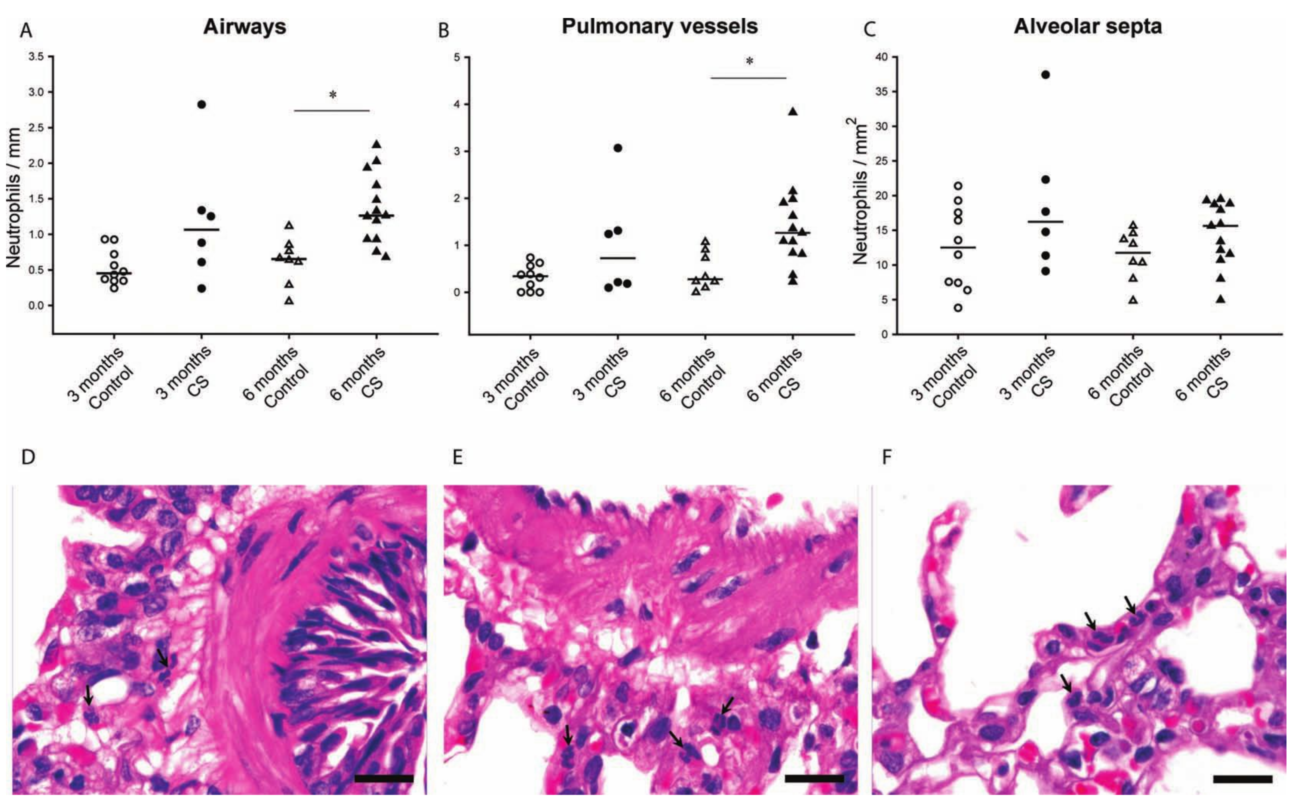

Figure 1. Neutrophilic infiltration in the lung of guinea pigs. Individual counts for neutrophils in the airways (A), pulmonary vessels (B) and alveolar septa (C) of controls and CS-exposed animals. Results are expressed as number of cells normalized by Pil in airways, Pim in vessels or square millimeter in alveolar septa. Horizontal bars represent median values. * p ≤ 0.05 CS-exposed vs. Control (Mann-Whitney rank sum test). Photomicrographs of an airway (D), a pulmonary vessel (E) and alveolar septa (F) of guinea pigs exposed to CS (H&E stain. Scale bar, 20 mm). Arrows show infiltrating neutrophils.

Table 1. Number of neutrophils, macrophages and eosinophils in lung structures after different periods of cigarette smoke exposure

			3 months		6 months	
			Control (n = 10)	CS-Exposed (n = 6)	Control (n = 8)	CS-Exposed (n = 13)
Neutrophils	Airways (cells/mm)	All airways	0.4 (0.3–0.7)	1.1 (0.6–1.3)	0.6 (0.4–0.8)	1.3 (0.9–1.7)*
		Larger airways	0.7 (0.6–1.2)	1.4 (0.7–1.9)	0.6 (0.4–0.6)	1.3 (1.0–1.5)*
		Smaller airways	0.3 (0.0–0.4)	0.7 (0.2–1.3)	0.7 (0.1–0.8)	1.3 (0.9–2.0)*
	Vessels (cells/mm)	All vessels	0.3 (0.0–0.6)	0.7 (0.2–1.3)	0.3 (0.2–0.8)	1.3 (0.8–1.9)*
		Larger vessels	0.0 (0.0–0.5)	0.8 (0.3–2.1)*	0.5 (0.2–0.6)	0.8 (0.5–2.1)*
		Smaller vessels	0.0 (0.0–0.4)	0 .4 (0.0–1.4)	0.0 (0.0–0.4)	1.5 (0.8–18)*
	Alveolar septa (cells/mm^2)		12.5 (7.4–17.5)	16.2 (11.3–22.3)	11.7 (9.2–14.1)	15.6 (11.4–18.8)
Macrophages	Airways (cells/mm)	All airways	0.2 (0.1–0.3)	0.2 (0.2–0.5)	0.1 (0.0–0.4)	0.4 (0.3–0.6)*
		Larger airways	0.1 (0.0–0.3)	0.2 (0.1–0.3)	0.2 (0.0–0.3)	0.4 (0.3–0.5)
		Smaller airways	0.0 (0.0–0.4)	0.3 (0.0–0.6)	0.0 (0.0–0.4)	0.6 (0.1–0.9)
	Vessels (cells/mm)	All vessels	0.1 (0.0–0.4)	0.3 (0.3–1.2)	0.0 (0.0–0.0)	1.0 (0.53–1.6)*
		Larger vessels	0.2 (0.0–0.6)	0.5 (0.0–0.7)	0.0 (0.0–0.0)	0.6 (0.0–1.4)*
		Smaller vessels	0.0 (0.0–0.0)	0.7 (0.0–2.9)*	0.0 (0.0–0.0)	1.2 (0.8–1.6)*
	Alveolar septa (cells/mm^2)		1.1 (0.0–2.6)	5.3 (2.6–6.5)*	0.0 (0.0–0.6)	6.6 (2.7–10.3)*
Eosinophils	Airways (cells/mm)	All airways	3.0 (1.7–3.3)	4.5 (3.2–4.8)*	1.5 (0.8–2.4)	5.0 (4.1–6.3)*
		Larger airways	3.7 (2.9–4.7)	4.3 (3.1–9.2)	1.9 (1.1–3.5)	5.1 (4.1–7.0)*
		Smaller airways	2.1 (1.0–3.1)	3.4 (1.3–5.8)	1.1 (0.2–1.7)	4.2 (3.6–6.0)*
	Vessels (cells/mm)	All vessels	0.5 (0.2–1.0)	1.6 (1.2–3.0)*	0.6 (0.2–0.8)	1.6 (0.9–2.8)*
		Larger vessels	0.4 (0.3–0.8)	1.8 (0.6–3.6)*	0.3 (0.1–0.8)	0.7 (0.2–1.2)
		Smaller vessels	0.7 (0.0–1.2)	2.2 (1.4–3.1)	0.0 (0.0–1.0)	2.0 (1.0–3.4)*
	Alveolar septa (cells/mm^2)		4.3 (1.8–8.8)	10.2 (8.7–16.4)	0.5 (0.0–1.9)	7.1 (5.6–7.6)*

Values are median and IQR.
* $p \leq 0.05$ CS-exposed vs. Control (Mann-Whitney rank sum test).

increased, suggesting a progression of the inflammatory process with prolonged CS exposure.

CS-exposed animals showed an increased number of macrophages infiltrating alveolar septa, after both 3 and 6 months. The number of macrophages also increased in the adventitia of both pulmonary vessels and airways after 6 months of exposure (Figure 2 and Table 1).

The number of eosinophils increased in airways and vessels, after both 3 and 6 months of exposure to CS. The number of eosinophils also increased in alveolar septa after 6 months. Eosinophilic infiltrate was greater in the airways than in the vessels. We did not observe any differences between larger and smaller airways (Figure 3 and Table 1).

Lymphoid follicles were identified close to the airways and vessels in CS-exposed animals after 6 months of exposure (Figure 4). Whereas 46% of CS-exposed animals showed follicles after 6 months of exposure, they were practically absent in sham-exposed animals ($p < 0.05$, Fisher exact test).

Morphometric assessments of airways

The morphometric measurements in airways from control and CS-exposed groups are shown in Table 2 and Figure 5. Airways were classified into larger and smaller airways according to whether they fell above or below the median value of Pil.

Compared with the control group, the airway wall was thicker in the CS-exposed group after 6 months of exposure. This enlargement was apparent for both larger and smaller airways, although after 6 months of exposure the differences were more pronounced in smaller airways. It is worth noting that there was an enlargement of airway wall thickness with time, which was essentially due to the enlargement of the mucosa+submucosa, probably as a result of the maturation of lung structures during growth.

Adventitia. A significant thickening of the adventitia was observed after 6 months of CS-exposure; this was more prominent in the smaller airways.
Muscularis. A significant thickening was shown after 6 months of CS exposure, particularly in smaller airways; this was due to the increase in smooth muscle content, as shown by α-smooth muscle actin immunoreactivity.
Mucosa+submucosa. Significant enlargement of the inner wall, comprising the epithelium and the submucosa, was observed in CS-exposed animals as

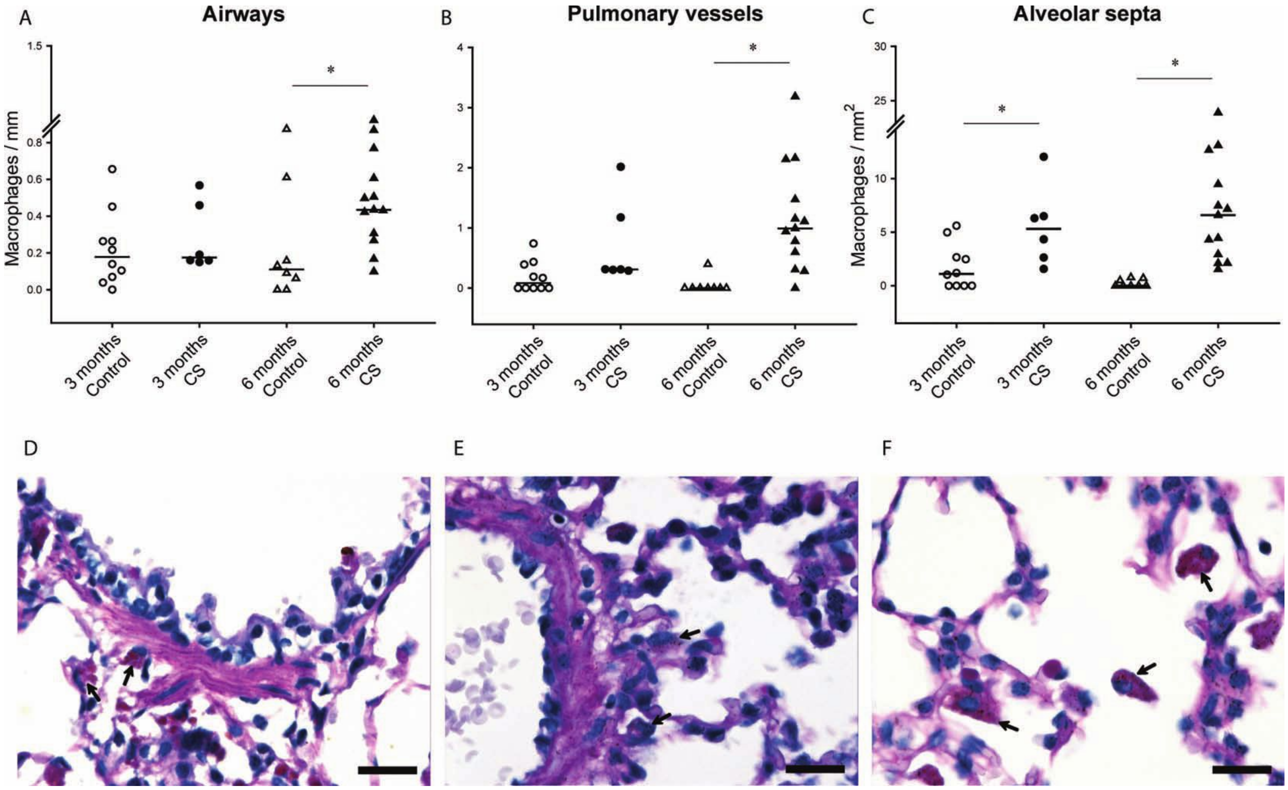

Figure 2. Macrophage infiltration in the lungs of guinea pigs. Individual count for macrophages in the airways (A), pulmonary vessels (B) and alveolar septa (C) of controls and CS-exposed animals. Results are expressed as number of cells normalized by Pil in airways, Pim in vessels or square millimeter in alveolar septa. Horizontal bars represent median values. * $p \leq 0.05$ CS-exposed vs. Control (Mann-Whitney rank sum test). Photomicrographs of an airway (D), a pulmonary vessel (E) and alveolar septa (F) of guinea pigs exposed to CS (PAS stain. Scale bar, 20 mm). Arrows show infiltrating macrophages.

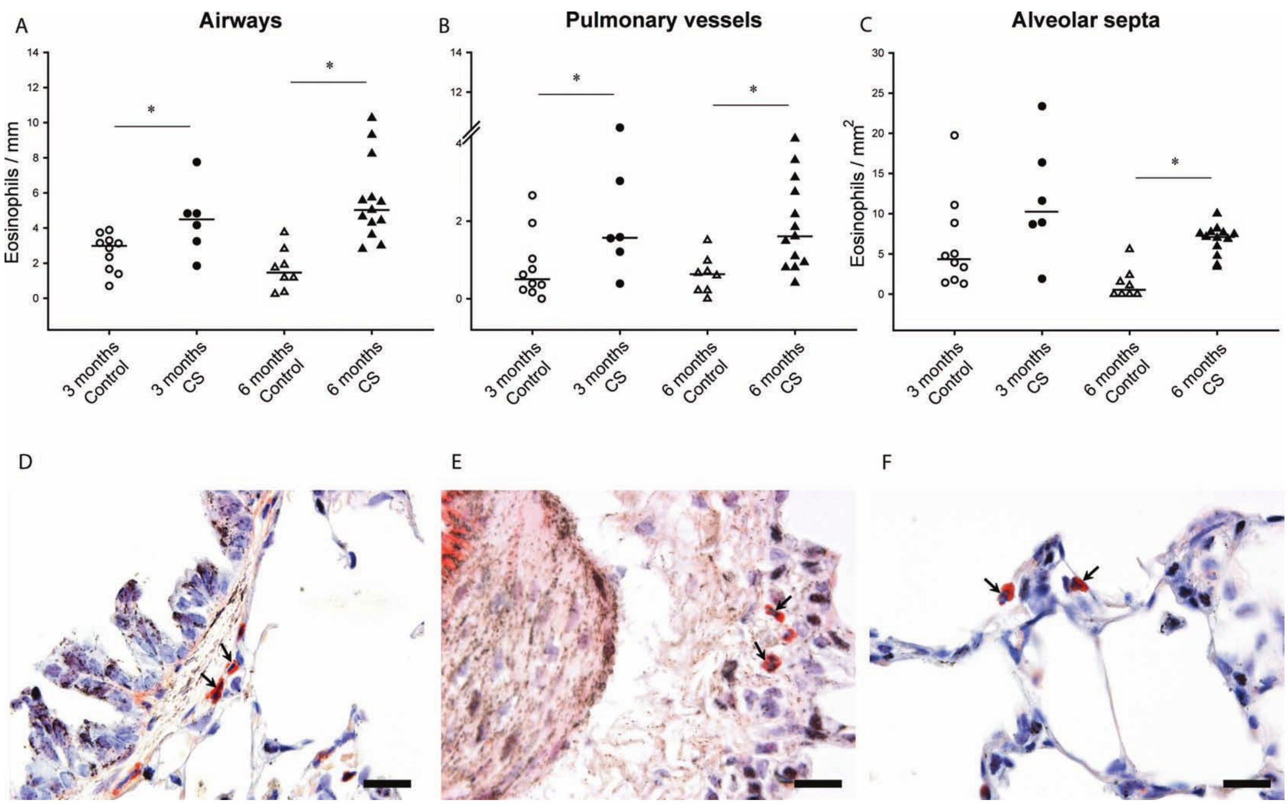

Figure 3. Eosinophil infiltration in the lungs of guinea pigs. Individual count for eosinophils in the airways (A), pulmonary vessels (B) and alveolar septa (C) of controls and CS-exposed animals. Results are expressed as number of cells normalized by Pil in airways, Pim in vessels or square millimeter in alveolar septa. Horizontal bars represent median values. * $p \leq 0.05$ CS-exposed vs. Control (Mann-Whitney rank sum test). Photomicrographs of an airway (D), a pulmonary vessel (E) and alveolar septa (F) of guinea pigs exposed to CS (Congo red stain. Scale bar, 20 mm). Arrows show infiltrating eosinophils.

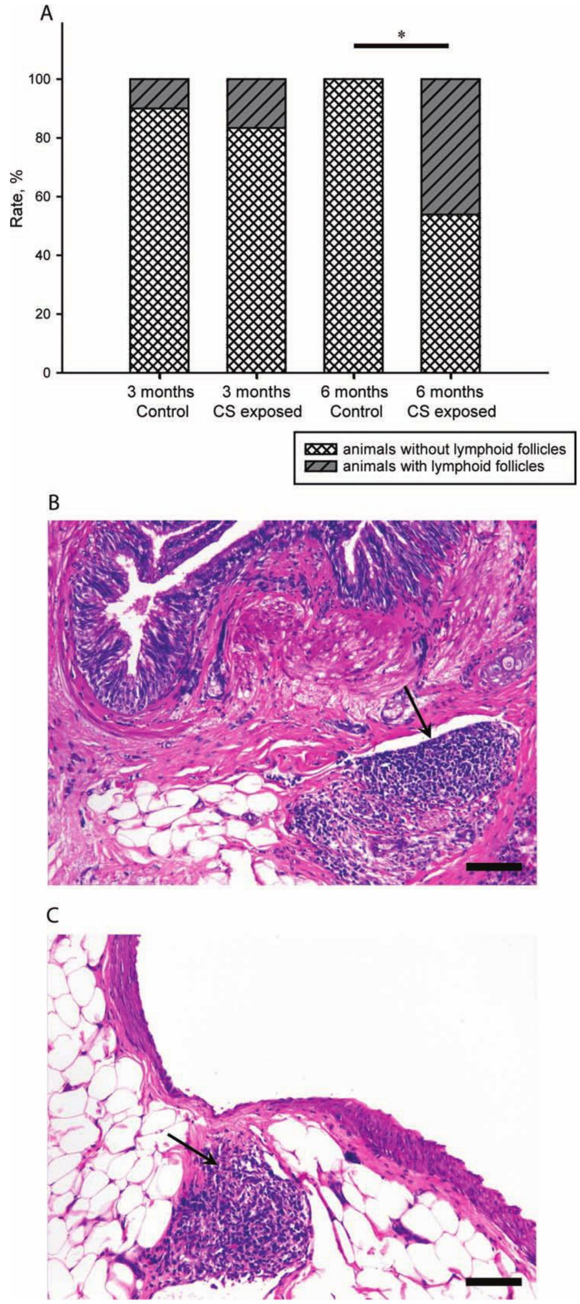

Figure 4. Pulmonary lymphoid follicles. Percentage of individuals with presence or absence of lymphoid follicles in lung tissue of control and CS-exposed groups (A).* $p < 0.05$ (Fisher exact test). Photomicrographs of lymphoid follicle (arrows) in peribronchial (B) and perivascular (C) lung tissue of CS-exposed guinea pigs at 6 months (H&E stain. Scale bar, 100 mm).

compared with controls, after both 3 and 6 months. There were no differences between the larger and smaller airways.

Emphysema. There was an increase in the mean distance between the alveolar septa in animals exposed to CS for 6 months (control vs. exposed: 64 ± 6 vs. 73 ± 5 μm, p = 0.001).

Morphological evaluation of pulmonary vessels

The morphometric measurements of intrapulmonary vessels are shown in Table 3. There was a trend towards a greater proportion of intrapulmonary vessels with double elastic laminas in animals exposed to CS during 6 months. The number of vessels with positive immunoreactivity to α-smooth muscle actin was higher in animals exposed to CS, after both 3 and 6 months. No differences were observed in the proportion of vessels with positive immunoreactivity to desmin (Table 3).

Fibrosis

Collagen deposition was evaluated under both bright field and polarized light microscopy in both the alveolar septa and the muscular layer of airways. The results for total collagen and both thick- and thin-fibre collagen are shown in Table 4 and Figure 6.

There was an increase in the proportion of collagen deposition in both the septa and the airways in animals exposed to CS for 6 months. The increase in collagen was more pronounced in smaller airways than in larger airways.

We analyzed the extension of thick- and thin-fibre collagen under polarized light. There was a greater deposition of thick-fibre collagen after 6 months of CS exposure in both the alveolar septa and the muscular layer of airways.

Correlations

The number of peribronchial neutrophils correlated with the thickness of the airway wall and its different layers, particularly in smaller airways (Figure 7 and Supplementary Table 1), and also with the alveolar size (r = 0.43, p = 0.01). The number of macrophages infiltrating the airways correlated with the wall thickness of smaller airways (Figure 7 and Supplementary Table 2) and the alveolar size (r = 0.37, p = 0.03). The macrophages in alveolar septa also correlated with the alveolar size (r = 0.45, p = 0.06). Moreover, the deposition of total (Figure 8) and thick-fibre collagen (r = 0.42, p = 0.01) in alveolar septa correlated positively with the degree of emphysema.

The number of peribronchial eosinophils correlated weakly with the thickness of the airway wall and its different layers (Supplementary Table 3). Only perivascular eosinophils correlated weakly with the number of α-actin-positive intrapulmonary vessels (r = 0.36, p = 0.03; Supplementary Figure 1).

Discussion

The present study shows that guinea pigs chronically exposed to CS develop an inflammatory reaction in all their pulmonary structures, clearly apparent after 6 months of exposure, as well as morphological changes in those structures. The changes in airway structure were pronounced, especially in smaller airways, and correlated with the number of infiltrating neutrophils and macrophages. Animals exposed to CS also developed a muscularization of small pulmonary vessels that was unrelated to the neutrophilic or macrophagic

Table 2. Morphological characteristics of airways

		3 months		6 months		ANOVA		
		Control (n = 10)	CS-Exposed (n = 6)	Control (n = 8)	CS-Exposed (n = 13)	CS Exposure	Time of Exposure	Interaction
Extended-airways radius (µm)		174 ± 32	193 ± 39	205 ± 37	228 ± 33	0.093	0.010	0.844
Total Wall Thickness (µm)	All airways	37.1 ± 4.5	45.2 ± 11.4	46.7 ± 6.6	66.9 ± 12.3*	≤0.001	≤0.001	0.072
	Larger airways	46.0 ± 6.7	57.2 ± 14.7	58.7 ± 7.4	75.9 ± 17.8*	0.005	0.002	0.533
	Smaller airways	28.5 ± 4.3	35.8 ± 14.3	33.8 ± 5.3	56.0 ± 6.5*	<0.001	<0.001	0.008
Thickness of Adventitia (µm)	All airways	11.1 ± 2.9	13.1 ± 5.7	11.9 ± 5.3	21.2 ± 6.4*	0.004	0.020	0.052
	Larger airways	13.4 ± 6.4	16.6 ± 6.0	14.9 ± 9.2	20.2 ± 6.7	0.091	0.301	0.656
	Smaller airways	10.2 ± 3.7	10.3 ± 9.6	7.7 ± 4.5	22.3 ± 7.0*	0.002	0.036	0.002
Thickness of Mucosa+submucosa (µm)	All airways	12.8 ± 1.9	15.7 ± 3.3*	19.9 ± 2.5	25.4 ± 4.8*	0.002	≤0.001	0.274
	Larger airways	16.2 ± 2.3	18.4 ± 4.4	22.8 ± 2.9	29.7 ± 7.6	0.019	≤0.001	0.200
	Smaller airways	10.8 ± 2.1	12.8 ± 2.1	16.6 ± 3.7	20.6 ± 4.7	0.020	≤0.001	0.422
Thickness of Muscularis (µm)	All airways	13.2 ± 2.0	16.5 ± 6.7	15.0 ± 2.6	20.3 ± 5.7*	0.011	0.086	0.538
	Larger airways	19.3 ± 3.1	21.9 ± 8.5	19.1 ± 3.7	24.9 ± 9.5	0.102	0.579	0.521
	Smaller airways	9.1 ± 1.5	10.8 ± 2.5	10.0 ± 1.8	14.2 ± 4.2*	0.007	0.040	0.215
Smooth Muscle Content (µm)	All airways	11.7 ± 2.5	14.6 ± 7.5	11.7 ± 2.6	16.4 ± 5.0*	0.022	0.564	0.578
	Larger airways	18.0 ± 3.5	20.3 ± 9.1	15.7 ± 4.1	20.1 ± 8.3	0.160	0.605	0.647
	Smaller airways	7.7 ± 1.7	8.6 ± 2.2	7.2 ± 1.5	10.7 ± 3.9*	0.023	0.432	0.165

Values are mean ± SD.
* p ≤ 0.05 CS-exposed vs. Control (*t*-test).

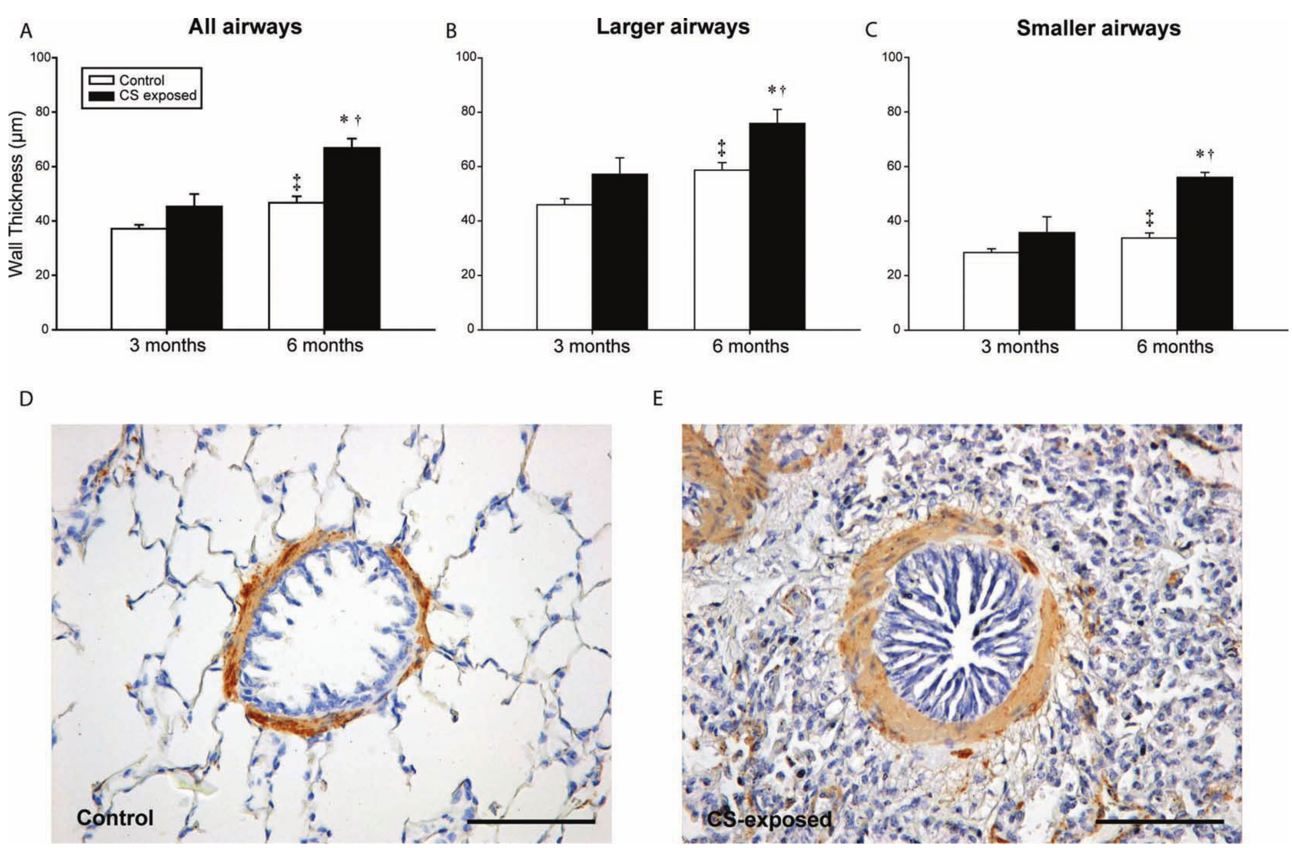

Figure 5. Morphometry of airways. Bar graphs show mean ± SEM of airway wall thickness, in all (A), larger (B) and smaller (C) airways in both control and CS-exposed guinea pigs, for 3 and 6 months of exposure. Immunohistochemistry for SMC a-actin in airways of a control (D) and a CS-exposed (E) animal. Scale bar, 100 mm. * p ≤ 0.05 CS-exposed vs. Control, ‡ p£0.05 6 months Control vs. 3 months Control and † p ≤ 0.05 6 months CS-exposed vs. 3 months CS-exposed (t-test).

Table 3. Morphological characteristics of vessels

	3 months		6 months		ANOVA		
	Control (n = 10)	CS-Exposed (n = 6)	Control (n = 8)	CS-Exposed (n = 13)	CS Exposure	Time of Exposure	Interaction
Vessels with double elastic lamina (per mm^2)	0.3 ± 0.4	0.4 ± 0.6	0.3 ± 0.4	0.6 ± 0.5	0.199	0.403	0.574
Vessels α-actin+ (per mm^2)	2.4 ± 0.9	4.8 ± 2.0*	2.7 ± 1.0	4.0 ± 1.2*	<0.001	0.550	0.195
Vessels desmin+ (per mm^2)	1.9 ± 0.9	3.0 ± 2.6	1.3 ± 1.3	1.7 ± 1.4	0.194	0.069	0.534

Values are mean ± SD.
* $p \leq 0.05$ CS-exposed vs. Control (*t*-test).

infiltrate. In addition to thickening of airway walls, animals exposed to CS presented deposition of collagen in alveolar septa, which ran in parallel with the severity of the inflammatory process. After 6 months of exposure, emphysema was apparent, and this was associated with collagen deposition and an increased number of macrophages and neutrophils infiltrating the bronchial wall, and of macrophages in alveolar septa.

To our knowledge, this is the first longitudinal study evaluating the characteristics of the inflammatory cell burden in the various lung tissue structures of guinea pigs exposed to CS. Our data reveal that animals exposed to CS mimic some of the inflammatory characteristics shown in smokers, supporting the validity of this species as an experimental model of COPD.

Neutrophils

The results of the present study show that in control animals, neutrophils were preferentially located in the alveolar septa, whereas the number of infiltrating neutrophils in the airways was low. The number of neutrophils in the airways of CS-exposed animals increased progressively over time and was clearly apparent after 6 months of exposure. A consistent infiltrate was also found around pulmonary vessels, indicating that the inflammatory reaction affects these lung structures and can be detected after 3 months of exposure, while becoming clearly apparent after 6 months. These findings are consistent with studies in humans showing a non-uniform distribution of inflammatory cells in both smokers with and without COPD, and a correlation between neutrophil numbers and pack-years of smoking (16). The accumulation of neutrophils is considered one of the key events in the pathogenesis of lung injury in smokers, particularly in the development of pulmonary emphysema (17), because these cells can induce protease-antiprotease and/or oxidant-antioxidant imbalance(s).

In this respect, it is important to note that neutrophilic inflammatory reaction correlated with the thickness of the airway wall and its different layers, particularly in smaller airways, and with interseptal distance,

Table 4. Collagen deposition in airways

		3 months		6 months	
		Control (n = 10)	CS-Exposed (n = 6)	Control (n = 8)	CS-Exposed (n = 13)
Total Collagen (μm)	All airways	1.06 (0.70–2.30)	2.51 (0.96–3.47)	0.85 (0.36–1.49)	2.25 (1.38–3.19)*
	Larger airways	1.79 (0.69–3.00)	2.46 (1.52–4.61)	1.33 (0.54–2.67)	2.50 (1.69–3.48)
	Smaller airways	1.07 (0.36–1.79)	1.18 (0.57–3.21)	0.48 (0.18–0.98)	1.87 (0.85–2.64)*
Thick Collagen (μm)	All airways	0.10 (0.09–0.16)	0.25 (0.14–1.10)	0.17 (0.01–0.53)	0.28 (0.20–0.66)
	Larger airways	0.26 (0.16–0.59)	0.40 (0.21–1.61)	0.33 (0.02–1.26)	0.39 (0.24–0.73)
	Smaller airways	0.06 (0.01–0.12)	0.09 (0.04–0.50)	0.01 (0–0.09)	0.16 (0.09–0.26)*
Thin Collagen (μm)	All airways	0.26 (0.12–0.34)	0.09 (0.04–0.54)	0.13 (0.08–0.19)	0.12 (0.08–0.21)
	Larger airways	0.31 (0.18–0.46)	0.12 (0.05–0.64)	0.17 (0.11–0.25)	0.14 (0.08–0.19)
	Smaller airways	0.19 (0.07–0.30)	0.06 (0.02–0.39)	0.10 (0.06–0.13)	0.09 (0.05–0.30)

Values are median and IQR.
* $p \leq 0.05$ CS-exposed vs. Control (Mann-Whitney rank sum test).

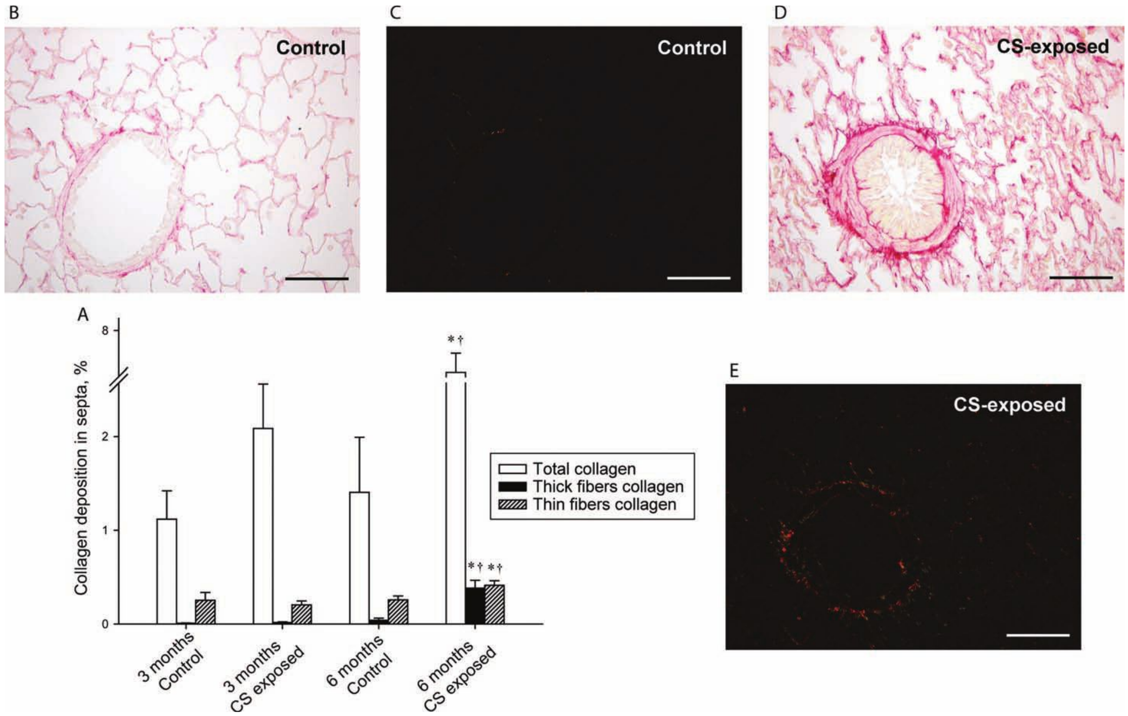

Figure 6. Collagen deposition in the lungs. Bar graphs show mean ± SEM of the percentage of area occupied by total collagen and thick and thin collagen fibres in the alveolar septa of control and CS-exposed guinea pigs (A). Photomicrographs of lung sections stained with Sirius red. Total collagen fibers were seen in red under bright field (B and D) and orange to red (thick collagen fibres) or green (thin collagen fibres) under polarized light (C and E). Scale bars, 100 mm. * $p \leq 0.05$ CS-exposed vs. Control and † $p \leq 0.05$ 6 months CS-exposed vs. 3 months CS-exposed (Mann-Whitney rank sum test).

suggesting that neutrophils may participate in airway remodelling and emphysema. Interestingly, Churg et al. (18) demonstrated that the administration of metalloproteinase inhibitors can ameliorate morphological emphysema and enhance small-airway remodelling, thereby strengthening the role of neutrophil proteases in this condition. They did not, however, evaluate the inflammatory infiltrate to test the origin of metalloproteinases. The present study extends these previous results and identifies neutrophils as a key component in airway remodelling and emphysema.

Macrophages

An increased number of macrophages in the bronchial tree of subjects with COPD (19) has been related to emphysema, suggesting they can also induce an elastolytic inflammatory response in airways exposed to CS (20). In animals exposed to CS, we observed a greater increase in the number of macrophages in the alveolar septa compared with the airway adventitia. Moreover, there was a positive relationship between the alveolar size and the number of macrophages in the bronchial tree and alveolar septa, thereby providing evidence of their theoretical potential in this condition. Macrophages appear to play a pivotal role in the pathophysiology of COPD and can account for most of the known features of the disease (21).

In humans, macrophages are located at sites of alveolar wall destruction and their numbers in the airways also correlate with the severity of COPD (22). Studies of emphysematous lung tissue from human subjects have shown a direct relationship between alveolar macrophage density in the parenchyma and severity of lung destruction (23). Our findings, and the distribution pattern of macrophages in CS-exposed animals, are similar to observations made in humans, emphasizing the critical role of CS in these cells.

Eosinophils

Apart from neutrophils and macrophages, there is evidence that eosinophils may also play a role in COPD and that patients with eosinophilic inflammation may represent a distinct phenotype of the disease. Although eosinophilic airway inflammation is usually considered a feature of asthma, its presence in large- and small-airway tissue samples and in 20%–40% of induced sputum samples has been demonstrated in patients with stable COPD. Airway eosinophilia increases during COPD exacerbations (24–26).

In guinea pigs, eosinophils were the predominant cells and were homogenously distributed in airways, pulmonary vessels and septa, and they correlated weakly with morphological changes in smaller airways and small intrapulmonary vessels. We do not rule out the possibility that the eosinophilic reaction elicited by CS exposure may be a specific feature of the guinea pig, along with its enhanced bronchial hyperresponsiveness, but the presence of eosinophilic bronchitis in

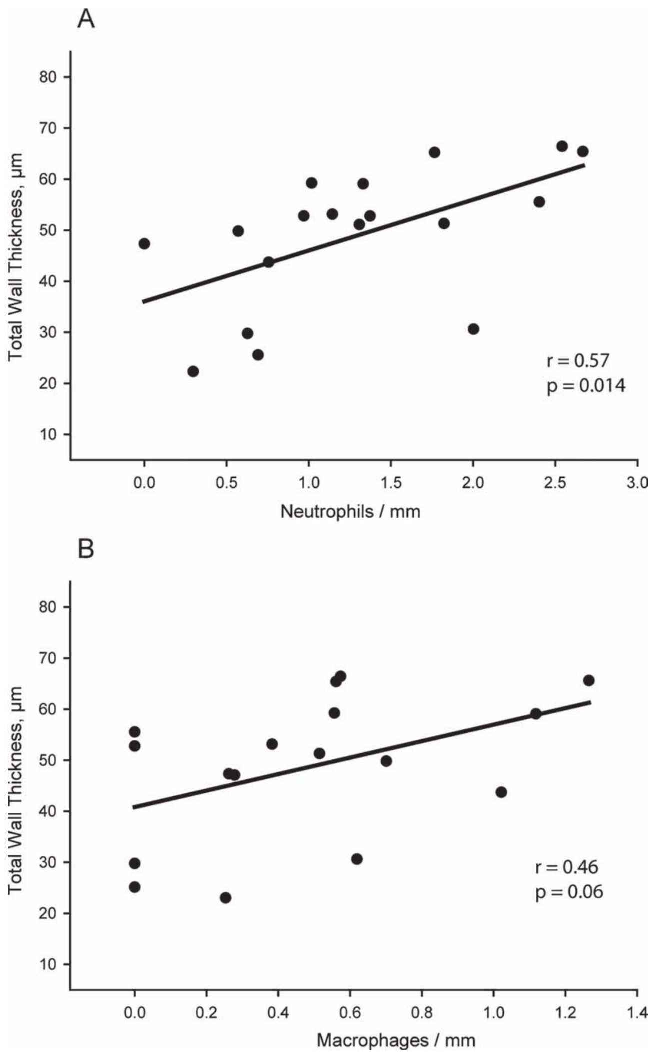

Figure 7. Correlations between inflammatory infiltrate and remodelling. Linear regression of neutrophils (A) and macrophages (B) with the thickness of total wall in smaller airways. Solid circles are CS-exposed animals independently of time of exposure.

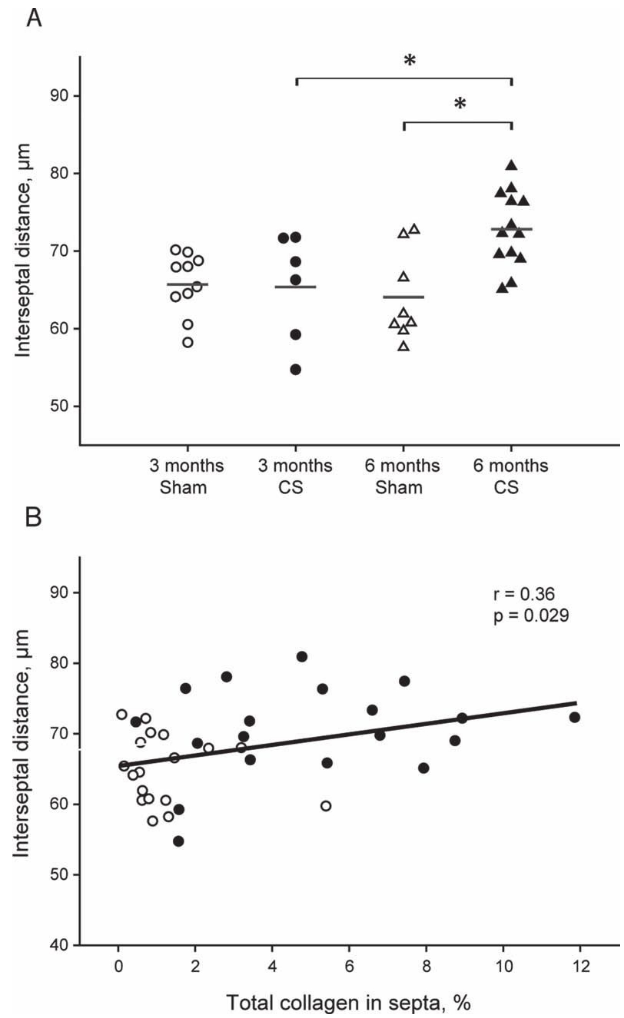

Figure 8. Emphysema in the lungs and correlation with fibrosis. Dot plot showing individual interseptal distance in each experimental group and mean (horizontal bars) (A). *p ≤ 0.05 (t-test). Linear regression of total collagen in septa with the mean linear intercept of alveolar septa (B). Solid circles are CS-exposed animals and open circles are sham-exposed animals independently of time of exposure.

smokers who are not asthmatics suggests a potential role of CS in the recruitment of eosinophils in lung structures (27).

Lymphocytes

Inflammation mediated by lymphocytes in the lung is considered a key component of COPD (28;29). These inflammatory cells, which persist long after ceasing to smoke (30), are diffusely distributed and might play an important role in the onset and maintenance of a chronic inflammatory response throughout the lung. In addition, T and B cells aggregate into organized lymphoid follicles in close proximity to the airways and within the lung parenchyma (3;6). It has been reported that the number of airways containing lymphoid follicles is increased in severe COPD (GOLD stages 3 and 4) when compared with patients in stages GOLD 0 to 2 (6). We evaluated the presence of lymphoid follicles in the lungs of guinea pigs. In our study, there was an increased proportion of lungs with lymphoid follicles in animals exposed for 6 months to CS. Moreover, there was a trend towards a positive correlation between follicle size and the wall thickness of smaller airways.

Lung fibrosis

Recent studies have demonstrated areas of lung fibrosis in some smokers. Furthermore, the association of emphysema with fibrosis has been recognized as a specific entity, with a poor outcome (31–33). In guinea pigs exposed to CS, we observed collagen deposition in airways and alveolar septa. Moreover, some degree of fibrosis has been observed in the airways of smokers (6;12;34). The mechanisms of fibrosis around the airways are not yet understood, but they probably involve an attempt to repair chronic inflammation. Our results concur with those of Wright et al. (14), who showed increased amounts of thick collagen fibres in the small-airway walls in a model of guinea pig exposed to CS. We also observed marked fibrosis in alveolar septa, fitting with an increase in emphysema. These septal areas could be more susceptible to damage and repair overlapping emphysematous lesions (33). Interestingly, we observed airway inflammation preceded by airway remodelling, supporting the role of inflammation in lung remodelling (4,35,36). We observed an increase in thick collagen fibres, especially in smaller airways, in contrast to thin fibres. Thick collagen fibres have been associated with scarring and could modulate the stiffness of tissues (37).

The study has some limitations. Inflammatory cells were identified by a combination of histochemical staining and standard morphological criteria. Immunostaining with monoclonal antibodies would have provided more specific identification of inflammatory cells. Unfortunately, most of the commercially available antibodies are not sensitive or specific enough for immunohistochemical characterization in the guinea pig. We conducted preliminary immunohistochemical analyses with several commercially available antibodies but they lacked the specificity, selectivity and reproducibility required by our experimental conditions. Accordingly, we used standard histochemical and morphological criteria to distinguish the inflammatory cell populations.

Conclusions

In summary, our study has fully characterized a pleiotropic inflammatory reaction induced by chronic CS exposure in the airways, pulmonary vessels and alveolar septa of the guinea-pig lung. The inflammatory reaction was composed of neutrophils, macrophages and eosinophils and persisted over time, especially in smaller airways and vessels. The intensity of the neutrophilic and macrophagic infiltrate correlates with smaller airway remodelling and emphysema, emphasizing the crucial role of these cells in morphological changes associated with COPD. The remodelling of small pulmonary vessels was not associated with neutrophil and macrophage infiltration but slightly correlated with that of eosinophils.

In animals exposed to CS, areas of collagen deposition were apparent in alveolar septa and smaller airways and were associated with the enlargement of the alveolar size. Therefore, CS-induced inflammatory reaction not only leads to lung damage but also to a repair process. All in all, this indicates that the effects of CS on the guinea pig lungs mimic those observed in patients diagnosed with COPD, further supporting the use of this animal model in studies of the clinical progression of COPD and therapeutic interventions.

Declaration of Interest

The authors report that they have no conflicts of interest. The authors are responsible for the writing of this paper. This manuscript was supported by grants from the Fondo de Investigación Sanitaria (04/1424), the European Commission (2005-018725) and Consorcios Estratégicos Nacionales en Investigación Técnica (CENIT).

References

1. Rivera RM, Cosio MG, Ghezzo H, Salazar M, Perez-Padilla R. Comparison of lung morphology in COPD secondary to cigarette and biomass smoke. Int J Tuberc Lung Dis 2008 Aug;12(8):972–7.
2. Cosio MG, Saetta M, Agusti A. Immunologic aspects of chronic obstructive pulmonary disease. N Engl J Med 2009 Jun 4;360(23):2445–54.
3. van der Strate BW, Postma DS, Brandsma CA, Melgert BN, Luinge MA, Geerlings M, Hylkema MN, van den BA, Timens W, Kerstjens HA. Cigarette smoke-induced emphysema: A role for the B cell? Am J Respir Crit Care Med 2006 Apr 1;173(7):751–8.
4. Turato G, Zuin R, Miniati M, Baraldo S, Rea F, Beghe B, Monti S, Formichi B, Boschetto P, Harari S, et al. Airway inflammation in severe chronic obstructive pulmonary disease: relationship with lung function and radiologic emphysema. Am J Respir Crit Care Med 2002 Jul 1;166(1):105-10.
5. Retamales I, Elliott WM, Meshi B, Coxson HO, Pare PD, Sciurba FC, Rogers RM, Hayashi S, Hogg JC. Amplification of inflammation in emphysema and its association with latent adenoviral infection. Am J Respir Crit Care Med 2001 Aug 1;164(3):469–73.
6. Hogg JC, Chu F, Utokaparch S, Woods R, Elliott WM, Buzatu L, Cherniack RM, Rogers RM, Sciurba FC, Coxson HO, et al. The nature of small-airway obstruction in chronic obstructive pulmonary disease. N Engl J Med 2004 Jun 24;350(26):2645–53.
7. Cosio MG, Majo J, Cosio MG. Inflammation of the airways and lung parenchyma in COPD: role of T cells. Chest 2002 May;121(5 Suppl):160S–5S.
8. Wright JL, Churg A. A model of tobacco smoke-induced airflow obstruction in the guinea pig. Chest 2002 May;121(5 Suppl):188S–91S.
9. Ferrer E, Peinado VI, Diez M, Carrasco JL, Musri MM, Martinez A, Rodriguez-Roisin R, Barbera JA. Effects of cigarette smoke on endothelial function of pulmonary arteries in the guinea pig. Respir Res 2009;10:76.
10. Meyerholz DK, Griffin MA, Castilow EM, Varga SM. Comparison of histochemical methods for murine eosinophil detection in an RSV vaccine-enhanced inflammation model. Toxicol Pathol 2009 Feb;37(2):249–55.
11. White HJ, Garg BD. Early pulmonary response of the rat lung to inhalation of high concentration of diesel particles. J Appl Toxicol 1981 Apr;1(2):104–10.
12. Kuwano K, Bosken CH, Pare PD, Bai TR, Wiggs BR, Hogg JC. Small airways dimensions in asthma and in chronic obstructive pulmonary disease. Am Rev Respir Dis 1993 Nov;148(5):1220–5.
13. James AL, Hogg JC, Dunn LA, Pare PD. The use of the internal perimeter to compare airway size and to calculate smooth muscle shortening. Am Rev Respir Dis 1988 Jul;138(1):136–9.
14. Wright JL, Postma DS, Kerstjens HA, Timens W, Whittaker P, Churg A. Airway remodeling in the smoke exposed guinea pig model. Inhal Toxicol 2007 Sep;19(11):915–23.
15. Hsia CC, Hyde DM, Ochs M, Weibel ER. An official research policy statement of the American Thoracic Society/European Respiratory Society: standards for quantitative assessment of lung structure. Am J Respir Crit Care Med 2010 Feb 15;181(4):394–418.
16. Turato G, Zuin R, Saetta M. Pathogenesis and pathology of COPD. Respiration 2001;68(2):117–28.
17. Janoff A. Elastases and emphysema. Current assessment of the protease-antiprotease hypothesis. Am Rev Respir Dis 1985 Aug;132(2):417–33.
18. Churg A, Wang R, Wang X, Onnervik PO, Thim K, Wright JL. Effect of an MMP-9/MMP-12 inhibitor on smoke-induced emphysema and airway remodelling in guinea pigs. Thorax 2007 Aug;62(8):706–13.
19. Di SA, Turato G, Maestrelli P, Mapp CE, Ruggieri MP, Roggeri A, Boschetto P, Fabbri LM, Saetta M. Airflow limitation in

chronic bronchitis is associated with T-lymphocyte and macrophage infiltration of the bronchial mucosa. Am J Respir Crit Care Med 1996 Feb;153(2):629–32.
20. Churg A, Wang RD, Tai H, Wang X, Xie C, Dai J, Shapiro SD, Wright JL. Macrophage metalloelastase mediates acute cigarette smoke-induced inflammation via tumor necrosis factor-alpha release. Am J Respir Crit Care Med 2003 Apr 15;167(8):1083–9.
21. Shapiro SD. The macrophage in chronic obstructive pulmonary disease. Am J Respir Crit Care Med 1999 Nov;160(5 Pt 2):S29–S32.
22. Di SA, Capelli A, Lusuardi M, Balbo P, Vecchio C, Maestrelli P, Mapp CE, Fabbri LM, Donner CF, Saetta M. Severity of airflow limitation is associated with severity of airway inflammation in smokers. Am J Respir Crit Care Med 1998 Oct;158(4):1277–85.
23. Finkelstein R, Fraser RS, Ghezzo H, Cosio MG. Alveolar inflammation and its relation to emphysema in smokers. Am J Respir Crit Care Med 1995 Nov;152(5 Pt 1):1666–72.
24. Gorska K, Krenke R, Korczynski P, Kosciuch J, Domagala-Kulawik J, Chazan R. Eosinophilic airway inflammation in chronic obstructive pulmonary disease and asthma. J Physiol Pharmacol 2008 Dec;59 Suppl 6:261–70.
25. Saetta M, Di Stefano A, Maestrelli P, Turato G, Ruggieri MP, Roggeri A, Calcagni P, Mapp CE, Ciaccia A, Fabbri LM. Airway eosinophilia in chronic bronchitis during exacerbations. Am J Respir Crit Care Med 1994 Dec;150(6 Pt 1):1646–52.
26. Snoeck-Stroband JB, Lapperre TS, Gosman MM, Boezen HM, Timens W, ten Hacken NH, Sont JK, Sterk PJ, Hiemstra PS. Chronic bronchitis sub-phenotype within COPD: inflammation in sputum and biopsies. Eur.Respir.J. 2008 Jan;31(1):70–7.
27. Papi A, Romagnoli M, Baraldo S, Braccioni F, Guzzinati I, Saetta M, Ciaccia A, Fabbri LM. Partial reversibility of airflow limitation and increased exhaled NO and sputum eosinophilia in chronic obstructive pulmonary disease. Am J Respir Crit Care Med 2000 Nov;162(5):1773–7.
28. Saetta M, Di Stefano A, Maestrelli P, Ferraresso A, Drigo R, Potena A, Ciaccia A, Fabbri LM. Activated T-lymphocytes and macrophages in bronchial mucosa of subjects with chronic bronchitis. Am Rev Respir Dis 1993 Feb;147(2):301–6.
29. Cosio MG. Autoimmunity, T-cells and STAT-4 in the pathogenesis of chronic obstructive pulmonary disease. Eur Respir J 2004 Jul;24(1):3–5.
30. Gamble E, Grootendorst DC, Hattotuwa K, O'Shaughnessy T, Ram FS, Qiu Y, Zhu J, Vignola AM, Kroegel C, Morell F, et al. Airway mucosal inflammation in COPD is similar in smokers and ex-smokers: a pooled analysis. Eur Respir J 2007 Sep;30(3):467–71.
31. Cottin V, Nunes H, Brillet PY, Delaval P, Devouassoux G, Tillie-Leblond I, Israel-Biet D, Court-Fortune, Valeyre D, Cordier JF. Combined pulmonary fibrosis and emphysema: a distinct underrecognised entity. Eur Respir J 2005 Oct;26(4):586–93.
32. Katzenstein AL, Mukhopadhyay S, Zanardi C, Dexter E. Clinically occult interstitial fibrosis in smokers: classification and significance of a surprisingly common finding in lobectomy specimens. Hum Pathol 2010 Mar;41(3):316–25.
33. Washko GR, Hunninghake GM, Fernandez IE, Nishino M, Okajima Y, Yamashiro T, Ross JC, Estepar RS, Lynch DA, Brehm JM, et al. Lung volumes and emphysema in smokers with interstitial lung abnormalities. N Engl J Med 2011 Mar 10;364(10):897–906.
34. Kranenburg AR, Willems-Widyastuti A, Moori WJ, Sterk PJ, Alagappan VK, de Boer WI, Sharma HS. Enhanced bronchial expression of extracellular matrix proteins in chronic obstructive pulmonary disease. Am J Clin Pathol 2006 Nov;126(5):725–35.
35. O'Shaughnessy TC, Ansari TW, Barnes NC, Jeffery PK. Inflammation in bronchial biopsies of subjects with chronic bronchitis: inverse relationship of CD8+ T lymphocytes with FEV_1. Am J Respir Crit Care Med 1997 Mar;155(3):852–7.
36. Saetta M, Di Stefano A, Turato G, Facchini FM, Corbino L, Mapp CE, Maestrelli P, Ciaccia A, Fabbri LM. CD8+ T-lymphocytes in peripheral airways of smokers with chronic obstructive pulmonary disease. Am J Respir Crit Care Med 1998 Mar;157(3 Pt 1):822–6.
37. Suki B, Ito S, Stamenovic D, Lutchen KR, Ingenito EP. Biomechanics of the lung parenchyma: critical roles of collagen and mechanical forces. J Appl Physiol 2005 May;98(5):1892–9.

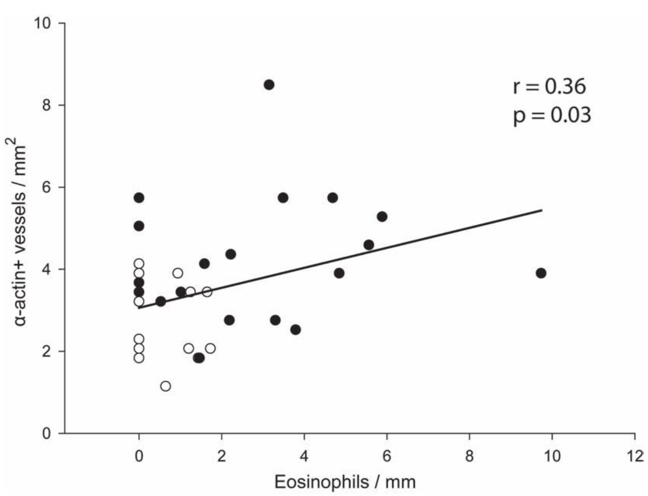

Supplementary Figure 9. Correlation between eosinophils and muscularization. Linear regression of perivascular eosinophils with the number of vessels per mm² positive to a-actin in lung tissue. Solid circles are CS-exposed animals and open circles are sham-exposed animals independently of time of exposure.

Notice of corrections: Corrections have been made to the captions of Figures 1–3, 5 and 6 since the original online publication of this article on 18 June, 2012.

APPENDICES

Supplementary Material - Methods

Animals and experimental model

Animals were provided with water supplemented with vitamin C (1 g/L; Roche Pharma, Madrid, Spain) and fed with a diet of standard chow *ad libitum*. Their body weights were measured weekly throughout the experimental period.

Morphological analysis of airways

Immunostaining. 5 μm serial sections were immunostained with a mouse monoclonal antibody against human smooth muscle α-actin (M0851; DakoCytomation, Glostrup, Denmark). Sections were deparaffined and hydrated. Peroxydase inhibition was performed in a hydrogen peroxide solution and sections were washed twice in PBS. Nonspecific antibody binding was blocked with nonimmune serum and incubated overnight at 4ºC with primary antibody (all reagents from DakoCytomation). Sites of primary antibody were revealed with an ABC system kit (PK-6102 kit; VectorLaboratories, Berlingame (CA), US) and DAB+chromogen solution as substrate (DakoCytomation). Sections were counterstained with Gill's hematoxilin.

Morphometric studies. To sample a comparable airway orientation so estimates represent true thicknesses of layers, only airways cut in cross section (a long-short diameter ratio of 2:1 or less) were evaluated. The smooth muscle perimeter Pos and Pis were defined respectively as the outer and the inner perimeter of the smooth muscle. The internal luminal perimeter (Pil) was defined as the perimeter of the airway lumen. The areas outlined by Pos, Pis and Pil were also determined (Aos, Ais and Ail). Thickness of smooth muscle layer was calculated as the difference in the areas surrounded by the outer and the inner perimeter of the smooth muscle divided by Pil ((Aos – Ais) / Pil). Smooth muscle content was estimated by dividing the α-actin+ area in airway by the Pil. Mucosa+submucosa ((Ais - Ail) / Pil), adventitia (Aad / Pil) and total wall thickness ((Aad + (Aos – Ail)) / Pil) were also calculated, where Aad is the area of adventitia.

Collagen deposition

The slides, after deparaffining were taken through distilled water and stained in saturated picric acid with 0.1% Sirius red. Airways and alveolar septa were captured at a magnification of x160 and x320, respectively, for fibrosis evaluation.

Under polarized light microscopy, collagen fibres of different thickness emit different colours [14]. The thick and denser collagen fibres brighten orange to red, whereas the thinner collagen fibres are detected green.

Supplementary Table 1. Relationship between neutrophilic infiltrate and morphometric parameters of stratified airways

	Adventitial Neutrophils (cells/mm Pil)		
	All Airways (n=37)	**Larger Airways** (n=37)	**Smaller Airways** (n=37)
Total Wall Thickness (μm)	r = 0.564 p < 0.001	r = 0.265 p = 0.123	r = 0.727 p < 0.001
Thickness of Adventitia (μm)	r = 0.625 p < 0.001	r = 0.388 p = 0.019	r = 0.613 p < 0.001
Thickness of Mucosa+submucosa (μm)	r = 0.429 p = 0.008	r = 0.136 p = 0.428	r = 0.524 p < 0.001
Thickness of Muscularis (μm)	r = 0.326 p = 0.049	r = 0.090 p = 0.602	r = 0.658 p < 0.001
Smooth Muscle Content (μm)	r = 0.226 p = 0.179	r = 0.054 p = 0.754	r = 0.503 p = 0.001

Supplementary Table 2. Relationship between macrophagic infiltrate and morphometric parameters of stratified airways

	Adventitial Macrophages (cells/mm Pil)		
	All Airways (n=37)	**Larger Airways** (n=37)	**Smaller Airways** (n=37)
Total Wall Thickness (μm)	r = 0.502 p = 0.001	r = 0.339 p = 0.046	r = 0.474 p = 0.003
Thickness of Adventitia (μm)	r = 0.394 p = 0.016	r = 0.257 p = 0.130	r = 0.407 p = 0.014
Thickness of Mucosa+submucosa (μm)	r = 0.387 p = 0.018	r = 0.266 p = 0.123	r = 0.322 p = 0.052
Thickness of Muscularis (μm)	r = 0.490 p = 0.002	r = 0.233 p = 0.179	r = 0.504 p = 0.001
Smooth Muscle Content (μm)	r = 0.407 p = 0.012	r = 0.222 p = 0.199	r = 0.510 p = 0.001

Supplementary Table 3. Relationship between eosinophilic infiltrate and morphometric parameters of stratified airways

	Adventitial Eosinophils (cells/mm Pil)		
	All Airways (n=37)	**Larger Airways** (n=37)	**Smaller Airways** (n=37)
Total Wall Thickness (µm)	r = 0.529 p < 0.001	r = 0.298 p = 0.087	r = 0.268 p = 0.126
Thickness of Adventitia (µm)	r = 0.566 p < 0.001	r = 0.266 p = 0.123	r = 0.245 p = 0.162
Thickness Mucosa+submucosa (µm)	r = 0.369 p = 0.024	r = 0.119 p = 0.490	r = 0.219 p = 0.206
Thickness of Muscularis (µm)	r = 0.370 p = 0.024	r = 0.324 p = 0.054	r = 0.207 p = 0.234
Smooth Muscle Content (µm)	r = 0.336 p = 0.042	r = 0.363 p = 0.029	r = 0.173 p = 0.319

1.1.- Resultados principales

Células inflamatorias

Neutrófilos. El número de neutrófilos en la vía aérea y los vasos pulmonares aumentó con la exposición durante 6 meses al HC, independientemente del tamaño de la vía aérea y los vasos pulmonares. El número de neutrófilos ya aumentó con la exposición durante 3 meses, sugiriendo una progresión del infiltrado neutrofílico al prolongar la exposición al HC.

Macrófagos. Los animales expuestos al HC mostraron mayor número de macrófagos infiltrando septo alveolar, tanto a los 3 como a los 6 meses de exposición. En vasos pulmonares y vía aérea aumentaron los macrófagos sólo tras 6 meses de exposición.

Eosinófilos. El número de eosinófilos incrementó en la vía aérea y los vasos pulmonares, tanto después de 3 como de 6 meses de exposición al HC. El infiltrado eosinofílico fue mayor en la vía aérea que en los vasos pulmonares y no se observaron diferencias según el calibre de vía aérea. En el septo alveolar aumentó tras 6 meses de exposición.

Folículos linfoides. El porcentaje de animales en los que se observaron folículos linfoides próximos a la vía aérea y a los vasos pulmonares fue mayor en los expuestos al HC durante 6 meses. En los animales no expuestos prácticamente no se observaron folículos linfoides.

Evaluación morfométrica de la vía aérea y enfisema

La exposición al HC durante 6 meses produjo un engrosamiento de la pared bronquial debido tanto al engrosamiento de la capa muscular por el incremento de músculo liso como al de la capa adventicia, y fue más prominente en la vía aérea más pequeña. También se observó un engrosamiento de la pared bronquial con el tiempo y con el HC tanto a los 3 como a los 6 meses, debido al engrosamiento de la mucosa y la submucosa.

Enfisema. Se produjo un incremento de la distancia media entre los septos alveolares en los animales expuestos durante 6 meses al HC.

Evaluación morfológica de los vasos pulmonares

El número de vasos positivos para α-actina de músculo liso fue mayor en los animales expuestos al HC tanto a los 3 como a los 6 meses. La proporción de vasos intrapulmonares de pequeño tamaño con láminas elásticas dobles tendió a aumentar con la exposición durante 6 meses al HC y no hubo diferencias en la proporción de vasos desmina+.

Fibrosis

La proporción de colágeno total y fibras de colágeno gruesas depositadas en el septo alveolar y en la capa muscular de la vía aérea, principalmente la más distal, incrementó en los animales expuestos durante 6 meses al HC.

Correlaciones

Tanto el infiltrado de neutrófilos como de macrófagos peribronquiales correlacionó con el remodelado de la pared bronquial, particularmente en la vía aérea de menor calibre, y también con el enfisema. En el septo alveolar el infiltrado por macrófagos y el depósito de colágeno total y de las fibras más gruesas también correlacionó con el enfisema pulmonar.

El número de eosinófilos peribronquiales y perivasculares sólo correlacionó débilmente con el remodelado bronquial y vascular, respectivamente.

2.- Segundo artículo

Effects of Aclidinium Bromide in a Cigarette Smoke-Exposed Guinea Pig Model of COPD.

David Domínguez-Fandos, Elisabet Ferrer, Raquel Puig-Pey, Cristina Carreño, Neus Prats, Mònica Aparici, Melina Mara Musri, Amadeu Gavaldà, Víctor Ivo Peinado, Montserrat Miralpeix, Joan Albert Barberà.

Artículo publicado en American Journal of Respiratory Cell and Molecular Biology 2014 Feb;50(2):337-46.

ORIGINAL RESEARCH

Effects of Aclidinium Bromide in a Cigarette Smoke–Exposed Guinea Pig Model of Chronic Obstructive Pulmonary Disease

David Domínguez-Fandos[1], Elisabet Ferrer[1], Raquel Puig-Pey[1], Cristina Carreño[2], Neus Prats[2], Mònica Aparici[2], Melina Mara Musri[1], Amadeu Gavaldà[2], Víctor I. Peinado[1,3], Montserrat Miralpeix[2], and Joan A. Barberà[1,3]

[1]Department of Pulmonary Medicine, Hospital Clínic-Institut d'Investigacions Biomèdiques August Pi i Sunyer, University of Barcelona, Barcelona, Spain; [2]Almirall S.A. R&D Center, Barcelona, Spain; and [3]Centro de Investigación Biomédica en Red de Enfermedades Respiratorias, Spain

Abstract

Long-acting muscarinic antagonists are widely used to treat chronic obstructive pulmonary disease (COPD). In addition to bronchodilation, muscarinic antagonism may affect pulmonary histopathological changes. The effects of long-acting muscarinic antagonists have not been thoroughly evaluated in experimental models of COPD induced by chronic exposure to cigarette smoke (CS). We investigated the effects of aclidinium bromide on pulmonary function, airway remodeling, and lung inflammation in a CS-exposed model of COPD. A total of 36 guinea pigs were exposed to CS and 22 were sham exposed for 24 weeks. Animals were nebulized daily with vehicle, 10 μg/ml, or 30 μg/ml aclidinium, resulting in six experimental groups. Pulmonary function was assessed weekly by whole-body plethysmography, determining the enhanced pause (Penh) at baseline, after treatment, and after CS/sham exposure. Lung changes were evaluated by morphometry and immunohistochemistry. CS exposure increased Penh in all conditions. CS-exposed animals treated with aclidinium showed lower baseline Penh than untreated animals ($P = 0.02$). CS induced thickening of all bronchial wall layers, airspace enlargement, and inflammatory cell infiltrate in airways and septa. Treatment with aclidinium abrogated the CS-induced smooth muscle enlargement in small airways ($P = 0.001$), and tended to reduce airspace enlargement ($P = 0.054$). Aclidinium also attenuated CS-induced neutrophilia in alveolar septa ($P = 0.04$). We conclude that, in guinea pigs chronically exposed to CS, aclidinium has an antiremodeling effect on small airways, which is associated with improved respiratory function, and attenuates neutrophilic infiltration in alveolar septa. These results indicate that, in COPD, aclidinium may exert beneficial effects on lung structure in addition to its bronchodilator action.

Keywords: acetylcholine/pharmacology; airway resistance; emphysema; inflammation; muscarinic antagonists

Clinical Relevance

Patients with chronic obstructive pulmonary disease (COPD) benefit from regular treatment with long-acting muscarinic antagonists (LAMAs). It has been postulated that LAMAs might exert lung effects that go beyond their bronchodilating action. Our results indicate that, in a cigarette smoke–exposed guinea pig model of COPD, aclidinium bromide, a new LAMA, abrogated smooth muscle enlargement in small airways and attenuated neutrophilic infiltration in alveolar septa, in addition to improving respiratory function. These findings show that LAMAs might exert beneficial effects on lung structure additional to their bronchodilator action.

Long-acting muscarinic antagonists (LAMAs) are first-choice drugs for the treatment of patients with stable chronic obstructive pulmonary disease (COPD) (1). Among other outcomes, treatment with LAMAs significantly reduces the frequency of COPD exacerbation episodes (2) and lowers the rate of decline in FEV_1 in some patients (3), suggesting that their

(Received in original form March 12, 2013; accepted in final form August 26, 2013)

This work was supported by a grant from the program for National Strategic Consortia in Technical Investigation, Center for Industrial Technological Development, Spanish Ministry of Economy and Competitiveness.

Author Contributions: D.D.-F., E.F., R.P.-P., C.C., and N.P. conducted the experimental work and were involved in the acquisition and analysis of the data. D.D.-F., E.F., R.P-.P., M.A., M.M.M., A.G., V.I.P., M.M., and J.A.B. contributed to the conception, design, and data interpretation of the study. A.G., M.M., and J.A.B. were involved in the planning and coordination of the study. D.D.-F., V.I.P., A.G., M.M., and J.A.B. contributed to the writing of the article or substantial involvement in its critical revision before submission.

Correspondence and requests for reprints should be addressed to Joan A. Barberà, M.D., Ph.D., Servei de Pneumologia, Hospital Clínic, Villarroel 170, 08036 Barcelona, Spain. E-mail: jbarbera@clinic.ub.es

This article has an online supplement, which is accessible from this issue's table of contents at www.atsjournals.org

Am J Respir Cell Mol Biol Vol 50, Iss 2, pp 337–346, Feb 2014

Originally Published in Press as DOI: 10.1165/rcmb.2013-0117OC on September 13, 2013
Internet address: www.atsjournals.org

effects may go beyond pure bronchodilator action (4).

Muscarinic receptor activation may induce the secretion of cytokines and leukotrienes from inflammatory and epithelial cells (5–7), induce the proliferation of fibroblasts (8), enhance the response of smooth muscle cells to growth factors (9, 10), and modulate smooth muscle cell contractile protein expression and contractility (8). Indeed, studies in experimental models of airflow obstruction have shown that treatment with LAMAs diminishes the number of inflammatory cells in bronchoalveolar lavage (BAL) (11, 12), reduces the release of inflammatory cytokines by airway smooth muscle cells (7), and counteracts the remodeling process in the airways (12, 13), providing evidence that anticholinergic therapy may add substantial therapeutic benefits to the bronchodilating action of LAMAs in the management of COPD.

The majority of experimental studies on muscarinic antagonists have been conducted in experimental models of allergic asthma (13–16), pulmonary damage induced by LPS instillation (17), and short-term exposure to cigarette smoke (CS) (11). Little is known about the effects of LAMAs on experimental models of COPD induced by long-term exposure to CS, which are the models of COPD that more closely reproduce the anatomical and mechanical changes occurring in patients with COPD by using the same causative agent (18, 19).

Aclidinium bromide is a novel, inhaled LAMA that has been recently approved for the treatment of COPD (20–22). In preclinical studies, aclidinium has demonstrated potent muscarinic-antagonist activity, comparable to ipratropium bromide and tiotropium bromide, and long duration of action (20). In clinical trials conducted in patients with COPD, aclidinium produced sustained bronchodilation over 24 hours, increased exercise tolerance (23), improved airflow obstruction, reduced the perception of dyspnea, and delayed the first exacerbation (24–26).

On the basis of the potent affinity of aclidinium for the M_3 muscarinic receptor (20), the receptor that mediates the proinflammatory and proliferative actions of acetylcholine (4, 5, 9), and its inhibitory effect on myofibroblastic differentiation (27), we hypothesized that aclidinium would exert antiremodeling effects and reduce the inflammatory cell infiltrate in lung tissue in experimental COPD. Accordingly, the present study aimed to

Table 1: Assessment of Respiratory Function by Unrestrained Whole-body Plethysmography

	Vehicle		Ac 10 (μg/ml)		Ac 30 (μg/ml)		Two-Way ANOVA Main Effects P Value		
	Sham Exposed (n = 8)	CS Exposed (n = 10)	Sham Exposed (n = 7)	CS Exposed (n = 6)	Sham Exposed (n = 7)	CS Exposed (n = 8)	CS Exposure	Ac	Interaction
Enhanced pause, arbitrary units									
Baseline	10.0 (9.2–10.4)	18.9 (17.3–23.8)	9.6 (8.5–10.2)	15.1 (13.6–20.0)	8.9 (7.7–10.0)	13.7 (11.7–20.2)	<0.001	0.023	0.487
After nebulization	11.2 (10.5–12.7)	26.6 (24.6–28.8)	10.9 (9.5–12.9)	19.4 (16.4–25.6)	10.6 (10.1–12.1)	17.6* (14.2–20.4)	—	—	0.049
After CS	11.3 (10.7–12.8)	126.3 (80.6–132.6)	11.4 (10.6–11.7)	94.7 (82.1–96.8)	10.9 (9.8–11.3)	72.9 (57.7–87.2)	<0.001	0.024	0.163
Breathing frequency, arbitrary units									
Baseline	2,409 (2,219–2,951)	2719 (2,625–2,818)	2,580 (2,409–2,707)	2,812 (2,666–3,006)	2,071 (2,014–2,105)	2,839 (2,447–2,957)	<0.001	0.056	0.157
After nebulization	1,900 (1,812–2,182)	2176 (2,115–2,202)	1,984 (1,928–2,185)	2,327 (2,143–2,552)	1,690 (1,575–1,791)†,‡	2,347 (2,258–2,404)	—	—	0.011
After CS	1,845 (1,749–1,896)	2316 (2,010–2,492)	1,879 (1,764–1,949)	2,494 (2,366–2,761)	1,808 (1,669–1,855)	2,463 (2,053–2,804)	⩽0.001	0.579	0.338
Tidal volume, arbitrary units									
Baseline	17,192 (15,591–18,862)	17,189 (15,034–18,190)	17,424 (15,482–18,111)	17,419 (16,029–20,638)	14,522 (14,255–15,344)	16,979 (15,540–18,553)	0.171	0.332	0.246
After nebulization	13,822 (12,620–14,452)	13,774 (13,356–14,791)	14,527 (13,719–14,971)	14,196 (12,054–16,392)	11,421†,‡ (11,032–12,998)	14,437 (13,989–15,342)	—	—	0.024
After CS	12,905 (11,862–13,534)	22,749 (20,101–27,916)	13,261 (13,037–13,846)	23,744 (22,031–26,398)	12,433 (11,834–13,157)	22,592 (21,018–25,651)	⩽0.001	0.655	0.977

Definition of abbreviations: Ac, aclidinium bromide; Ac10, aclidinium 10 μg/ml; Ac30, aclidinium 30 μg/ml; CS, cigarette smoke.
Values are median (interquartile range) of the area under the curve of measurements obtained weekly during 6 months.
*$P < 0.05$ compared with vehicle + CS exposed.
†$P < 0.05$ compared with vehicle + sham exposed.
‡$P < 0.05$ compared with Ac10 + sham exposed.

investigate the effects of two different doses of aclidinium on the histopathological changes and inflammatory cell infiltrate in the lungs of guinea pigs chronically exposed to CS. This is a well established experimental model of COPD that develops morphological and physiological alterations that resemble and mimic those seen in patients (18, 28, 29).

Some of the results of these studies have been previously reported in the form of abstracts (30, 31).

Materials and Methods

Experimental Groups

A total of 58 male guinea pigs were divided into two groups: exposed, using a nose-only system, to the smoke of six cigarettes per day, 5 days per week, for 6 months (n = 36); and sham-exposed (n = 22). Before CS or sham exposure, the animals were treated with distilled water (vehicle), 10 μg/ml, or 30 μg/ml of aclidinium solution using an ultrasonic nebulizer (Devilbiss Ultraneb 3000; Somerset, PA), resulting in six experimental groups.

All animal procedures were approved by the ethics review board on animal research of the University of Barcelona, and complied with national and international guidelines.

Assessment of Respiratory Function and Cough

Respiratory function was assessed by unrestrained whole-body plethysmography. Assessments were performed weekly at the following time points: 24 hours after last CS or sham exposure (baseline), 30 minutes after nebulization of aclidinium or vehicle, and 10 minutes after the CS or sham exposure (*see* Figure E1 in the online supplement).

At each time point, we recorded the breathing frequency (Bf), tidal volume, and enhanced pause (Penh), which reflects changes in the waveform of the box pressure signal from both inspiration and expiration, related to the timing comparison of early and late expiration (32).

To investigate the antitussive properties of aclidinium, the number of cough episodes was assessed using the method described by Lewis and colleagues (33). Briefly, during the first minute after CS exposure, coughs were counted *de visu* once a week for the last 16 weeks of the study.

Lung Morphometric and Immunohistochemical Analysis

After death, the lungs were removed, inflated, and fixed under constant pressure. The thickness of the mucosa plus submucosa, muscularis, and adventitia, as well as the area showing positive immunoreaction to α-actin, was measured in 10 airways. The median internal luminal perimeter of each airway (34) was used as a reference to normalize the morphometric assessments and group them by airway size. Goblet cells were counted in the airway epithelium of 10 cross-sectioned airways, stained with Alcian blue.

Pulmonary emphysema was evaluated in hematoxylin and eosin–stained tissue sections by measuring the mean linear intercept of alveolar septa in 20 randomly selected fields. Vascular remodeling was evaluated by assessing the number of intrapulmonary vessels under 50-μm diameter showing positive immunostaining to α-actin and expressed as vessels per square millimeter.

Identification and differential counting of neutrophils, eosinophils, and lymphoid follicles were performed in each animal, in 5-μm serial sections stained with hematoxylin and eosin, in 10 airways and 20 microscopic fields of lung parenchyma, as previously described (28). Macrophages were counted on sections stained with periodic acid-Schiff. Lymphoid follicles were assessed by measuring their area and normalized by the number of airways.

Data Analysis

Normally distributed variables are expressed as mean (± SD), and nonnormally distributed variables as median and interquartile range.

To analyze the evolution of plethysmographic respiratory parameters (Bf, Penh, tidal volume) assessed weekly over the course of the 6-month study period,

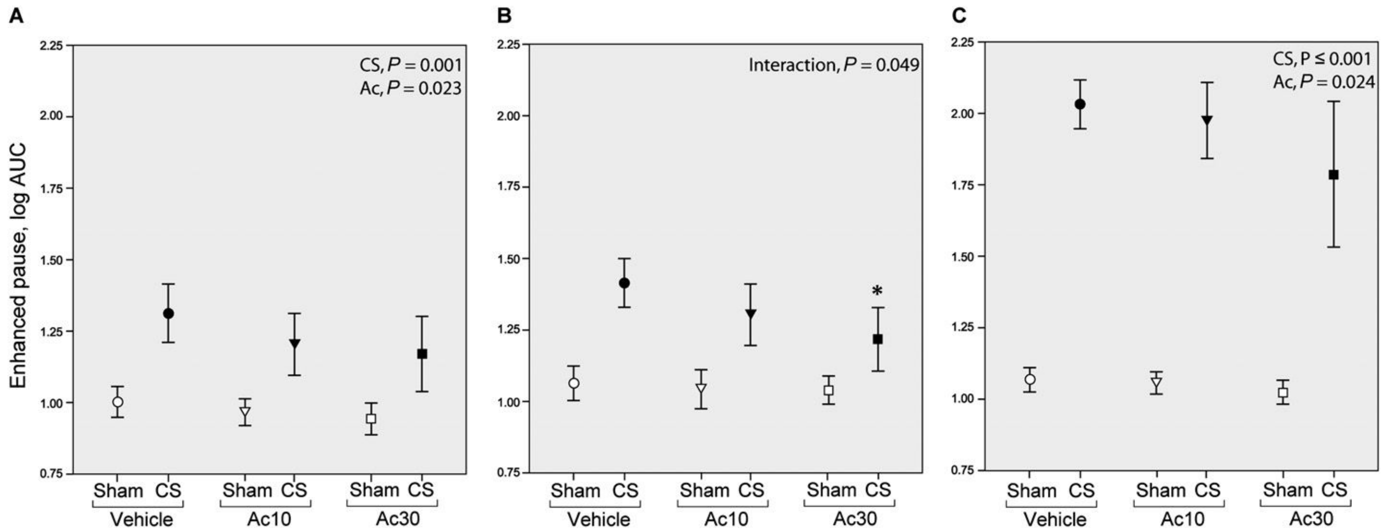

Figure 1. Average value of the enhanced pause (Penh) assessed by unrestrained whole-body plethysmography in guinea pigs exposed to cigarette smoke (CS) or sham, treated with vehicle, aclidinium bromide (Ac) 10 μg/ml (Ac10) or 30 μg/ml (Ac30). Measurements obtained at baseline (*A*), 30 minutes after treatment nebulization (*B*), and 10 minutes after CS or sham exposure (*C*) are shown. *P* values denote the main effects assessed with the two-way ANOVA, CS exposure and Ac treatment, as well as their interaction. *Graph symbols* show the mean log-transformed area under the curve (AUC) of Penh, and *bars* show the 95% confidence interval. *Post hoc* pairwise comparisons were performed when significant interaction was shown in the ANOVA. *P < 0.05 compared with control group (vehicle).

we calculated the area under the curve of all measurements performed in each animal as a summary measure.

Comparisons between groups were performed using a two-way ANOVA. The main effects of CS exposure, aclidinium, and their interaction were analyzed. When significant, *post hoc* pairwise comparisons were performed using the Student-Newman-Keuls test. Relationships between variables were assessed using the Pearson's correlation test. A P value less than 0.05 was considered significant.

Results

The guinea pigs showed normal behavior and activity during the experimental procedures, and tolerated well the administration of aclidinium. A total of 12 of the CS-exposed animals died during the study (4 in the group treated with vehicle, 6 in the group treated with 10 μg/ml aclidinium, and 2 in the group treated with 30 μg/ml aclidinium), whereas all the nonexposed animals completed the study. Similar mortality rates have been observed in guinea pigs exposed to CS (28, 29). There were no significant differences in mortality among the groups of animals exposed to CS. Lung morphometric and immunohistochemical assessment analyses were performed in the animals that completed the whole study period.

Respiratory Function

The average value of Penh at baseline, assessed by the area under the curve of all the measurements obtained during the study period, was higher in animals exposed to CS than in the sham-exposed group (P = 0.001). Treatment with aclidinium resulted in a significant decrease in Penh (P = 0.023), without any difference between treatment doses (Table 1, Figures 1A and E2).

At 30 minutes after treatment nebulization, a significant interaction between CS exposure and aclidinium on Penh was observed in the ANOVA (P = 0.049), reducing the Penh value in CS-exposed animals treated with aclidinium in a dose-dependent manner (Table 1, Figure 1B).

CS exposure elicited a significant 4- to 6-fold increase in Penh immediately after exposure (Table 1). In CS-exposed animals treated with aclidinium, there was a trend

Table 2: Lung Morphometric Assessments

	Airway Size (Per Internal Perimeter)	Vehicle		Ac 10 (*μg/ml*)		Ac 30 (*μg/ml*)		Two-Way ANOVA Main Effects *P* Value		
		Sham Exposed (*n* = 8)	CS Exposed (*n* = 10)	Sham Exposed (*n* = 7)	CS Exposed (*n* = 6)	Sham Exposed (*n* = 7)	CS Exposed (*n* = 8)	CS Exposure	Ac	Interaction
Airways										
Wall thickness, μm	All airways	61 ± 14	113 ± 36	71 ± 14	94 ± 17	73 ± 11	99 ± 21	≤0.001	0.852	0.145
	>Median	66 ± 8	108 ± 9	73 ± 5	99 ± 8	79 ± 5	106 ± 6	≤0.001	0.645	0.471
	<Median	57 ± 9	120 ± 52	68 ± 15	81 ± 17	66 ± 9	95 ± 24	≤0.001	0.414	0.050
Mucosa + submucosa thickness, μm	All airways	28 ± 5	56 ± 27	34 ± 6	47 ± 9	32 ± 5	46 ± 9	≤0.001	0.848	0.284
	>Median	27 ± 2	53 ± 6	33 ± 3	50 ± 4	31 ± 2	45 ± 3	≤0.001	0.741	0.361
	<Median	29 ± 5	59 ± 38	34 ± 5	41 ± 8	33 ± 4	46 ± 10	0.006	0.603	0.219
Muscular thickness, μm	All airways	19 ± 1	31 ± 3	21 ± 2	23 ± 3	23 ± 1	25 ± 1	0.009	0.599	0.057
	>Median	21 ± 2	32 ± 5	23 ± 2	26 ± 3	27 ± 2	31 ± 2	0.042	0.475	0.475
	<Median	16 ± 3	32 ± 9	19 ± 7	18 ± 4*	20 ± 3	21 ± 5*	—	—	0.001
Adventitia thickness, μm	All airways	15 ± 7	26 ± 11	16 ± 8	24 ± 6	18 ± 7	28 ± 10	≤0.001	0.562	0.839
	>Median	17 ± 4	23 ± 3	16 ± 3	24 ± 4	21 ± 3	29 ± 4	0.014	0.292	0.941
	<Median	12 ± 5	30 ± 17	15 ± 7	22 ± 6	15 ± 5	29 ± 15	≤0.001	0.704	0.404
Lumen area, $10^4 \times \mu m^2$	All airways	13.2 ± 5.2	9.5 ± 3.7	11.9 ± 6.7	7.5 ± 3.7	9.3 ± 4.2	8.1 ± 3.6	0.030	0.270	0.623
	>Median	16.9 ± 7.1	12.0 ± 5.0	17.2 ± 9.1	9.5 ± 5.4	11.3 ± 5.4	10.5 ± 4.8	0.021	0.280	0.340
	<Median	8.9 ± 3.0	6.0 ± 2.4	7.2 ± 4.0	5.2 ± 2.9	7.2 ± 2.7	6.7 ± 3.1	0.059	0.513	0.535
Goblet cells, mm^{-1}	All airways	1.9 ± 2.6	16.8 ± 12.6	2.7 ± 2.8	16.4 ± 5.4	4.9 ± 5.9	13.1 ± 7.6	≤0.001	0.979	0.428
	>Median	3.2 ± 4.1	22.8 ± 14.6	6.2 ± 8.4	17.9 ± 11.4	9.2 ± 10.3	15.9 ± 10.6	≤0.001	0.968	0.229
	<Median	0.2 ± 0.5	6.0 ± 5.5	1.0 ± 1.9	7.0 ± 6.1	0.1 ± 0.2	9.9 ± 8.9	≤0.001	0.589	0.485
Parenchyma										
Interseptal distance, μm		34.2 ± 2.3	48.5 ± 9.1	36.8 ± 3.4	41.8 ± 3.9	38.3 ± 8.0	43.3 ± 5.4	≤0.001	0.654	0.054
Intrapulmonary vessels										
SM α-actin$^+$ vessels, mm^{-2}		2.1 ± 1.2	7.9 ± 4.1	1.8 ± 2.0	6.1 ± 1.9	1.6 ± 1.0	5.1 ± 3.2	≤0.001	0.208	0.459

Definition of abbreviations: Ac, aclidinium bromide; CS, cigarette smoke; SM, smooth muscle.
Values are mean ± SD.
*P < 0.05 compared with vehicle + CS exposed.

toward attenuated reactivity, with a lower increase in Penh immediately after CS exposure (P = 0.053). The absolute value of Penh after exposure was also reduced in animals treated with aclidinium (P = 0.024), an effect that was particularly marked in CS-exposed animals treated with the 30-μg/ml dose (Table 1, Figure 1C).

In animals exposed to CS, the breathing pattern differed from that of the sham-exposed group, showing higher Bf at baseline (Table 1). There was also a trend toward higher Bf at baseline in guinea pigs treated with aclidinium. After treatment nebulization, both the Bf and the tidal volume were lower in sham-exposed guinea pigs treated with 30 μg/ml aclidinium, compared with animals nebulized with vehicle (Table 1). CS exposure significantly changed the breathing pattern, increasing both the Bf and the tidal volume (Table 1). No effect of aclidinium on the breathing pattern was observed after CS exposure.

Cough Episodes

CS induced cough episodes in exposed guinea pigs (0 ± 0 vs. 10 ± 8 accumulated episodes per animal at Week 24 in sham- and CS-exposed animals, respectively; $P \leqslant 0.001$; Figure E3). There was a trend toward fewer cough episodes in CS-exposed animals treated with 30 μg/ml aclidinium (Figure E3). Aclidinium in sham animals did not induce cough.

CS-exposed guinea pigs treated with 30 μg/ml aclidinium also showed better tolerance of CS, presenting less frequent episodes of bronchoconstriction during or after the exposure (data not shown).

Histological Assessments

Airways. CS exposure induced significant enlargement of the bronchial wall, especially in small airways, with a consequent reduction in the lumen area. This enlargement was dependent on the thickening of all bronchial wall layers: mucosa plus submucosa, muscularis, and adventitia (Table 2). The enlarged muscular layer in CS-exposed animals was due to greater smooth muscle content, as shown by positive immunoreaction to α-actin (Figure 2) (data not shown).

In guinea pigs exposed to CS and treated with aclidinium, the increase in bronchial wall thickness in smaller airways (internal perimeter below the median) was less pronounced than in CS-exposed, untreated animals (Table 2). This effect was particularly apparent in the muscular layer, because, in animals exposed to CS and treated with aclidinium, the thickness of the muscularis did not differ from that of sham-exposed animals, and was significantly lower than in CS-exposed, untreated animals (Figure 2G). Thus, aclidinium at the two tested doses abrogated the enlargement of the muscular layer induced by CS, in particular in small airways (Table 2, Figure 2). The smooth muscle content in the airways, evaluated by immunoreactivity to α-actin, in animals exposed to CS and treated with aclidinium, was similar to that of sham-exposed animals and significantly lower than that of CS-exposed, untreated guinea pigs (data not shown).

No significant differences related to aclidinium were observed in the thickness of the mucosal and adventitial layers (Table 2).

Exposure to CS gave rise to a marked increase in bronchial goblet cells, in particular in larger airways, but treatment with aclidinium did not modify the number of bronchial goblet cells (Table 2, Figure E4).

Lung parenchyma. Development of pulmonary emphysema, assessed as the increase in the mean distance between alveolar septa, was observed in animals exposed to CS. There was a trend toward less enlargement of airspace size in animals

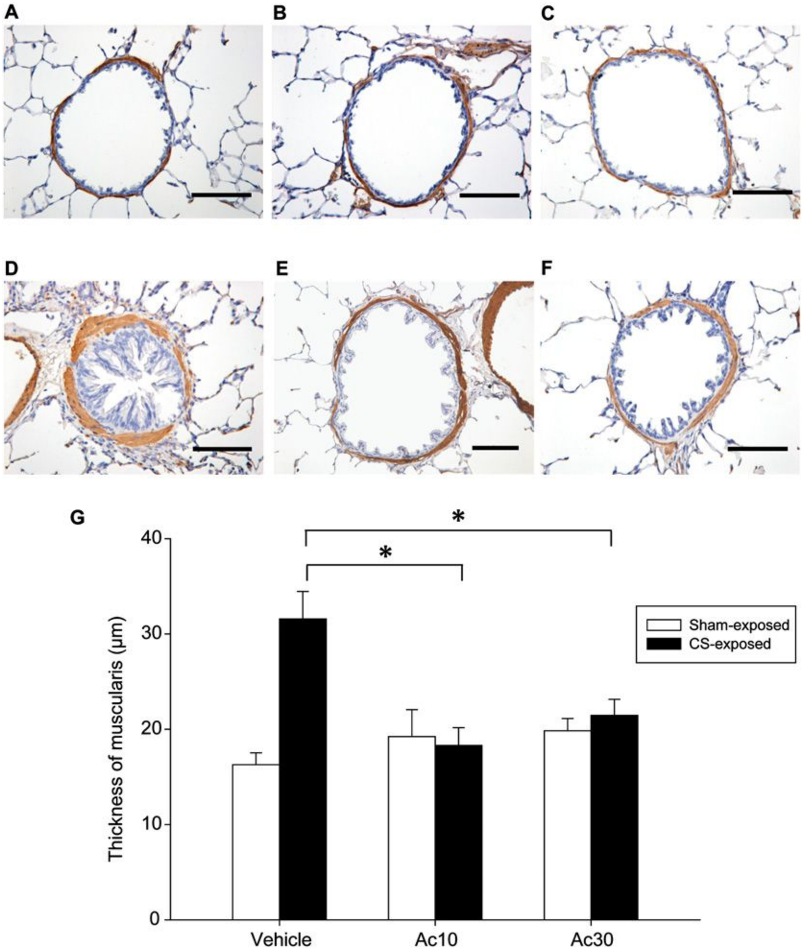

Figure 2. Assessment of smooth muscle content in small airways (lumen perimeter below the median value). Photomicrographs of airways immunostained with anti–α-actin antibody in sham-exposed guinea pigs treated with vehicle (*A*), 10 μg/ml Ac (*B*), or 30 μg/ml Ac (*C*); and CS-exposed guinea pigs treated with vehicle (*D*), 10 μg/ml Ac (*E*), or 30 μg/ml Ac (*F*). *Scale bar*, 100 μm. The *bar graph* shows the morphometric assessment of the muscular layer thickness in the six experimental groups (*G*). The two-way ANOVA showed significant interaction between CS exposure and Ac treatment (P = 0.001). *$P < 0.05$ compared with control group (vehicle).

exposed to CS and treated with aclidinium ($P = 0.054$) (Table 2, Figure E5).

Intrapulmonary vessels. CS exposure induced the muscularization of small intrapulmonary vessels, as shown by an increased proportion of vessels exhibiting positive immunoreactivity to α-actin (Figure E6). The administration of aclidinium did not significantly modify the changes induced by CS in pulmonary vessels (Table 2).

Inflammatory cells. The number of inflammatory cells was increased in animals exposed to CS, both in the alveolar septa and in the airways (Figure 3, Table E1). In the alveolar septa, the administration of aclidinium was associated with a decreased number of neutrophils ($P = 0.039$), without any difference in the number of macrophages or eosinophils (Figure 3). In the airways, treatment with aclidinium did not affect the number of infiltrating neutrophils or eosinophils (Figure 3, Table E1).

The presence of lymphoid follicles was a prominent feature of guinea pigs exposed to CS, in keeping with previous reports (28). Treatment with aclidinium did not modify the number or size of lymphoid structures induced by CS exposure (Figure E7).

Correlations

In CS-exposed animals, the area under the curve of baseline Penh correlated significantly with the thickness of the airway muscular layer, particularly in smaller airways ($r = 0.67$, $P < 0.001$; Figure 4) and with emphysema ($r = 0.66$, $P < 0.001$; Figure 4). Furthermore, the numbers of neutrophils and eosinophils infiltrating the airways correlated with the wall thickness of smaller airways ($r = 0.61$, $P = 0.002$ and $r = 0.66$, $P < 0.001$, respectively; Figure E8).

Discussion

Results of the present study show that, in guinea pigs chronically exposed to CS, the administration of aclidinium exerted an antiremodeling effect on the airways that was associated with reduced respiratory resistance. Furthermore, aclidinium slightly attenuated the neutrophilic infiltrate in the alveolar septa induced by CS exposure.

Chronic exposure to CS increased respiratory resistance, as assessed by whole-body plethysmography, in line with previous observations in this experimental model (35, 36). Such an increase in respiratory resistance could be attributed to histopathological changes taking place in the airways and lung parenchyma, because baseline Penh strongly correlated with airway muscular thickness and airspace size. Therefore, in the CS-exposed guinea pig model, airway remodeling and emphysema account for increased respiratory resistance (36); this is similar to what occurs in COPD.

Treatment with aclidinium significantly reduced the respiratory resistance over the study period, and attenuated the acute hyperresponsiveness induced by CS exposure. These effects could be attributed, at least in part, to the antiremodeling effect of the drug on the airways, as animals exposed to CS and

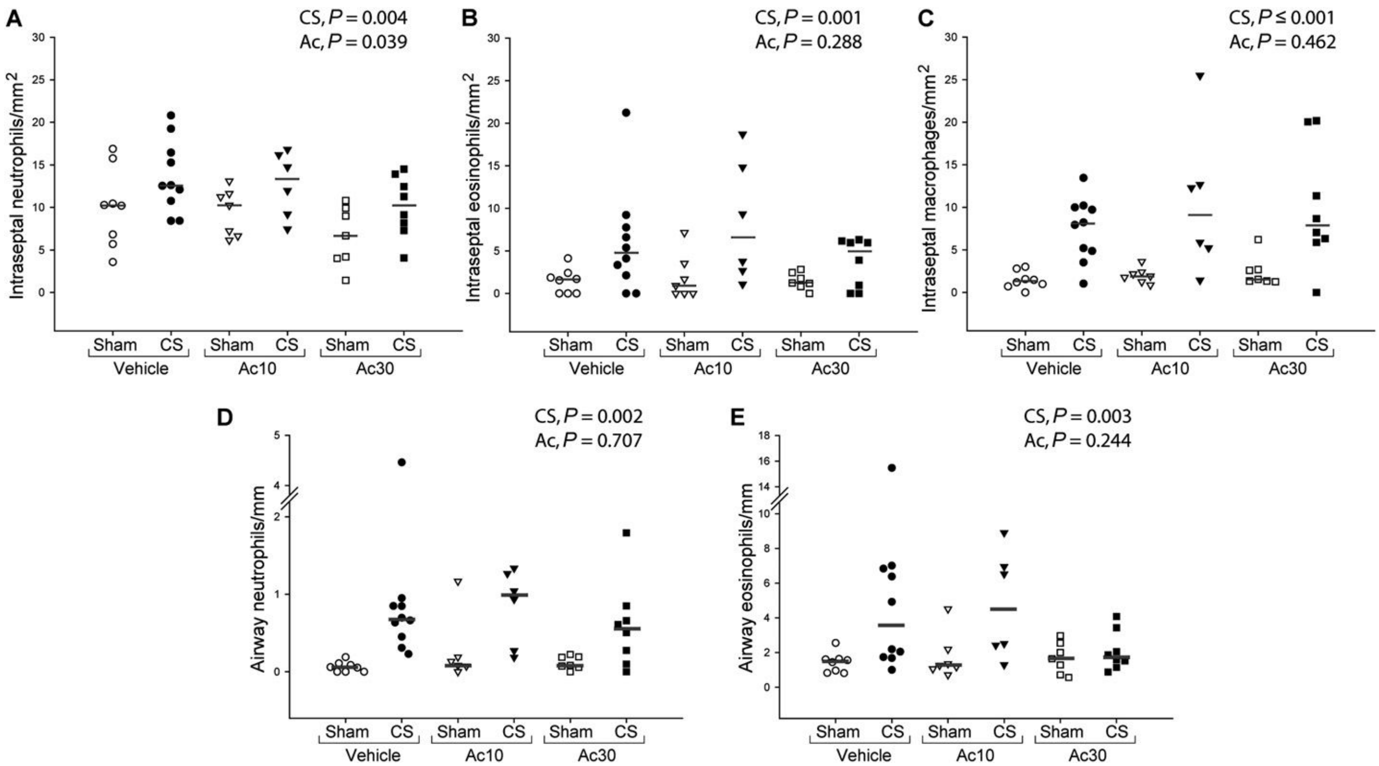

Figure 3. Immunohistochemical assessment of inflammatory cell infiltrate in guinea pig lungs. *Graphs* show the number of neutrophils (*A*), eosinophils (*B*), and macrophages (*C*) in alveolar septa, and the number of neutrophils (*D*) and eosinophils (*E*) in the airways. Assessments were performed in guinea pigs exposed to CS or sham, treated with vehicle, 10 μg/ml Ac (Ac10), or 30 μg/ml Ac (Ac30). *P* values denote the main effects assessed in the two-way ANOVA: CS exposure and Ac treatment.

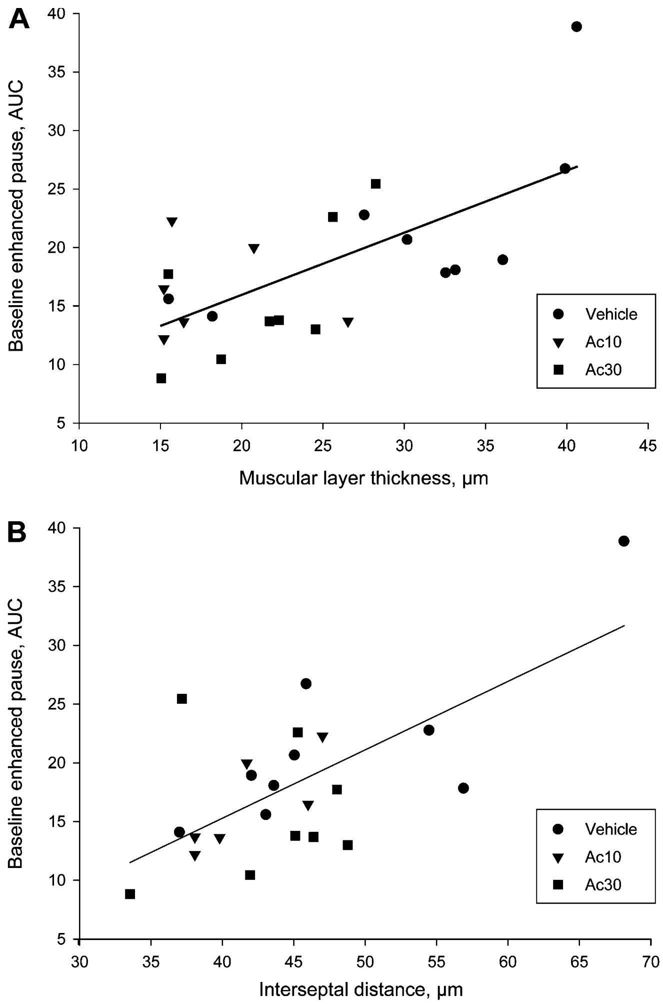

Figure 4. Correlations of the average value (AUC of all study measurements) of the Penh, assessed by unrestrained whole-body plethysmography, with the thickness of the muscular layer of small airways (lumen perimeter below the median value) (*A*) and the mean linear intercept of alveolar septa (*B*), in guinea pigs exposed to CS, treated with vehicle, 10 μg/ml Ac (Ac10), or 30 μg/ml Ac (Ac30). The Penh value was significantly correlated with both measurements ($r = 0.67$, $P < 0.001$ and $r = 0.66$, $P < 0.001$, respectively).

treated with aclidinium showed no enlargement of the airway smooth muscle. These observations suggest a major role for muscarinic activation in airway smooth muscle remodeling (4, 8, 9). Indeed, in a guinea pig model of allergic asthma, Gosens and colleagues (15) showed that the administration of the muscarinic antagonist, tiotropium, inhibited the increase in airway smooth muscle mass. The effects of aclidinium shown in the present study extend these previous observations, and provide evidence of the involvement of the cholinergic pathway in airway smooth muscle remodeling caused by chronic exposure to CS. In fact, Milara and colleagues (27) have shown that aclidinium attenuates fibroblast proliferation and migration, as well as the transition of fibroblasts into myofibroblasts in smokers and patients with COPD. These findings indicate that muscarinic antagonists may have a major impact on airway remodeling, in addition to their sustained bronchodilator effect. In fact, whereas the antiremodeling effect did not differ between the two aclidinium doses, the 30-μg/ml dose had a slightly greater effect on Penh and cough episodes, suggesting that higher doses might have exerted additional bronchodilator action. In any case, the demonstration of such antiremodeling activity of antimuscarinic therapy in a properly validated animal model of COPD (18, 19) strengthens the results of recent clinical trials showing the clinical efficacy of aclidinium in patients with COPD (24–26).

The cholinergic system participates in the inflammatory response, and muscarinic receptors have been shown to be expressed not only in the parasympathetic nervous system, but also in nearly all the cell types located in the airways (8, 37). Muscarinic M_3 receptor stimulation by CS induces the secretion of IL-8 by human airway smooth muscle cells (5). The M_3 receptor is the primary subtype involved in airway smooth muscle contraction and cell proliferation induced by methacholine (9, 38).

Acetylcholine has also been shown to be released from inflammatory cells (8, 39). Aclidinium has been reported to decrease the eosinophil cell count in BAL in a murine model of allergen-induced asthma (12). Tiotropium has also been shown to inhibit the CS-induced neutrophilic inflammation in BAL in mice (11). These findings suggest that muscarinic antagonists might attenuate the inflammatory component induced by airway damage. In our study, treatment with aclidinium was associated with a reduced number of neutrophils in the alveolar septa of guinea pigs exposed to CS, whereas other inflammatory cell types remained unaffected. There was also a trend toward a reduced number of neutrophils in sham-exposed animals treated with 30 μg/ml aclidinium. The observed effect on parenchymal neutrophils is consistent with the reduction in the number of neutrophils in BAL produced by tiotropium in mice exposed to CS (11). In contrast, the inflammatory influx induced by CS in the airways was unaffected by aclidinium. The latter finding is consistent with studies in patients with COPD, where treatment with tiotropium, either alone or in combination with fluticasone, failed to reduce the number of inflammatory cells in induced sputum (40). In addition, the limited anti-inflammatory effect of aclidinium on the airways might be species specific, result from the intense inflammatory reaction induced by CS exposure, or be related to the fact that we assessed airway neutrophils in the bronchial wall, which may provide a different inflammatory profile than sputum or BAL (41). Although wall thickness correlated with the intensity of inflammatory infiltrate in the airways, the contrasting effects of aclidinium on airway remodeling and inflammatory cell infiltrate suggest that the antiremodeling effect on airway smooth muscle was more probably due to the effect on signaling pathways regulated by muscarinic agonists (42, 43), rather than a direct effect on airway inflammatory cell recruitment.

The airspace size did not differ between CS-exposed, aclidinium-treated animals and control animals. Furthermore, if we pool the two doses of aclidinium, the mean distance between alveolar septa was significantly higher in CS-exposed, untreated guinea pigs than in CS-exposed, treated animals (48.5 ± 9.1 μm vs. 42.6 ± 4.7 μm; P = 0.023). Overall, our findings suggest that the drug could have a potential effect on preventing the development of emphysema. It is tempting to speculate that aclidinium reduced the neutrophilic influx induced by CS in the alveolar septa, and thus prevented the enlargement of airspace size; however, we did not find any relationship between the airspace size and the number of neutrophils in the alveolar septa.

Aclidinium might block the activation of signal transduction pathways associated with G protein–-linked muscarinic receptors, such as the RhoA/Rho-kinase cascade, thus improving the clearance of apoptotic cells (44). Indeed, the expression and function of RhoA is increased by proinflammatory cytokines in animal models of COPD (8). Therefore, we hypothesize that aclidinium might prevent the enlargement of airspace by attenuating the activation of G protein–dependent pathways in epithelial cells, thereby improving the homeostasis of lung parenchyma. Nevertheless, as recently pointed out (45), the effects of experimental drugs on emphysema should be treated with caution, as positive results in experimental models may not translate to humans.

The increased amount of goblet cells and mucus hypersecretion in the airway epithelium is a characteristic feature of smokers and patients with COPD (46, 47). Both CS exposure and cholinergic agonists are associated with an increased expression of MUC5AC mucin (48, 49). Aclidinium and other LAMAs may suppress MUC5AC expression (17, 48). In the present study, animals exposed to CS showed prominent goblet cell metaplasia in the airways, in keeping with previous observations in this experimental model (50). The administration of aclidinium did not modify the number of goblet cells in CS-exposed animals, even though it selectively inhibits CS-induced MUC5AC expression in the airways (48). Considering that the histochemical analysis of goblet cells may not correlate with the immunohistochemical expression of MUC5AC (51), we cannot rule out that, in our experimental model, aclidinium might have had an inhibitory effect on MUC5AC without altering goblet cell hyperplasia.

This study has some limitations. First, inflammatory cells were identified by a combination of histochemical staining and standard morphological criteria. Immunostaining with monoclonal antibodies would have provided more specific identification of inflammatory cells. Unfortunately, most of the commercially available antibodies are not sensitive or specific enough to achieve high selectivity and reproducibility in the guinea pig. Accordingly, we used standard histochemical and morphological criteria to distinguish the inflammatory cell populations. Second, the present study shows an inhibitory effect of aclidinium bromide on smooth muscle cell proliferation, but the specific pathways involved in this process were not evaluated. Third, the effects of aclidinium were assessed using a preventive design, where treatment was instituted from Day 1 of smoke exposure. Whether or not the effects of the drug will be the same once the structural abnormalities are already in place remains to be established. The latter should be addressed in future studies in this experimental model.

In conclusion, the present study, conducted in a validated animal model of COPD, shows potential therapeutic benefits for aclidinium beyond a direct effect on respiratory function improvement, in preventing airway remodeling, reducing the neutrophilic infiltrate in alveolar septa, and, to some extent, avoiding the development of emphysema. These results strengthen the evidence shown in clinical studies for the potential benefits of aclidinium in the treatment of COPD. ■

Author disclosures are available with the text of this article at www.atsjournals.org.

Acknowledgments: The authors thank Ingrid Victoria from Hospital Clínic, and Raquel Otal, Pepi Torres, Anna Domènech, and Mariona Aulí from Almirall S.A. R&D Center for technical assistance. They also acknowledge the personnel of Almirall S.A. R&D Center and Lluís de Jover for their valuable contributions.

References

1. Vestbo J, Hurd SS, Agustí AG, Jones PW, Vogelmeier C, Anzueto A, Barnes PJ, Fabbri LM, Martinez FJ, Nishimura M, *et al*. Global strategy for the diagnosis, management, and prevention of chronic obstructive pulmonary disease: GOLD executive summary. *Am J Respir Crit Care Med* 2013;187:347–365.
2. Karner C, Chong J, Poole P. Tiotropium versus placebo for chronic obstructive pulmonary disease. *Cochrane Database Syst Rev* 2012;7:CD009285.
3. Decramer M, Celli B, Kesten S, Lystig T, Mehra S, Tashkin DP; UPLIFT Investigators. Effect of tiotropium on outcomes in patients with moderate chronic obstructive pulmonary disease (UPLIFT): a prespecified subgroup analysis of a randomised controlled trial. *Lancet* 2009;374:1171–1178.
4. Bateman ED, Rennard S, Barnes PJ, Dicpinigaitis PV, Gosens R, Gross NJ, Nadel JA, Pfeifer M, Racké K, Rabe KF, *et al*. Alternative mechanisms for tiotropium. *Pulm Pharmacol Ther* 2009;22:533–542.
5. Gosens R, Rieks D, Meurs H, Ninaber DK, Rabe KF, Nanninga J, Kolahian S, Halayko AJ, Hiemstra PS, Zuyderduyn S. Muscarinic M3 receptor stimulation increases cigarette smoke–induced IL-8 secretion by human airway smooth muscle cells. *Eur Respir J* 2009;34:1436–1443.
6. Profita M, Bonanno A, Montalbano AM, Ferraro M, Siena L, Bruno A, Girbino S, Albano GD, Casarosa P, Pieper MP, *et al*. Cigarette smoke extract activates human bronchial epithelial cells affecting non-neuronal cholinergic system signalling *in vitro*. *Life Sci* 2011;89:36–43.
7. Suzaki I, Asano K, Shikama Y, Hamasaki T, Kanei A, Suzaki H. Suppression of IL-8 production from airway cells by tiotropium bromide *in vitro*. *Int J Chron Obstruct Pulmon Dis* 2011;6:439–448.
8. Gosens R, Zaagsma J, Meurs H, Halayko AJ. Muscarinic receptor signaling in the pathophysiology of asthma and COPD. *Respir Res* 2006;7:73.
9. Gosens R, Nelemans SA, Grootte Bromhaar MM, McKay S, Zaagsma J, Meurs H. Muscarinic M3-receptors mediate cholinergic synergism of mitogenesis in airway smooth muscle. *Am J Respir Cell Mol Biol* 2003; 28:257–262.
10. Krymskaya VP, Orsini MJ, Eszterhas AJ, Brodbeck KC, Benovic JL, Panettieri RA Jr, Penn RB. Mechanisms of proliferation synergy by receptor tyrosine kinase and G protein–coupled receptor activation in human airway smooth muscle. *Am J Respir Cell Mol Biol* 2000;23:546–554.
11. Wollin L, Pieper MP. Tiotropium bromide exerts anti-inflammatory activity in a cigarette smoke mouse model of COPD. *Pulm Pharmacol Ther* 2010;23:345–354.

12. Damera G, Jiang M, Zhao H, Fogle HW, Jester WF, Freire J, Panettieri RA Jr. Aclidinium bromide abrogates allergen-induced hyperresponsiveness and reduces eosinophilia in murine model of airway inflammation. *Eur J Pharmacol* 2010;649:349–353.
13. Bos IS, Gosens R, Zuidhof AB, Schaafsma D, Halayko AJ, Meurs H, Zaagsma J. Inhibition of allergen-induced airway remodelling by tiotropium and budesonide: a comparison. *Eur Respir J* 2007;30: 653–661.
14. Buels KS, Jacoby DB, Fryer AD. Non-bronchodilating mechanisms of tiotropium prevent airway hyperreactivity in a guinea-pig model of allergic asthma. *Br J Pharmacol* 2012;165:1501–1514.
15. Gosens R, Bos IS, Zaagsma J, Meurs H. Protective effects of tiotropium bromide in the progression of airway smooth muscle remodeling. *Am J Respir Crit Care Med* 2005;171: 1096–1102.
16. Ohta S, Oda N, Yokoe T, Tanaka A, Yamamoto Y, Watanabe Y, Minoguchi K, Ohnishi T, Hirose T, Nagase H, *et al*. Effect of tiotropium bromide on airway inflammation and remodelling in a mouse model of asthma. *Clin Exp Allergy* 2010;40: 1266–1275.
17. Pera T, Zuidhof A, Valadas J, Smit M, Schoemaker RG, Gosens R, Maarsingh H, Zaagsma J, Meurs H. Tiotropium inhibits pulmonary inflammation and remodelling in a guinea pig model of COPD. *Eur Respir J* 2011;38:789–796.
18. Wright JL, Churg A. Animal models of cigarette smoke–induced COPD. *Chest* 2002; 122(6 Suppl)301S–306S.
19. Wright JL, Churg A. A model of tobacco smoke–induced airflow obstruction in the guinea pig. *Chest* 2002; 121(5 Suppl)188S–191S.
20. Gavaldà A, Miralpeix M, Ramos I, Otal R, Carreño C, Viñals M, Doménech T, Carcasona C, Reyes B, Vilella D, *et al*. Characterization of aclidinium bromide, a novel inhaled muscarinic antagonist, with long duration of action and a favorable pharmacological profile. *J Pharmacol Exp Ther* 2009;331:740–751.
21. European Medicines Agency. Eklira Genuair and Bretaris Genuair (aclidinium bromide) [Internet]. London: European Medicines Agency; c2012 [updated 2013 Aug 8; accessed 2013 Jul 29]. Available from: http://www.ema.europa.eu/ema/index.jsp?curl=pages/medicines/human/medicines/002211/human_med_001571.jsp&mid=WC0b01ac058001d124
22. U.S. Food and Drug Administration. Turdoza Pressair (aclidinium bromide) [Internet]. Silver Spring, MD: U.S. Food and Drug Administration; c2012 [accessed 2013 Jul 29]. Available from: http://www.accessdata.fda.gov/scripts/cder/drugsatfda/index.cfm?fuseaction=Search.DrugDetails
23. Maltais F, Celli B, Casaburi R, Porszasz J, Jarreta D, Seoane B, Caracta C. Aclidinium bromide improves exercise endurance and lung hyperinflation in patients with moderate to severe COPD. *Respir Med* 2011;105:580–587.
24. Fuhr R, Magnussen H, Sarem K, Llovera AR, Kirsten AM, Falqués M, Caracta CF, Garcia Gil E. Efficacy of aclidinium bromide 400 μg twice daily compared with placebo and tiotropium in patients with moderate to severe COPD. *Chest* 2012;141:745–752.
25. Kerwin EM, D'Urzo AD, Gelb AF, Lakkis H, Garcia Gil E, Caracta CF; ACCORD I Study Investigators. Efficacy and safety of a 12-week treatment with twice-daily aclidinium bromide in COPD patients (ACCORD COPD I). *COPD* 2012;9:90–101.
26. Jones PW, Singh D, Bateman ED, Agusti A, Lamarca R, de Miquel G, Segarra R, Caracta C, Garcia Gil E. Efficacy and safety of twice-daily aclidinium bromide in COPD patients: the ATTAIN study. *Eur Respir J* 2012;40:830–836.
27. Milara J, Serrano A, Peiró T, Gavaldà A, Miralpeix M, Morcillo EJ, Cortijo J. Aclidinium inhibits human lung fibroblast to myofibroblast transition. *Thorax* 2012;67:229–237.
28. Domínguez-Fandos D, Peinado VI, Puig-Pey R, Ferrer E, Musri MM, Ramírez J, Barberà JA. Pulmonary inflammatory reaction and structural changes induced by cigarette smoke exposure in the guinea pig. *COPD* 2012;9:473–484.
29. Ferrer E, Peinado VI, Díez M, Carrasco JL, Musri MM, Martínez A, Rodríguez-Roisin R, Barberà JA. Effects of cigarette smoke on endothelial function of pulmonary arteries in the guinea pig. *Respir Res* 2009;10:76.
30. Domínguez-Fandos D, Puig-Pey R, Ferrer E, Carreño C, Aparici M, Beleta J, Prats N, Miralpeix M, Gavaldà A, Peinado VI, *et al*. Effects of aclidinium bromide on airway remodeling in guinea pigs exposed to cigarette smoke for 6 months [abstract]. Presented at the American Thoracic Society International Conference. May 13–18, 2011, Denver, CO.
31. Ferrer E, Domínguez-Fandos D, Puig-Pey R, Carreño C, Aparici M, Beleta J, Prats N, Miralpeix M, Gavaldà A, Peinado VI, *et al*. Effects of aclidinium bromide on respiratory function in guinea pigs exposed to cigarette smoke for 6 months [abstract]. Presented at the American Thoracic Society International Conference. May 13–18, 2011, Denver, CO.
32. Lomask M. Further exploration of the Penh parameter. *Exp Toxicol Pathol* 2006;57:13–20.
33. Lewis CA, Ambrose C, Banner K, Battram C, Butler K, Giddings J, Mok J, Nasra J, Winny C, Poll C. Animal models of cough: literature review and presentation of a novel cigarette smoke-enhanced cough model in the guinea-pig. *Pulm Pharmacol Ther* 2007;20:325–333.
34. James AL, Hogg JC, Dunn LA, Paré PD. The use of the internal perimeter to compare airway size and to calculate smooth muscle shortening. *Am Rev Respir Dis* 1988;138:136–139.
35. Olea E, Ferrer E, Prieto-Lloret J, Gonzalez-Martin C, Vega-Agapito V, Gonzalez-Obeso E, Agapito T, Peinado V, Obeso A, Barbera JA, *et al*. Effects of cigarette smoke and chronic hypoxia on airways remodeling and resistance: clinical significance. *Respir Physiol Neurobiol* 2011;179:305–313.
36. Wright JL, Postma DS, Kerstjens HA, Timens W, Whittaker P, Churg A. Airway remodeling in the smoke exposed guinea pig model. *Inhal Toxicol* 2007;19:915–923.
37. Gwilt CR, Donnelly LE, Rogers DF. The non-neuronal cholinergic system in the airways: an unappreciated regulatory role in pulmonary inflammation? *Pharmacol Ther* 2007;115:208–222.
38. Roffel AF, Elzinga CR, Zaagsma J. Muscarinic M3 receptors mediate contraction of human central and peripheral airway smooth muscle. *Pulm Pharmacol* 1990;3:47–51.
39. Wessler I, Kirkpatrick CJ. Acetylcholine beyond neurons: the non-neuronal cholinergic system in humans. *Br J Pharmacol* 2008;154: 1558–1571.
40. Perng DW, Tao CW, Su KC, Tsai CC, Liu LY, Lee YC. Anti-inflammatory effects of salmeterol/fluticasone, tiotropium/fluticasone or tiotropium in COPD. *Eur Respir J* 2009;33:778–784.
41. Wen Y, Reid DW, Zhang D, Ward C, Wood-Baker R, Walters EH. Assessment of airway inflammation using sputum, BAL, and endobronchial biopsies in current and ex-smokers with established COPD. *Int J Chron Obstruct Pulmon Dis* 2010;5: 327–334.
42. Pieper MP, Chaudhary NI, Park JE. Acetylcholine-induced proliferation of fibroblasts and myofibroblasts *in vitro* is inhibited by tiotropium bromide. *Life Sci* 2007;80:2270–2273.
43. Gosens R, Bromhaar MM, Tonkes A, Schaafsma D, Zaagsma J, Nelemans SA, Meurs H. Muscarinic M(3) receptor-dependent regulation of airway smooth muscle contractile phenotype. *Br J Pharmacol* 2004;141:943–950.
44. Richens TR, Linderman DJ, Horstmann SA, Lambert C, Xiao YQ, Keith RL, Boé DM, Morimoto K, Bowler RP, Day BJ, *et al*. Cigarette smoke impairs clearance of apoptotic cells through oxidant-dependent activation of RhoA. *Am J Respir Crit Care Med* 2009; 179:1011–1021.
45. Churg A, Sin DD, Wright JL. Everything prevents emphysema: are animal models of cigarette smoke–induced chronic obstructive pulmonary disease any use? *Am J Respir Cell Mol Biol* 2011;45: 1111–1115.
46. Saetta M, Turato G, Baraldo S, Zanin A, Braccioni F, Mapp CE, Maestrelli P, Cavallesco G, Papi A, Fabbri LM. Goblet cell hyperplasia and epithelial inflammation in peripheral airways of smokers with both symptoms of chronic bronchitis and chronic airflow limitation. *Am J Respir Crit Care Med* 2000;161: 1016–1021.
47. Innes AL, Woodruff PG, Ferrando RE, Donnelly S, Dolganov GM, Lazarus SC, Fahy JV. Epithelial mucin stores are increased in the large airways of smokers with airflow obstruction. *Chest* 2006;130: 1102–1108.

48. Cortijo J, Mata M, Milara J, Donet E, Gavaldà A, Miralpeix M, Morcillo EJ. Aclidinium inhibits cholinergic and tobacco smoke–induced MUC5AC in human airways. *Eur Respir J* 2011;37:244–254.
49. Caramori G, Di Gregorio C, Carlstedt I, Casolari P, Guzzinati I, Adcock IM, Barnes PJ, Ciaccia A, Cavallesco G, Chung KF, *et al*. Mucin expression in peripheral airways of patients with chronic obstructive pulmonary disease. *Histopathology* 2004;45:477–484.
50. Ardite E, Peinado VI, Rabinovich RA, Fernández-Checa JC, Roca J, Barberà JA. Systemic effects of cigarette smoke exposure in the guinea pig. *Respir Med* 2006;100:1186–1194.
51. Caramori G, Casolari P, Di Gregorio C, Saetta M, Baraldo S, Boschetto P, Ito K, Fabbri LM, Barnes PJ, Adcock IM, *et al*. MUC5AC expression is increased in bronchial submucosal glands of stable COPD patients. *Histopathology* 2009;55:321–331.

ONLINE DATA SUPPLEMENT

Effects of Aclidinium Bromide in a Cigarette Smoke-Exposed Guinea Pig Model of COPD

David Domínguez-Fandos, Elisabet Ferrer, Raquel Puig-Pey, Cristina Carreño, Neus Prats, Mònica Aparici, Melina Mara Musri, Amadeu Gavaldà, Víctor I. Peinado, Montserrat Miralpeix and Joan A. Barberà

SUPPLEMENTARY MATERIALS AND METHODS

Animals used in the study

Fifty-eight male Hartley guinea pigs (~415 g in weight) were purchased from Harlam Ibérica, Spain. The animals were fed a diet of standard chow *ad libitum* and provided with water supplemented with vitamin C (1 g/L; Roche Pharma, Madrid, Spain). They were weighed weekly throughout the experimental protocol. The ethical review board on animal research of the University of Barcelona approved the experimental protocols of the study, which was performed in accordance with institutional guidelines that comply with national (Generalitat de Catalunya decree 214/1997, DOGC 2450) and international (Guide for the Care and Use of Laboratory Animals, National Institutes of Health, 85-23, 1985) laws and policies.

Cigarette-smoke exposure

Guinea pigs were divided into two groups at random: sham-exposed (room air) (n=22) and exposed to the smoke of non-filtered research cigarettes (3R4F; Kentucky University Research, Lexington, KY, USA) (n=36, 5 days/week, for 24 weeks), using a nose-only system (E1) (Protowerx Design Inc, Langley, British Columbia, Canada). Over the first three weeks, the amount of cigarettes was increased gradually to habituate the animals. From the fourth week onward, the animals began to be exposed to the total load of cigarettes (6 per day).

Administration of aclidinium bromide

Micronized aclidinium bromide was synthesized and provided by Almirall S.A. (Barcelona, Spain). The animals from each group were treated daily for 6 months with either distilled water (vehicle), 10 µg/mL (Ac10) or 30 µg/mL (Ac30) of aclidinium solution. Thus, six final groups were used: vehicle+sham, vehicle+cigarette smoke (CS), Ac10+sham, Ac10+CS, Ac30+sham, and Ac30+CS. Animals treated with vehicle or aclidinium were nebulized with an ultrasonic nebulizer (Devilbiss Ultraneb 3000, Somerset, PA, USA) in methacrylate chambers for 12 minutes, 1 hour before exposure to CS or air (sham). For the first 2 minutes the nebulizer was switched on and for the following 4 minutes it was switched off (E2). This procedure was repeated twice. The nebulization was directed at guinea pigs via a gas mixture containing 5% CO_2, 21% O_2, and 74% N_2 (Air Liquide, Barcelona, Spain).

Aclinidinium concentrations (10 and 30 µg/mL) selected in this study were below to those that produce adverse effects in long-term toxicological studies in rats and dogs (3 and 6 months). In addition, the bronchoprotective effect in front of acetylcholine challenge in guinea pigs at 30 µg/mL was lower than 50% after 24 hours of aclidinium administration (E2). Taken together, the aclidinium concentrations used in this chronic study are not supramaximal.

Unrestrained whole-body plethysmography

Respiratory function was measured weekly in conscious guinea pigs by unrestrained whole-body plethysmography (Buxco Research Systems, Wilmington, NC, USA). Guinea pigs that breathed spontaneously were placed inside the chambers. The recording period started when the animals had adapted (no scratching, sniffing, or chewing) and data was collected and averaged for 3 minutes. Pressure signals were fed into a computer for visualization, storage, and offline analysis with specific software. Measured ventilatory parameters included breathing frequency (Bf) and tidal volume (TV). Respiratory resistance was assessed by the enhanced pause (Penh) (E3, E4). Penh is a unit-less index described as:

$$Penh = PEF/PIF \times (Te/Rt-1)$$

Where PEF is the peak of expiratory height, PIF is the peak of inspiratory height, Te is the expiratory time, and Rt is the time to expire 65% of the volume.

Measurements were recorded at three different points: 24 hours after the last exposure to CS (baseline), 30 minutes after nebulization of aclidinium or vehicle, and 10 minutes after exposure to CS or sham (Figure E1). At the end of the study, the area under the curve (AUC) for each parameter (Penh, TV, and Bf) assessed along the 6 months of study (Figure E2) was calculated using a logistic curve-fitting equation for each animal.

Assessment of cough

The number of cough episodes during the first minute after CS exposure was counted *de visu* once a week in each animal for the last 16 weeks of the study by two independent observers. The criterion for cough was a characteristic high sound with the mouth open, which was easily distinguished from a sneeze (E5).

Lung-tissue preparation

Twenty-four hours after their last exposure to CS, the animals were anesthetized with 50 mg/kg ketamine and 7 mg/kg xylazine by intramuscular puncture.

A blood sample (500 µL) was collected from each animal to evaluate hematological parameters. The differential blood-cell count, including lymphocytes, eosinophils, neutrophils, monocytes, and total white blood cells, was analyzed by hematology analyzer (Sysmex, Kobe, Japan).

The lungs of each guinea pig were removed, inflated, and fixed for 24 hours with 4% formaldehyde by airway instillation under constant pressure of 30 cm H_2O. After sampling, tissue blocks were dehydrated and lung sections were embedded in paraffin or frozen using optimal cut temperature (O.C.T; Tissue-Tek, Sakura Finetek, Zoeterwoude, The Netherlands).

Morphometric analysis of airways

Tissue preparation and airway sampling. Paraffin blocks were cut into serial sections 5 µm thick and placed on glass slides for histological examination. Ten cross-sectional airways stained with hematoxylin-eosin per animal were randomly photographed at a magnification of x320 using a Leica DM5000 B light microscope with a Leica DFC300 FX digital camera (Leica Microsystems Imaging Solutions Ltd, Cambridge, UK).

Stereological methods and measurements of airway dimensions. Airways cut in a reasonable cross-section (a long-short diameter ratio up to 2:1) were evaluated. Images were analyzed by planimetry using Image-Pro Plus 4.5 software (Media Cybernetics, Carlsbad, CA, USA). Different morphological dimensions were measured on each airway (E6) in sections immunostained with primary monoclonal mouse anti-human smooth muscle α-actin (M0851; DakoCytomation, Glostrup, Denmark). The smooth-muscle perimeters Pos and Pis were defined respectively as the perimeter of the outer and inner border of the muscular layer. The areas outlined by Pos and Pis were also determined (Aos and Ais). The perimeter of the airway lumen (internal luminal perimeter, Pil) and its outlined area (luminal area, Ail) were also defined. Thickness of the muscular layer was calculated as the difference in Aos and Ais divided by Pil ((Aos – Ais) / Pil). Airway smooth-muscle content in muscular layer was calculated in airways immunostained with smooth-muscle α-actin by dividing the α-actin$^+$ area in the muscular layer by the Pil. Mucosa+submucosa ((Ais - Ail) / Pil), adventitial (Aad / Pil), and total wall thickness ((Aad + (Aos – Ail)) / Pil) were also calculated, where Aad is the area of the adventitial layer.

Because the histological examination of airways in the guinea pig shows no differences between different branches, to identify their position in the airway tree and normalize assessments by size the median Pil value in the airways was used as an internal reference parameter (E7), not only to normalize assessments by airway size but also to group the airway into larger (above the median) or smaller (under the median). Median Pil value is obtained with all the airways analyzed.

Inflammatory cells

Histological examination of inflammatory cells was performed in 5 μm-thick serial sections stained with hematoxylin-eosin to identify neutrophils, eosinophils, and lymphoid follicles. Macrophages were counted on sections stained with periodic acid-Schiff. Ten airways cut in a reasonable cross-section at a magnification of x320 and 20 fields of parenchyma (x640) were randomly selected and photographed. In the airways, cell counting was related to Pil and in the alveolar septa it was expressed as number of cells per septa area. Sections of lung tissue were examined for the presence or absence of lymphoid follicles. When these were present, the sum of the area occupied by all the lymphoid follicles was calculated and normalized by the number of airways.

Data analysis

Normally distributed variables are expressed as mean±standard deviation in tables and as mean±standard error of the mean in figures. Non-normally distributed variables are expressed as median and interquartile range.

To analyze the evolution of plethysmographic respiratory parameters (Bf, TV, Penh), assessed weekly throughout the 6-month study period, we calculated the AUC of all the measurements performed in each animal as a summary measure.

Comparisons between groups were carried out using a two-way analysis of variance. The main effects of CS exposure, aclidinium and their interaction were analyzed. When significant, *post-hoc* pairwise comparisons were performed using the Student-Newman-Keuls test. In the Penh, expressed as AUC value, a logarithmic transformation was performed in order to normalize distributions since data were not homoscedastic, and followed a non-normal distribution.

To investigate whether some of the parameters evaluated may differ according to the size of the airways or the pulmonary vessels (E8), specific assessments were carried out in airways and vessels with Pil and internal elastic lamina perimeter (Pim) values, above (larger) or below (smaller) the median value. Relationships between variables were assessed using the Pearson's correlation test. A P value < 0.05 was considered significant.

References

E1. Ardite E, Peinado VI, Rabinovich RA, Fernandez-Checa JC, Roca J, Barbera JA. Systemic effects of cigarette smoke exposure in the guinea pig. *Respir Med* 2006;100:1186–1194.

E2. Gavaldà A, Miralpeix M, Ramos I, Otal R, Carreño C, Viñals M, Doménech T, Carcasona C, Reyes B, Vilella D, Gras J, Cortijo J, Morcillo E, Llenas J, Ryder H, Beleta J. Characterization of aclidinium bromide, a novel inhaled muscarinic antagonist, with long duration of action and a favorable pharmacological profile. *J Pharmacol Exp Ther* 2009;331:740–751.

E3. Hamelmann E, Schwarze J, Takeda K, Oshiba A, Larsen GL, Irvin CG, Gelfand EW. Noninvasive measurement of airway responsiveness in allergic mice using barometric plethysmography. *Am J Respir Crit Care Med* 1997;156:766–775.

E4. Lomask M. Further exploration of the Penh parameter. *Exp Toxicol Pathol* 2006;57 Suppl 2:13–20.

E5. Lewis CA, Ambrose C, Banner K, Battram C, Butler K, Giddings J, Mok J, Nasra J, Winny C, Poll C. Animal models of cough: literature review and presentation of a novel cigarette smoke-enhanced cough model in the guinea pig. *Pulm Pharmacol Ther* 2007;20:325–333.

E6. Kuwano K, Bosken CH, Pare PD, Bai TR, Wiggs BR, Hogg JC. Small airways dimensions in asthma and in chronic obstructive pulmonary disease. *Am Rev Respir Dis* 1993;148:1220–1225.

E7. James AL, Hogg JC, Dunn LA, Pare PD. The use of the internal perimeter to compare airway size and to calculate smooth muscle shortening. *Am Rev Respir Dis* 1988;138:136–139.

E8. Dominguez-Fandos D, Peinado VI, Puig-Pey R, Ferrer E, Musri MM, Ramirez J, Barbera JA. Pulmonary inflammatory reaction and structural changes induced by cigarette smoke exposure in the Guinea pig. *COPD* 2012;9:473–484.

TABLE

TABLE E1. CHARACTERISTICS OF INFLAMMATORY CELL INFILTRATE

			Vehicle		Ac10 µg/ml		Ac30 µg/ml		Two-way ANOVA main effects (*P* Value)		
			Sham-exposed *(n=8)*	CS-exposed *(n=10)*	Sham-exposed *(n=7)*	CS-exposed *(n=6)*	Sham-exposed *(n=7)*	CS-exposed *(n=8)*	CS exposure	Ac	Interaction
Intraseptal (cells/mm^2)	Neutrophils		10.2 (6.3-13.1)	12.6 (10.8-16.4)	10.2 (6.8-11.5)	13.3 (9.2-16.2)	6.7 (4.1-9.7)	10.2 (7.7-13.2)	0.004	0.039	0.988
	Macrophages		1.3 (0.8-2.2)	8.1 (4.9-10.0)	1.9 (1.4-2.3)	9.1 (5.2-12.7)	1.5 (1.3-2.7)	7.9 (6.1-15.7)	≤0.001	0.462	0.747
	Eosinophils		1.6 (0.0-2.1)	4.7 (2.1-7.7)	0.9 (0.0-3.1)	6.5 (2.7-14.8)	1.2 (0.9-2.3)	4.9 (0.5-6.1)	0.001	0.288	0.414
Airways (cells/mm)	Neutrophils	All airways	0.1 (0.0-0.1)	0.7 (0.4-0.8)	0.1 (0.0-0.2)	1.0 (0.3-1.3)	0.1 (0.1-0.2)	0.6 (0.2-0.8)	0.002	0.707	0.598
		Larger airways	0.1 (0.0-0.2)	0.4 (0.3-0.7)	0.1 (0.0-0.4)	0.4 (0.1-0.9)	0.1 (0.02-0.1)	0.8 (0.2-1.0)	0.014	0.890	0.646
		Smaller airways	0.0 (0.0-0.0)	0.8 (0.3-1.6)	0.0 (0.0-0.2)	1.3 (0.8-1.5)	0.0 (0.0-0.2)	0.3 (0.0-0.5)	0.002	0.291	0.276
	Eosinophils	All airways	1.5 (0.9-1.6)	3.6 (1.7-6.8)	1.3 (1.1-2.0)	4.5 (2.4-6.9)	1.6 (0.9-2.4)	1.7 (1.3-2.7)	0.003	0.244	0.186
		Larger airways	1.6 (1.3-2.1)	3.0 (1.8-5.4)	1.2 (1.1-1.4)	2.6 (1.6-4.8)	1.7 (1.0-2.5)	1.7 (1.2-3.0)	0.046	0.386	0.346
		Smaller airways	1.0 (0.5-1.5)	3.5 (1.2-10.4)	1.4 (0.8-2.2)	5.7 (1.3-9.9)	1.7 (0.5-2.3)	2.0 (0.8-2.4)	0.003	0.167	0.156
Lymphoid follicles (µm^2)			5688±6803	27043±27518	1593±4216	12952±11346	2056±3542	17337±18195	0.002	0.268	0.686

Definition of abbreviations: Ac = aclidinium; ANOVA = analysis of variance; CS = cigarette smoke.
Values are median (interquartile range) and mean±standard deviation.

FIGURE LEGENDS

Figure E1.

Experimental protocol diagram for the measurement of lung-function parameters. Once a week, pulmonary function was evaluated using unrestrained whole-body plethysmography system at three different points: baseline, 30 minutes after nebulization, and 10 minutes after cigarette smoke (CS)/sham exposure.

Figure E2.

Evolution of weekly measurements of the enhanced pause (Penh), evaluated by unrestrained whole plethysmography, at baseline, during the 6 months of the study period. Values are median at each weekly measurement of animals in each experimental group. As a summary measure of all the assessments, the area under the curve (AUC) was calculated for each animal. The median AUC of each experimental group is shown. Ac10 = aclidinium 10 μg/mL; Ac30 = aclidinium 30 μg/mL; CS = cigarette smoke.

Figure E3.

Accumulated coughs per animal during the study. Symbols show the accumulated mean value in the six experimental groups. Ac10 = aclidinium 10 μg/mL; Ac30 = aclidinium 30 μg/mL; CS = cigarette smoke.

Figure E4.

Goblet cell metaplasia in airways. (A) Number of muco-secretory cells in the epithelial surface of airways in all the airways analyzed (left panel), in airways with internal perimeter above the median (central panel), and in airways with internal perimeter below the median (right panel). Assessments were performed in guinea pigs exposed to cigarette smoke (CS) or sham, treated with vehicle, aclidinium bromide (Ac) 10 (Ac10) or 30 (Ac30) μg/mL. Values are mean±standard error of the mean of each experimental group. P values denote the main effects in the two-way analysis of variance: CS, Ac.

(B) Microphotographs of transverse sections of airways stained with alcian blue in a representative case of each experimental group. Note the increased number of goblet cells, stained light blue, in the epithelium of CS-exposed animals. Scale bar, 50 μm.

Figure E5.

Assessment of pulmonary emphysema. (A) Airspace size, evaluated by the mean linear intercept, in the lung parenchyma. Assessments were performed in guinea pigs exposed to cigarette smoke (CS) or sham, treated with vehicle, aclidinium bromide (Ac) 10 (Ac10) or 30 (Ac30) μg/mL. Values are mean±standard error of the mean of each experimental group.

P values denote the main effects in the two-way analysis of variance: CS, Ac. There was a trend toward significant interaction between CS and Ac ($P = 0.054$), given that the interseptal distance in CS-exposed animals treated with Ac was similar to that of their respective sham-exposed controls.

Microphotographs of lung parenchyma sections stained with hematoxylin of a sham-exposed guinea pig (B) and a CS-exposed (C) animal. Scale bar, 50 μm.

Figure E6.

Muscularization of small intrapulmonary arteries. (A) Bar charts showing the number of vessels with positive immunoreactivity for smooth-muscle α-actin. Assessments were performed in guinea pigs exposed to cigarette smoke (CS) or sham, treated with vehicle, aclidinium bromide (Ac) 10 (Ac10) or 30 (Ac30) μg/mL. Values are mean±standard error of the mean of each experimental group. P values denote the main effects in the two-way analysis of variance: CS, Ac.

Microphotographs of sections immunostained with smooth-muscle α-actin antibody of a sham-exposed (B) and CS-exposed (C) animal. Scale bar, 50 µm.

Figure E7.

Pulmonary lymphoid follicles. (A) Plots of individual counts of the area occupied by lymphoid follicles per number of airways. Assessments were performed in guinea pigs exposed to cigarette smoke (CS) or sham, treated with vehicle, aclidinium bromide (Ac) 10 (Ac10) or 30 (Ac30) µg/mL. The horizontal bars denote the mean value in each group.
P values denote the main effects in the two-way analysis of variance: CS, Ac.
Microphotographs of a lymphoid follicle in a guinea pig exposed to CS at low (B) (scale bar, 200 µm) and high (C) (scale bar, 50 µm) magnification.

Figure E8.

Correlations between inflammatory infiltrate and remodeling. Linear regression of neutrophils (A) and eosinophils (B) with the thickness of total wall in small airways (lumen perimeter below the median value). in guinea pigs exposed to cigarette smoke, treated with vehicle, aclidinium bromide (Ac) 10 (Ac10) or 30 (Ac30) µg/mL. The thickness of total wall in small airways was significantly correlated with both measurements (r = 0.61, $P = 0.002$ and r = 0.66, $P < 0.001$, respectively).

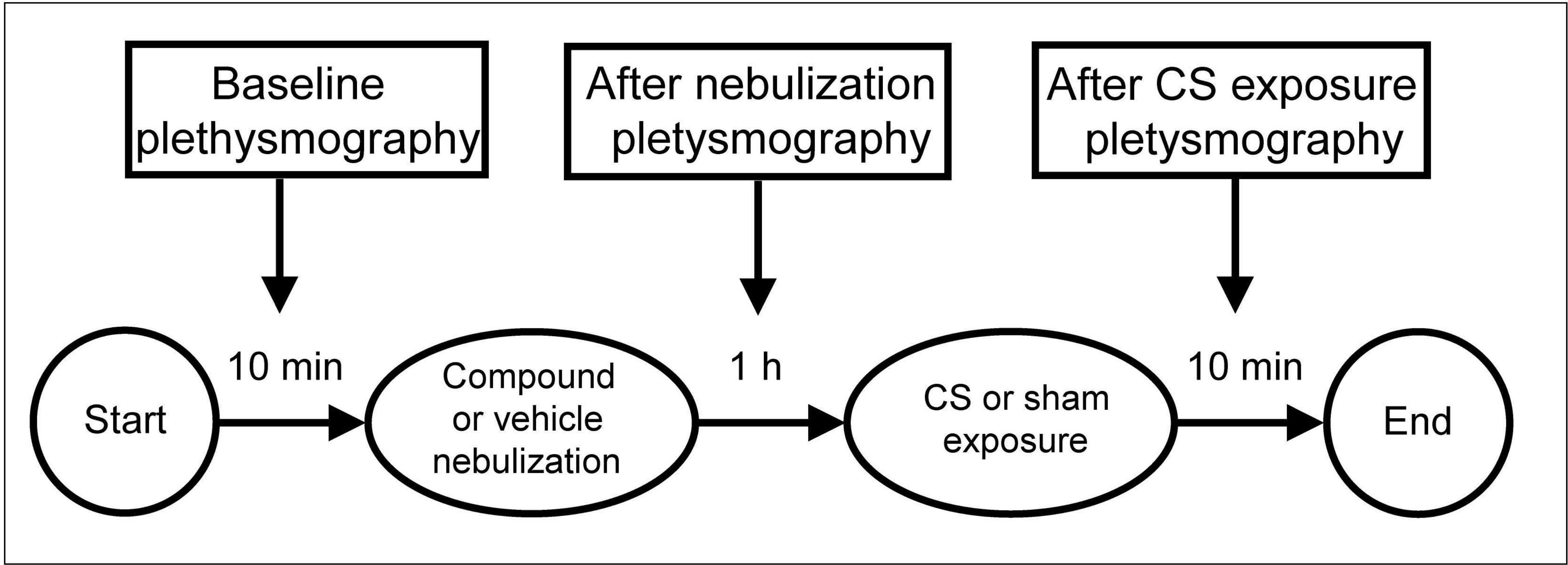
Baseline plethysmography
After nebulization pletysmography
After CS exposure pletysmography
Start
10 min
Compound or vehicle nebulization
1 h
CS or sham exposure
10 min
End

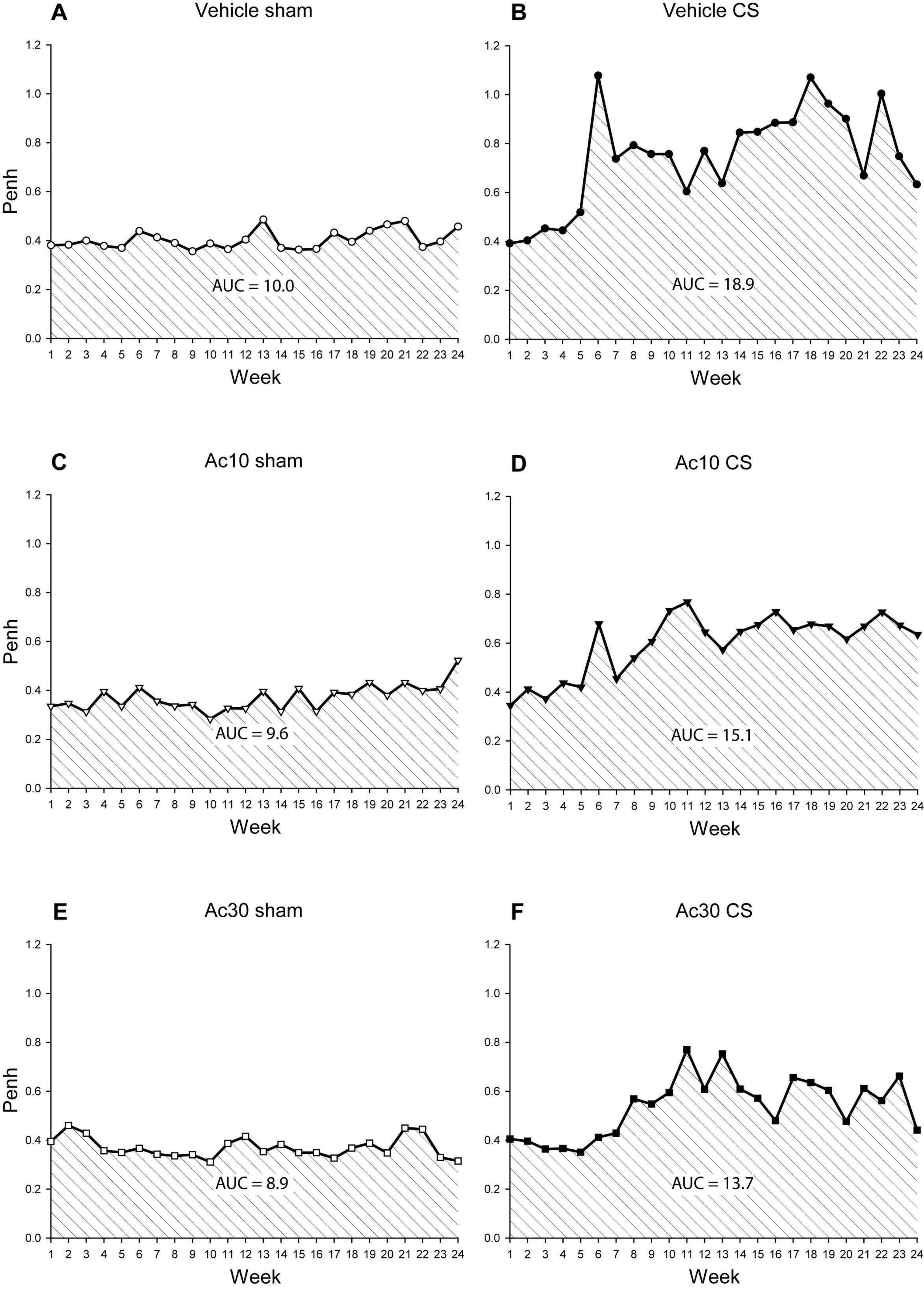

A
Vehicle sham
B
Vehicle CS
C
Ac10 sham
D
Ac10 CS
E
Ac30 sham
F
Ac30 CS
Penh
Week
AUC = 10.0
AUC = 18.9
AUC = 9.6
AUC = 15.1
AUC = 8.9
AUC = 13.7

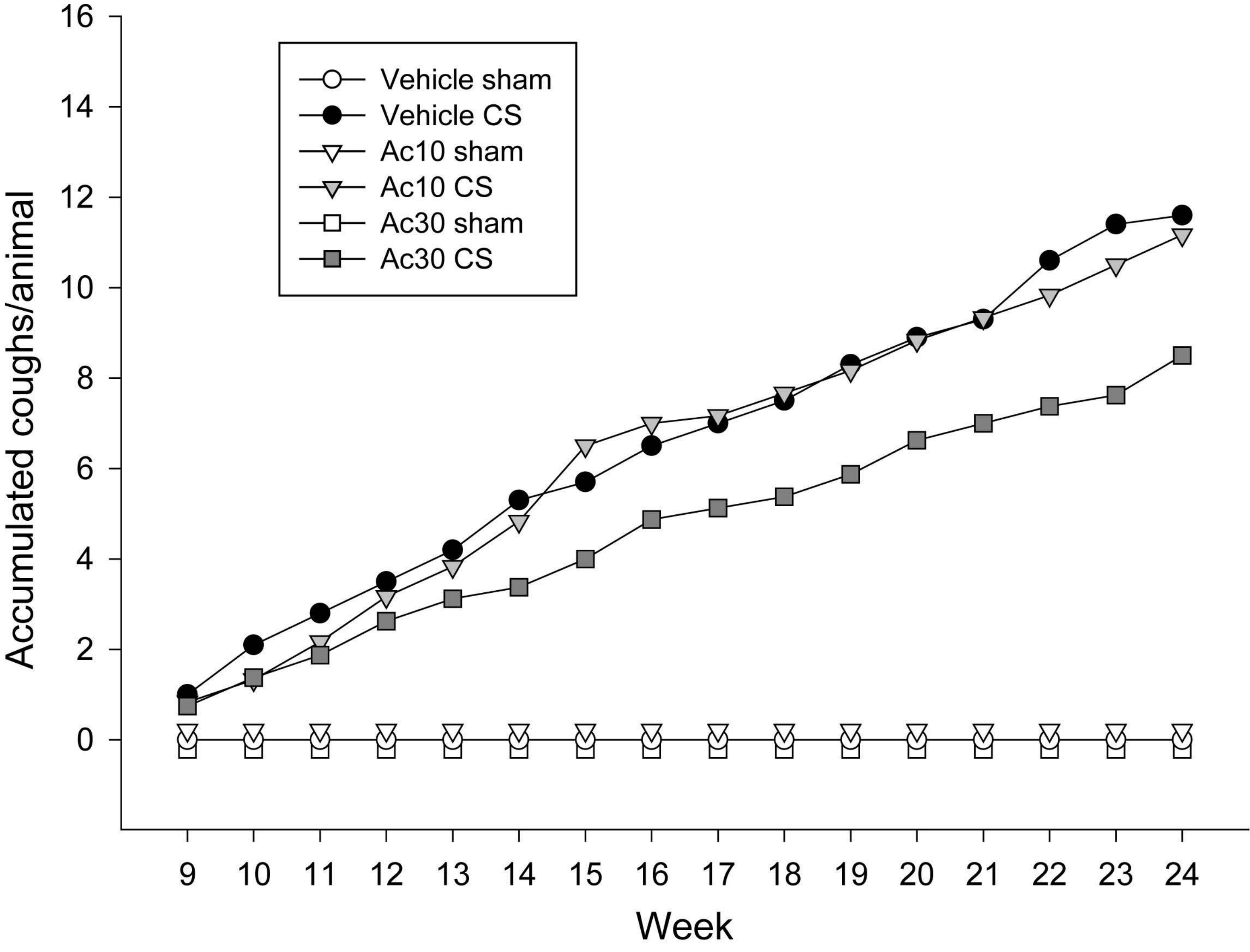

Vehicle sham
Vehicle CS
Ac10 sham
Ac10 CS
Ac30 sham
Ac30 CS
Accumulated coughs/animal
Week
0
2
4
6
8
10
12
14
16
9
10
11
12
13
14
15
16
17
18
19
20
21
22
23
24

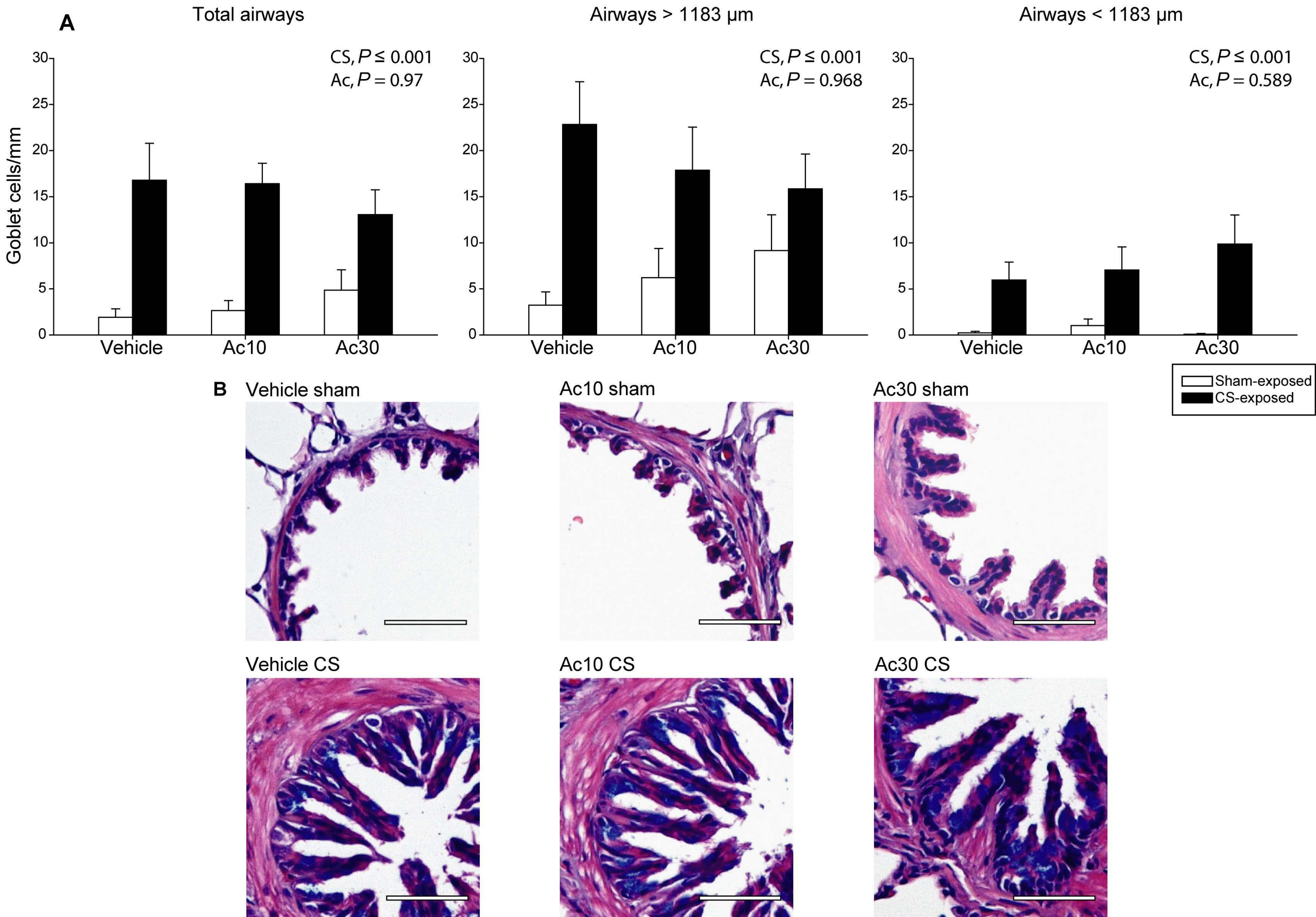
A
Total airways
Airways > 1183 µm
Airways < 1183 µm
Goblet cells/mm
CS, $P \leq 0.001$
Ac, $P = 0.97$
CS, $P \leq 0.001$
Ac, $P = 0.968$
CS, $P \leq 0.001$
Ac, $P = 0.589$
0
5
10
15
20
25
30
Vehicle
Ac10
Ac30
Sham-exposed
CS-exposed
B
Vehicle sham
Ac10 sham
Ac30 sham
Vehicle CS
Ac10 CS
Ac30 CS

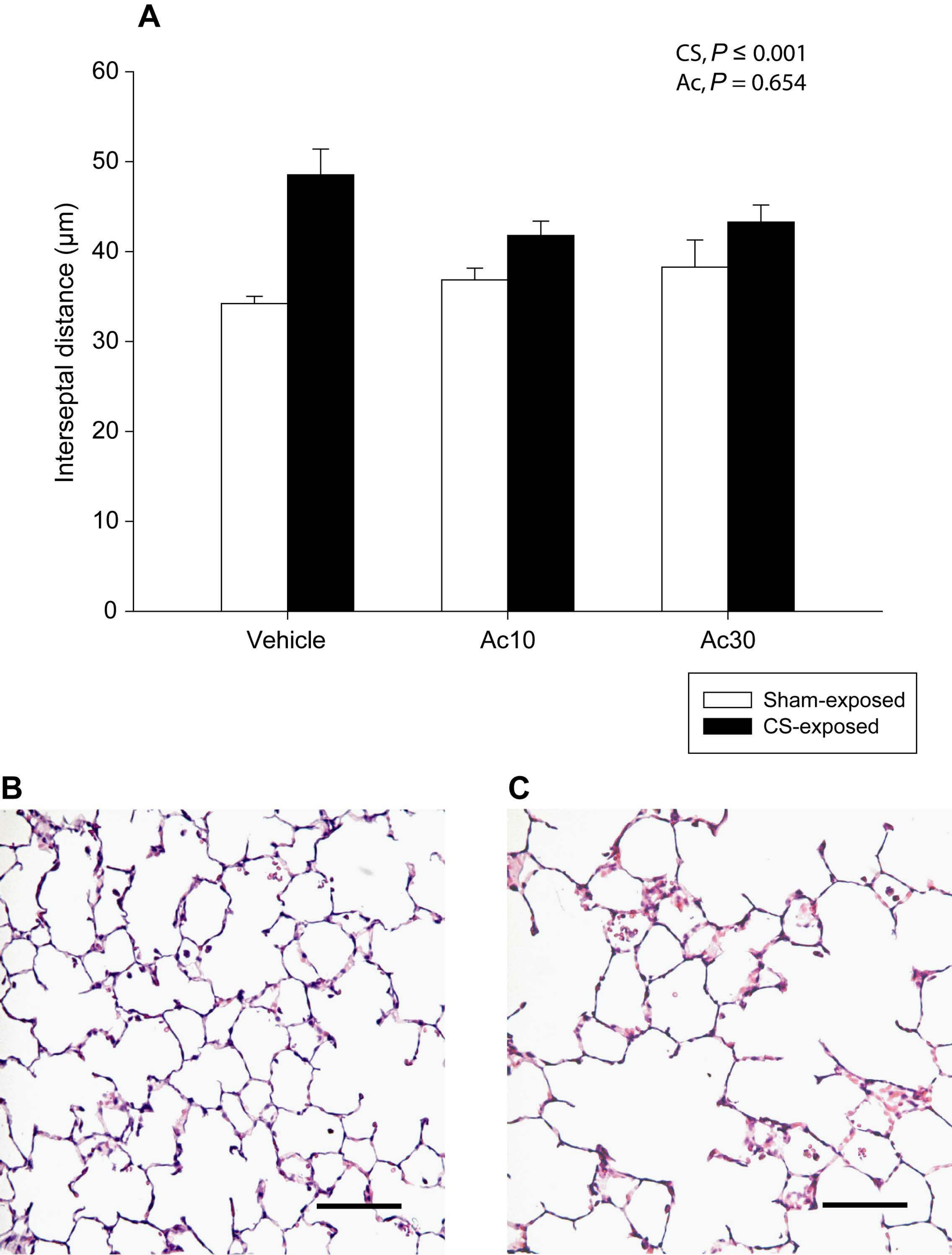
A
CS, P ≤ 0.001
Ac, P = 0.654
Interseptal distance (μm)
60
50
40
30
20
10
0
Vehicle
Ac10
Ac30
Sham-exposed
CS-exposed
B
C

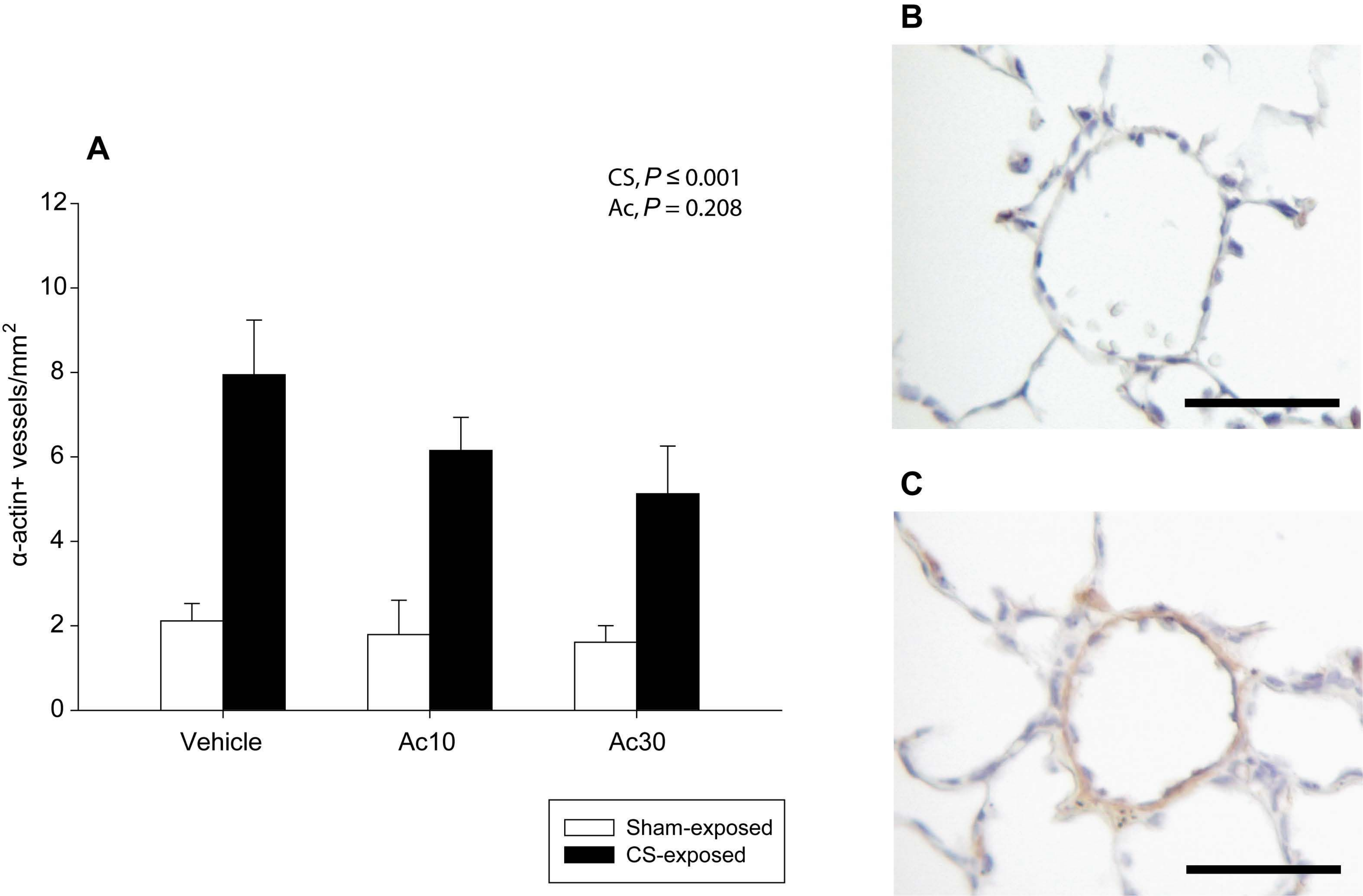

A
CS, $P \leq 0.001$
Ac, $P = 0.208$
α-actin+ vessels/mm^2
0
2
4
6
8
10
12
Vehicle
Ac10
Ac30
Sham-exposed
CS-exposed
B
C

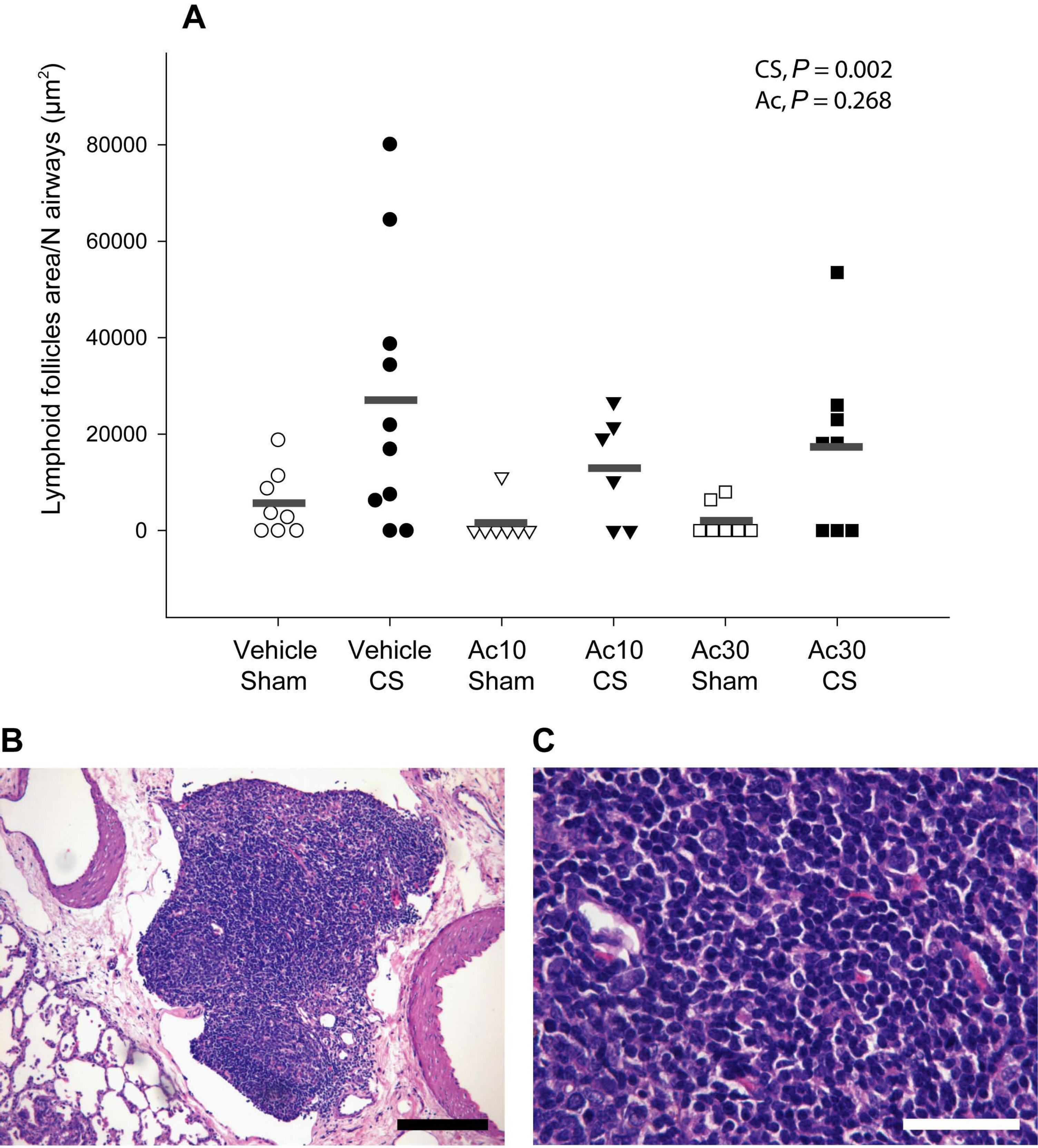
A
B
C
CS, P = 0.002
Ac, P = 0.268
Lymphoid follicles area/N airways (µm²)
80000
60000
40000
20000
0
Vehicle Sham
Vehicle CS
Ac10 Sham
Ac10 CS
Ac30 Sham
Ac30 CS

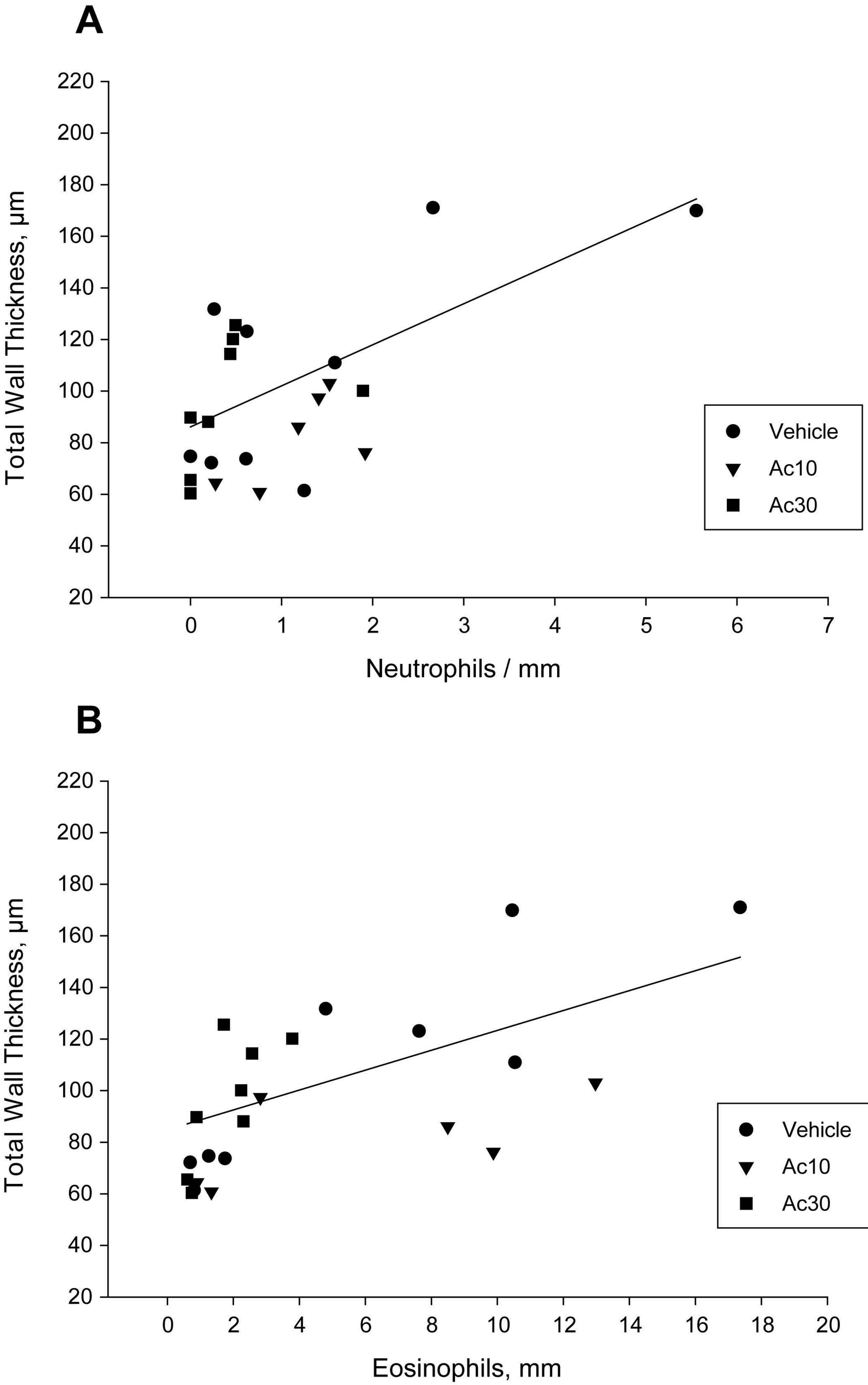
A
Total Wall Thickness, µm
220
200
180
160
140
120
100
80
60
40
20
0
1
2
3
4
5
6
7
Neutrophils / mm
Vehicle
Ac10
Ac30
B
Total Wall Thickness, µm
220
200
180
160
140
120
100
80
60
40
20
0
2
4
6
8
10
12
14
16
18
20
Eosinophils, mm
Vehicle
Ac10
Ac30

2.1.- Resultados principales

Función respiratoria

El valor medio del Penh (*enhanced pause*) a nivel basal a lo largo del estudio fue más elevado en los animales expuestos al HC. El tratamiento con aclidinio produjo una disminución del Penh, sin diferencias entre ambas dosis testadas. En cambio, después de la nebulización del fármaco la reducción del valor medio del Penh en los animales expuestos al HC fue mayor con la dosis de 30 μg/mL.

La exposición al HC produjo un aumento inmediato de 4 a 6 veces en el Penh. Esta reactividad tendió a ser menor en los animales tratados con aclidinio. Además, el valor medio de Penh después de la exposición al HC a lo largo del estudio también fue menos elevado con el tratamiento con aclidinio, particularmente con la dosis de 30 μg/mL.

La exposición al HC cambió el patrón respiratorio, produciendo un aumento de frecuencia respiratoria (FR) y volumen corriente (VC) sobre los que aclidinio no tuvo efecto. Los cobayos tratados con aclidinio también mostraron una tendencia a una mayor FR basal. Después de la nebulización del compuesto, tanto la FR como el VC fueron menos elevados en los cobayos no expuestos tratados con aclidinio 30 μg/mL.

Episodios de tos

El HC indujo episodios de tos en los cobayos. En los animales expuestos al HC la administración de aclidinio 30 μg/mL tendió a disminuir los episodios de tos y mostraron mejor tolerancia al HC, presentando menos episodios de broncoconstricción.

Análisis histológicos

Vía aérea: la exposición al HC indujo el engrosamiento de la pared bronquial a expensas de todas sus capas, especialmente de la vía aérea pequeña, provocando una reducción de su luz. El engrosamiento de la capa muscular fue debido al mayor contenido en músculo liso α-actina+. En los cobayos expuestos al HC y tratados con ambas dosis de aclidinio, este incremento del grosor de la pared bronquial fue menos acentuado, y fue particularmente evidente en la capa muscular y en la vía aérea pequeña. De hecho, el contenido en músculo liso en la vía aérea, en los animales expuestos al HC y tratados con aclidinio fue similar al de los animales no expuestos. Sin embargo, el grosor de la mucosa y adventicia no mostró diferencias debidas a aclidinio.

La exposición al HC provocó un incremento de células caliciformes en epitelio bronquial, en particular en la vía aérea más grande, que no se modificó con el tratamiento con aclidinio.

Parénquima pulmonar: se desarrolló enfisema en los animales expuestos al HC y hubo una tendencia a un menor aumento del tamaño de los espacios aéreos en los animales expuestos al HC tratados con aclidinio.

Vasos intrapulmonares: la exposición al HC indujo muscularización de los vasos intrapulmonares pequeños, que no se modificó con la administración de aclidinio.

Células inflamatorias: el infiltrado de células inflamatorias en el septo alveolar y la vía aérea estaba aumentado en los animales expuestos al HC. La administración de aclidinio se asoció a menor infiltración de neutrófilos en el septo alveolar. En cambio, su administración no modificó el número de macrófagos o eosinófilos intraseptales ni de neutrófilos o eosinófilos infiltrando la vía aérea. El tratamiento con aclidinio no modificó ni el número ni el tamaño de los folículos linfoides que indujo la exposición al HC.

<u>Correlaciones</u>

En los animales expuestos al HC, el valor de Penh a nivel basal correlacionó con el grosor de la capa muscular de la vía aérea, particularmente de la más pequeña, y también con el grado de enfisema. Además, el número de neutrófilos y eosinófilos que infiltran vía aérea correlacionó con el grosor de la pared de los bronquios de menor calibre.

3.- Tercer artículo

Sildenafil in a cigarette smoke-induced model of COPD in the guinea pig.

David Domínguez-Fandos, César Valdés, Elisabet Ferrer, Raquel Puig-Pey, Isabel Blanco, Olga Tura-Ceide, Tanja Paul, Víctor Ivo Peinado, Joan Albert Barberà.

Artículo remitido a European Respiratory Journal,
actualmente en segunda revisión.

European Respiratory Journal - Minor Revision decision on Manuscript ID ERJ-01399-2014.R1

Dear Dr Barbera:

Thank you very much for your submission to the ERJ. Your manuscript entitled "Sildenafil in a cigarette smoke-induced model of COPD in the guinea pig" has been evaluated by anonymous reviewers and the editors, and we are pleased to inform you that your manuscript has been accepted for publication in the ERJ, on the condition that the below reviewers' comments are adequately addressed.

Thank you in advance. We look forward to receiving your revised manuscript.

Yours sincerely,

Prof. Norbert Voelkel
European Respiratory Journal

Prof. M. Humbert
ERJ Chief Editor

Prof. A.T. Dinh-Xuan
Deputy Chief Editor

erj.chief-editors@ersnet.org

Sildenafil in a cigarette smoke-induced model of COPD in the guinea pig

David Domínguez-Fandos[1], César Valdés[1], Elisabet Ferrer[1], Raquel Puig-Pey[1], Isabel Blanco[1,2], Olga Tura-Ceide[1,2], Tanja Paul[1], Víctor I. Peinado[1,2] and Joan A. Barberà[1,2].

[1]Department of Pulmonary Medicine, Hospital Clínic-Institut d'Investigacions Biomèdiques August Pi i Sunyer (IDIBAPS), University of Barcelona, Barcelona, Spain; and [2]Centro de Investigación Biomédica en Red (CIBER) de Enfermedades Respiratorias, Madrid, Spain.

Address for correspondence and reprint requests: Joan A. Barberà; Servei de Pneumologia, Hospital Clínic, Villarroel 170, 08036 Barcelona, Spain. Fax: (+34) 93 227 5455. E-mail: jbarbera@clinic.ub.es

Total word count: 2999

ABSTRACT

Sildenafil, a phosphodiesterase-5 inhibitor used to treat pulmonary hypertension (PH), may have effects on pulmonary vessel structure and function. We evaluated the effects of sildenafil in a cigarette smoke (CS)-exposed model of chronic obstructive pulmonary disease (COPD).

Forty-two guinea pigs were exposed to CS or sham-exposed and treated with sildenafil or vehicle for 12 weeks, divided into 4 groups. Assessments included: respiratory resistance, pulmonary artery pressure (PAP), right ventricle (RV) hypertrophy, endothelial function of the pulmonary artery (PA), and lung vessels and parenchymal morphometry.

CS-exposed animals showed increased PAP, RV hypertrophy, raised respiratory resistance, airspace enlargement, and intrapulmonary vessel remodelling. CS exposure also produced wall thickening, increased contractility and endothelial dysfunction in the main PA. CS-exposed animals treated with sildenafil showed lower PAP and a trend to less RV hypertrophy than CS-exposed only. Furthermore, sildenafil preserved the intrapulmonary vessel density and attenuated the airspace enlargement induced by CS. No differences in gas exchange, respiratory resistance, endothelial function and vessel remodelling were observed.

We conclude that in this experimental model of COPD, sildenafil prevents the development of PH and contributes to preserve the parenchymal and vascular integrity, reinforcing the notion that the nitric oxide-cGMP axis is perturbed by CS exposure.

Abstract word count: 199

Summary: Sildenafil reduces pulmonary vascular tone and contributes to preserve tissue integrity in experimental COPD.

This article has supplementary material accessible from www.erj.ersjournals.com

INTRODUCTION

Pulmonary hypertension (PH) is a frequent and serious complication of chronic obstructive pulmonary disease (COPD), triggered in part by cigarette smoke (CS) exposure [1]. The pathophysiology of PH in COPD involves endothelial dysfunction, imbalance of growth factors [2] and an enhanced inflammatory response [3] in pulmonary vessels. These factors, alone or in combination, induce smooth muscle cell (SMC) proliferation in the vessel wall leading to increased pulmonary vascular resistance.

Endothelial dysfunction in pulmonary arteries of COPD patients is associated with reduced endothelial nitric oxide synthase (eNOS) expression and impaired release of nitric oxide (NO) [4, 5]. Endothelial NO activates the soluble guanylate cyclase (sGC) resulting in the formation of the secondary messenger cyclic guanosine monophosphate (cGMP) [4, 6]. Intracellular cGMP decreases the concentration of intracellular calcium, thereby relaxing vascular SMC [7]. Endothelial NO may also inhibit SMC proliferation through cGMP-dependent mechanisms [8]. In the lung, cGMP is metabolised primarily by the action of phosphodiesterase-5 (PDE5). Inhibitors of PDE5, like sildenafil, enhance the NO-cGMP signalling pathway and exert vasodilator and anti-proliferative effects [9]. Studies in experimental models of PH induced by hypoxia [10] or monocrotaline [11, 12] have shown that sildenafil reduces pulmonary artery pressure (PAP), prevents RV hypertrophy and exerts an anti-remodelling effect in pulmonary vessels. Sildenafil is currently used for the treatment of pulmonary arterial hypertension [13].

In patients with COPD and associated PH, we have demonstrated that sildenafil decreases pulmonary vascular resistance acutely [14], but this effect did not translate into augmented exercise tolerance when administered during 3 months [15]. This limited influence on exercise tolerance could be due to the concomitant changes that occur in the lung parenchyma and airways of COPD patients.

The effects of sildenafil on lung structure have not been evaluated in experimental models of COPD. The utilization of guinea pigs exposed to CS is the most advantageous approach to reproduce COPD features by using the primary disease-causing agent [16, 17]. This species lacks hypoxic pulmonary vasoconstriction (HPV) but develops chronic PH after exposure to CS for relatively long periods [17]. The lack of HPV is an additional advantage to test the anti-remodelling effects of vasodilators minimizing a potential detrimental effect on gas exchange.

In a recent study we have demonstrated that the administration of a NO-independent sGC stimulator to guinea pigs chronically exposed to CS reduces pulmonary vascular resistance and prevents pulmonary vascular remodelling, as well as the development of emphysema [18]. Therefore, we hypothesized that sildenafil, which enhances the activity of cGMP by impeding its metabolization, might exert favourable effects on lung structure beyond its vasodilator action.

Accordingly, the present study aimed to evaluate the effects of sildenafil on pulmonary haemodynamics, endothelial function, and vascular and parenchymal remodelling, in guinea pigs chronically exposed to CS.

METHODS

Experimental groups

Forty-two male guinea pigs were divided into two groups: exposed to the smoke of 7 non-filtered research cigarettes/day (3R4F; Kentucky University Research; Lexington, KY, USA) (smoke content per cigarette: 11 mg total particulate matter, 9.4 mg tar, 0.73

mg nicotine, and 12 mg carbon monoxide), 5 days/week, for 12 weeks (n=26); and sham-exposed (n=16), using a nose-only system (Protowerx Design Inc; Langley, British Columbia, Canada). Daily after CS or sham exposure, animals were administered with a vehicle (distilled water, n=18), or treated with 1mg/kg of sildenafil citrate solution by gavage (n=24), resulting in four experimental groups. Sildenafil (UK-92,480-10) was kindly provided by Pfizer (Sandwich, Kent, UK).

All animal procedures were approved by the ethics review board on animal research of the University of Barcelona and complied with national and international guidelines.

Unrestrained whole-body plethysmography

Respiratory function was measured weekly by unrestrained whole-body plethysmography (Buxco Research Systems, Wilmington, NC, USA) as previously described [19]. Breathing frequency (Bf), tidal volume (TV), minute ventilation (MV) and respiratory resistance (enhanced pause (Penh)) [20] were recorded 10 min before exposure (baseline) and 10 min after CS or sham exposure.

Pulmonary haemodynamics and arterial oxygenation

At the end of the experimental protocol and 24h after the last exposure to CS and sildenafil dose, systolic (sPAP), diastolic (dPAP) and mean (mPAP) PAP were measured under anaesthesia in open-chest animals using a catheter placed in the main pulmonary artery through the RV and connected to a pressure transducer (Buxco Research Systems, Wilmington, NC, USA).

Arterial PO_2 (PaO_2) was analysed in blood sampled from the carotid artery, immediately after hemodynamic measurements. The animals were subsequently sacrificed.

Right ventricle hypertrophy

The heart was removed and RV and left ventricle plus the septum (LV+S) were dissected and weighed separately, and the ratio between RV and LV+S weight [RV/LV+S] was calculated.

Endothelial function

The main PA was isolated, cleaned of fat and connective tissue and cut into rings of 3 mm length. The left branch was placed in an organ bath chamber and attached to an isometric transducer (Panlab, Barcelona, Spain). After a period of stabilization, arteries were contracted with KCl (60 mM) to determine their viability and contractile capacity. Endothelial function was assessed in pre-contracted pulmonary artery rings as previously described [17], by measuring changes in wall tension in response to cumulative doses of adenosine diphosphate (ADP). At the end of the studies, main pulmonary artery rings were fixed and cryo-embedded for histological examination.

Morphometric and histological assessments

Explanted lungs were inflated and fixed with formalin under a constant pressure of 30 cmH_2O for 24h and then embedded in paraffin.

The wall thickness of the main pulmonary artery was measured in sections stained with elastin-Van Gieson. Vascular density was assessed as the number of pulmonary vessels per square millimetre of lung tissue. The number of small intrapulmonary vessels (diameter <50μm) showing positive immunostaining for smooth muscle (SM) α-actin or with double elastic laminas in orcein-stained sections were counted, and expressed as a percentage of the total number of small intrapulmonary vessels. Intrapulmonary vessels (diameter <50μm) immunostained for α-actin were further classified semi-quantitatively depending on the proportion of the vessel wall positive for α-actin into: non-muscularised, ≤1/4 of the vessel wall; partially muscularised, >1/4 - ≤3/4; or fully muscularised, >3/4.

The mean airspace size was evaluated in hematoxylin–stained tissue sections by measuring the mean linear intercept (MLI) of alveolar septa in 20 randomly selected fields.

Real Time-PCR

Total RNA was extracted from lung tissue using the RNeasy Micro Kit (Qiagen GmbH, Hilden, Germany). Total RNA was retrotranscribed and quantification of eNOS was performed by real-time PCR as previously described [17]. Expression of eNOS was normalized to β-actin expression as endogenous housekeeping gene and relative gene expression was analysed using the $2^{-\Delta\Delta Ct}$ method [21].

Data analysis

Results are expressed as mean±standard deviation (SD) or as median and interquartile range (IQR), depending on whether or not the variables followed a normal distribution. The progression of respiratory parameters (Penh, Bf, TV and MV) was assessed weekly throughout the 3 months of study and expressed as the area under the curve (AUC) of all measurements.

Comparisons between groups were carried out using a two-way analysis of variance (ANOVA), considering exposure to CS and sildenafil as main factors, and their interaction. When significant, *post-hoc* pairwise comparisons were performed using the Student-Newman-Keuls test. Relationships between variables were assessed using the Pearson's correlation test. A p-value <0.05 was considered as significant.

RESULTS

Pulmonary haemodynamics and right ventricle hypertrophy

Animals exposed to CS showed higher PAP than non-exposed animals ($p=0.005$) (Figure 1A and Table 1). Treatment with sildenafil prevented the increase of PAP induced by CS, and PAP values were similar to sham-exposed animals (Figure 1A and Table 1).

Untreated CS-exposed animals showed RV hypertrophy. In guinea pigs exposed to CS and treated with sildenafil the RV/LV+S ratio was lower than in the CS-exposed group, although not significantly, and not different from sham-exposed animals (Figure 1B).

Endothelial function and vascular contractility

The maximal contraction induced by KCl in pulmonary arteries was greater in animals exposed to CS (Table 1). Sildenafil treatment did not modify the contractile response of pulmonary arteries.

Endothelium-dependent relaxation induced by cumulative doses of ADP was slightly attenuated in animals exposed to CS, as suggested by a trend to a right shift (EC_{50}) ($p=0.096$) and a higher AUC ($p=0.058$) of the dose-response curve (Table 1 and Supplementary Figure 1). Concomitant treatment with sildenafil did not modify the endothelium-dependent vasodilator response.

Morphometric and histological assessments

Wall thickness of the main pulmonary artery was greater in animals exposed to CS (Supplementary Figure 2). No difference was observed in animals exposed to CS and treated with sildenafil (Table 2).

The proportion of small vessels (diameter <50μm) showing positive immunoreactivity to SM α-actin was higher in animals exposed to CS (Figure 2A-C and Table 2). When vessels were scored according to the degree of muscularisation, it was apparent that in the CS-exposed groups, there was a decrease in the proportion of non-muscularised vessels and a concomitant increase in the proportion of partially and fully muscularised intrapulmonary vessels (Figure 2A-C). Treatment with sildenafil did not modify changes induced by CS.

No significant differences between groups were observed in the proportion of arteries with double elastic lamina (Table 2).

Exposure to CS showed a trend to reduce the density of small intrapulmonary vessels. Animals treated with sildenafil showed greater small vessel density, thereby preventing the reduction induced by CS exposure (p=0.009) (Figure 3 and Table 2).

Development of pulmonary emphysema, assessed as an increased MLI, was observed in animals exposed to CS compared with the sham-exposed group (p=0.028) (Figure 4A-E and Table 2). Guinea pigs exposed to CS and treated with sildenafil showed intermediate MLI values that did not differ either from CS-exposed or from sham-exposed animals (Figure 4A-E and Table 2).

Gene expression of eNOS

No differences in the gene expression of eNOS in lung homogenates were observed between groups (Table 2).

Pulmonary function and blood gas measurements

Unrestrained whole body plethysmographic measurements performed before CS or sham exposure showed a trend to lower MV (p=0.051) (Supplementary Table 1). After

CS exposure a dramatic increase in TV, MV and Penh took place (Supplementary Figure 3B and Supplementary Table 1). The concomitant administration of sildenafil neither modified the pulmonary function at baseline nor after CS exposure (Supplementary Figure 3A and Supplementary Table 1).

Guinea pigs exposed to CS showed a trend to lower arterial PO_2 than non-exposed animals (p=0.138). The administration of sildenafil did not modify the PaO_2 value, neither in CS-exposed nor in non-exposed guinea pigs (Supplementary Table 1).

Correlations

In CS-exposed animals, the muscularisation of small pulmonary vessels correlated with the RV weight (r=0.55, p=0.01, Figure 2D) and the density of small intrapulmonary vessels was inversely related to RV hypertrophy (r=-0.52, p=0.01, Figure 3B). Furthermore, the MLI correlated with mPAP (r=0.56, p=0.01) and with the total number of small pulmonary vessels (r=-0.44, p=0.01, Figure 4F).

DISCUSSION

The present study evaluated the effects of sildenafil in guinea pigs chronically exposed to CS. Our results show that sildenafil prevented the increase in PAP and the subsequent RV hypertrophy, but did not modify pulmonary vascular remodelling induced by CS. Furthermore, sildenafil showed a trend to diminish the airspace enlargement induced by CS exposure and preserved the intrapulmonary vessel density.

The main effect observed in this study was the prevention of PH in CS-exposed animals treated with sildenafil. Whereas, guinea pigs exposed to CS showed increased mPAP and RV hypertrophy when compared with non-exposed animals, in keeping with previous studies [22, 23]; those CS-exposed, treated with sildenafil showed mPAP values and a RV/LV+S weight ratio similar to the non-exposed animals, confirming the vasodilator action of sildenafil in this experimental model [10, 11, 12]. The lack of increase in PAP was not accompanied by differences in lung vessel structure, since CS-exposed guinea pigs treated with sildenafil showed pulmonary artery wall thickening, muscularisation of small vessels, and proliferation of SMCs at similar levels to CS-exposed, untreated guinea pigs and significantly higher than in non-exposed animals. Therefore, in the current experimental setting sildenafil exerted vasodilator but not anti-remodelling effect on pulmonary arteries.

Previous studies in experimental models of PH induced by hypoxia have provided discrepant results regarding the anti-remodelling effect of sildenafil in pulmonary vessels. Whereas in some studies sildenafil prevented pulmonary vascular remodelling, along with the reduction of PAP [10, 24], in others it failed to exert anti-remodelling effect [25], despite reducing PAP, similar to what occurred in our study. We used a sildenafil dose similar to that approved in humans with pulmonary arterial hypertension [26] (1 mg/kg per day during 12 weeks; cumulative dose, 84 mg/kg), which is a low dose compared with previous studies in experimental models of PH induced by hypoxia [10, 24, 25, 27]. It is tempting to speculate that such a low dose could have been sufficient to exert vasodilation, but it was insufficient to produce an anti-remodelling effect. Nevertheless, in previous studies in experimental PH, a significant anti-remodelling effect has been shown with cumulative sildenafil doses of 180 mg/kg [24], whereas cumulative doses of 525 mg/kg failed to produce any anti-remodelling effect [25]. We cannot disregard that the absence of anti-remodelling effect of sildenafil on pulmonary vessels observed in our study could be attributed to the experimental conditions we used, since there are no previous studies with sildenafil conducted in guinea pigs or using CS exposure as a mechanism of pulmonary vascular damage. It is conceivable that the effect of CS exposure on pulmonary vessel structure could exceed those produced by hypoxia, which has been used in previous experimental settings. In fact, in a previous study conducted in guinea pigs we showed differences in the characteristics of pulmonary vascular remodelling between CS exposure and hypoxia [23].

Current observations with sildenafil in the guinea pig chronically exposed to CS contrast with the effects we have recently shown in this experimental model using a sGC stimulator (BAY 41-2272) [18]. With the latter compound we showed not only reduced pulmonary vascular resistance, but also less pulmonary vascular remodelling. Although no direct comparisons between the two drugs have been made, it is tempting to speculate that sGC stimulation might be more effective in increasing cGMP levels than PDE5 inhibition [28], thereby resulting in a more potent anti-remodelling effect.

Interestingly, the airspace size was lower and the small vessel density was higher in CS-exposed animals treated with sildenafil than in CS-exposed untreated animals and did not differ from non-exposed guinea pigs. Since the airspace size and the small intrapulmonary vessels density were significantly correlated, our data suggest that sildenafil contributed to preserve the structural integrity of the lung. In the present study, changes in airspace size were of small magnitude and therefore insufficient to produce any effect on respiratory resistance or gas exchange, akin to previous observations [18]. The preservation of the intrapulmonary vascular surface, which allows reduced vascular resistance, might explain the reduced PAP in sildenafil-treated animals despite the lack of change in vessel remodelling. The inverse relationship between small vessel density and RV hypertrophy also points to that direction, although we cannot disregard a direct effect of sildenafil on RV itself as a mechanism of reduced hypertrophy [24, 29]. We have observed similar effects employing a sGC stimulator, which prevented both pulmonary vascular remodelling and emphysema development in CS-exposed guinea pigs [18]. Taken together, this suggests that cGMP plays a key role in preserving the lung structure. The mechanisms underlying such effects of sildenafil were not explored in the present study, but the alluded previous study shows that increased production of cGMP by sGC stimulation increases mediators of vascular integrity and lung maintenance, such as VEFGA and FGF10, and antioxidant enzymes, such as SOD1; and reduces inflammation by preventing the activation and adherence of circulating inflammatory cells [18]. Accordingly, we hypothesize that the prevention of cGMP degradation by PDE5 inhibition with sildenafil contributed to preserve lung parenchyma and vascular integrity by similar mechanisms, namely antioxidant and antiflammatory effects, and up-regulation of mediators of vessel integrity. The fact that sGC stimulation exerts a greater effect on cGMP intracellular levels than the prevention of its degradation by the inhibition of PDE5 [28] might explain that in the current investigation the effects of sildenafil on vessel remodelling and airspace size were less pronounced than those observed with the sGC stimulator BAY 41-2272 [18]. On the other hand, there is evidence for a causative role of inducible nitric oxide synthase (iNOS) and peroxinitrite (ONOO-) in CS induced emphysema and vessel remodeling [30]. The effects of peroxinitrite that act in part through oxidizing sGC can also be prevented by increasing cGMP levels [18].

The study has some limitations. First, we used a preventive experimental design by starting sildenafil administration at the same time as CS exposure. Accordingly, we cannot state that sildenafil will exert similar effects once the structural changes induced by CS have already developed. Indeed, in patients with severe COPD and mild-to-moderate PH, sildenafil failed to improve exercise tolerance [15]. Second, we used a sildenafil dose similar to that approved in humans to treat pulmonary arterial hypertension [26]. Therefore, we cannot disregard that higher doses could have produced a greater impact on vessel remodelling and/or airspace size. Third, our data suggest that sildenafil contributed to preserve the structural integrity of the lung parenchyma although whether this is reflected in reduced compliance remains to be established. Finally, assessment of exercise function would have been informative to elucidate whether the effects of sildenafil might translate to patients with COPD. However, the effects of CS exposure on exercise tolerance in the guinea pig have not been documented and the inclusion of an exercise arm would have increased the complexity of our study.

In conclusion, the results of the present investigation show that sildenafil prevents the development of PH and RV hypertrophy in an experimental model of COPD induced by chronic exposure to CS. These effects are likely due to a vasodilator effect, along with the preservation of parenchymal integrity and vascular surface, since no effects on vessel remodelling were observed. Current results reinforce the notion that the NO-cGMP axis is perturbed by CS exposure and contributes to clarify the effects of sildenafil in COPD-associated PH. Further investigations are needed to determine the role of PDE5 inhibition once the disease is established.

SUPPORT STATEMENT

Supported by grants FIS PI09/00536 and PI13/00836, and R5-HCPB.

STATEMENT OF INTEREST

The authors report that they have no conflicts of interest regarding the content of the present investigation.

The authors are responsible for the writing of this paper.

ACKNOWLEDGMENTS

The authors would like to thank the personnel of the Department of Pathology at the Hospital Clínic and the animal housing facilities of the University of Barcelona.

REFERENCES

1. Thabut G, Dauriat G, Stern JB, Logeart D, Levy A, Marrash-Chahla R, Mal H. Pulmonary hemodynamics in advanced COPD candidates for lung volume reduction surgery or lung transplantation. *Chest* 2005; 127: 1531-1536.

2. Santos S, Peinado VI, Ramirez J, Morales-Blanhir J, Bastos R, Roca J, Rodriguez-Roisin R, Barbera JA. Enhanced expression of vascular endothelial growth factor in pulmonary arteries of smokers and patients with moderate chronic obstructive pulmonary disease. *Am J Respir Crit Care Med* 2003; 167: 1250-1256.

3. Peinado VI, Barbera JA, Abate P, Ramirez J, Roca J, Santos S, Rodriguez-Roisin R. Inflammatory reaction in pulmonary muscular arteries of patients with mild chronic obstructive pulmonary disease. *Am J Respir Crit Care Med* 1999; 159: 1605-1611.

4. Barbera JA, Peinado VI, Santos S, Ramirez J, Roca J, Rodriguez-Roisin R. Reduced expression of endothelial nitric oxide synthase in pulmonary arteries of smokers. *Am.J Respir Crit Care Med* 2001; 164: 709-713.

5. Peinado VI, Barbera JA, Ramirez J, Gomez FP, Roca J, Jover L, Gimferrer JM, Rodriguez-Roisin R. Endothelial dysfunction in pulmonary arteries of patients with mild COPD. *Am.J Physiol* 1998; 274: L908-L913.

6. Schermuly RT, Stasch JP, Pullamsetti SS, Middendorff R, Muller D, Schluter KD, Dingendorf A, Hackemack S, Kolosionek E, Kaulen C, Dumitrascu R, Weissmann N, Mittendorf J, Klepetko W, Seeger W, Ghofrani HA, Grimminger F. Expression and function of soluble guanylate cyclase in pulmonary arterial hypertension. *Eur Respir J* 2008; 32: 881-891.

7. Klinger JR, Abman SH, Gladwin MT. Nitric oxide deficiency and endothelial dysfunction in pulmonary arterial hypertension. *Am J Respir Crit Care Med* 2013; 188: 639-646.

8. Jeremy JY, Rowe D, Emsley AM, Newby AC. Nitric oxide and the proliferation of vascular smooth muscle cells. *Cardiovasc Res* 1999; 43: 580-594.

9. Ghofrani HA, Voswinckel R, Reichenberger F, Olschewski H, Haredza P, Karadas B, Schermuly RT, Weissmann N, Seeger W, Grimminger F. Differences in hemodynamic and oxygenation responses to three different phosphodiesterase-5 inhibitors in patients with pulmonary arterial hypertension: a randomized prospective study. *J Am Coll Cardiol* 2004; 44: 1488-1496.

10. Sebkhi A, Strange JW, Phillips SC, Wharton J, Wilkins MR. Phosphodiesterase type 5 as a target for the treatment of hypoxia-induced pulmonary hypertension. *Circulation* 2003; 107: 3230-3235.

11. Schermuly RT, Kreisselmeier KP, Ghofrani HA, Yilmaz H, Butrous G, Ermert L, Ermert M, Weissmann N, Rose F, Guenther A, Walmrath D, Seeger W, Grimminger F. Chronic sildenafil treatment inhibits monocrotaline-induced pulmonary hypertension in rats. *Am J Respir Crit Care Med* 2004; 169: 39-45.

12. Schafer S, Ellinghaus P, Janssen W, Kramer F, Lustig K, Milting H, Kast R, Klein M. Chronic inhibition of phosphodiesterase 5 does not prevent pressure-overload-induced right-ventricular remodelling. *Cardiovasc Res* 2009; 82: 30-39.

13. Galie N, Corris PA, Frost A, Girgis RE, Granton J, Jing ZC, Klepetko W, McGoon MD, McLaughlin VV, Preston IR, Rubin LJ, Sandoval J, Seeger W,

Keogh A. Updated treatment algorithm of pulmonary arterial hypertension. *J Am Coll Cardiol* 2013; 62: D60-D72.

14. Blanco I, Gimeno E, Munoz PA, Pizarro S, Gistau C, Rodriguez-Roisin R, Roca J, Barbera JA. Hemodynamic and gas exchange effects of sildenafil in patients with chronic obstructive pulmonary disease and pulmonary hypertension. *Am.J.Respir.Crit Care Med.* 2010; 181: 270-278.

15. Blanco I, Santos S, Gea J, Guell R, Torres F, Gimeno-Santos E, Rodriguez DA, Vilaro J, Gomez B, Roca J, Barbera JA. Sildenafil to improve respiratory rehabilitation outcomes in COPD: a controlled trial. *Eur Respir J* 2013; 42: 982-992.

16. Wright JL, Churg A. A model of tobacco smoke-induced airflow obstruction in the guinea pig. *Chest* 2002; 121: 188S-191S.

17. Ferrer E, Peinado VI, Diez M, Carrasco JL, Musri MM, Martinez A, Rodriguez-Roisin R, Barbera JA. Effects of cigarette smoke on endothelial function of pulmonary arteries in the guinea pig. *Respir Res* 2009; 10: 76.

18. Weissmann N, Lobo B, Pichl A, Parajuli N, Seimetz M, Puig-Pey R, Ferrer E, Peinado VI, Dominguez-Fandos D, Fysikopoulos A, Stasch JP, Ghofrani HA, Coll-Bonfill N, Frey R, Schermuly RT, Garcia-Lucio J, Blanco I, Bednorz M, Tura-Ceide O, Tadele E, Brandes RP, Grimminger J, Klepetko W, Jaksch P, Rodriguez-Roisin R, Seeger W, Grimminger F, Barbera JA. Stimulation of soluble guanylate cyclase prevents cigarette smoke-induced pulmonary hypertension and emphysema. *Am J Respir Crit Care Med* 2014; 189: 1359-1373.

19. Dominguez-Fandos D, Ferrer E, Puig-Pey R, Carreno C, Prats N, Aparici M, Musri MM, Gavalda A, Peinado VI, Miralpeix M, Barbera JA. Effects of aclidinium bromide in a cigarette smoke-exposed Guinea pig model of chronic obstructive pulmonary disease. *Am J Respir Cell Mol Biol* 2014; 50: 337-346.

20. Lomask M. Further exploration of the Penh parameter. *Exp Toxicol Pathol* 2006; 57 Suppl 2:13-20.

21. Livak KJ, Schmittgen TD. Analysis of relative gene expression data using real-time quantitative PCR and the 2(-Delta Delta C(T)) Method. *Methods* 2001; 25: 402-408.

22. Wright JL, Tai H, Churg A. Vasoactive mediators and pulmonary hypertension after cigarette smoke exposure in the guinea pig. *J Appl Physiol* 2006; 100: 672-678.

23. Ferrer E, Peinado VI, Castaneda J, Prieto-Lloret J, Olea E, Gonzalez-Martin MC, Vega-Agapito MV, Diez M, Dominguez-Fandos D, Obeso A, Gonzalez C, Barbera JA. Effects of cigarette smoke and hypoxia on the pulmonary circulation in the guinea pig. *Eur Respir J* 2011; 38: 617-627.

24. Weissmann N, Gerigk B, Kocer O, Nollen M, Hackemack S, Ghofrani HA, Schermuly RT, Butrous G, Schulz A, Roth M, Seeger W, Grimminger F. Hypoxia-induced pulmonary hypertension: different impact of iloprost, sildenafil, and nitric oxide. *Respir Med* 2007; 101: 2125-2132.

25. Zhao L, Mason NA, Morrell NW, Kojonazarov B, Sadykov A, Maripov A, Mirrakhimov MM, Aldashev A, Wilkins MR. Sildenafil inhibits hypoxia-induced pulmonary hypertension. *Circulation* 2001; 104: 424-428.

26. Galie N, Rubin LJ, Simonneau G. Phosphodiesterase inhibitors for pulmonary hypertension. *N Engl J Med* 2010; 362: 559-560.

27. Preston IR, Hill NS, Gambardella LS, Warburton RR, Klinger JR. Synergistic effects of ANP and sildenafil on cGMP levels and amelioration of acute hypoxic pulmonary hypertension. *Exp Biol Med (Maywood.)* 2004; 229: 920-925.

28. Stasch JP, Evgenov OV. Soluble guanylate cyclase stimulators in pulmonary hypertension. *Handb Exp Pharmacol* 2013; 218: 279-313.

29. Nagendran J, Archer SL, Soliman D, Gurtu V, Moudgil R, Haromy A, St Aubin C, Webster L, Rebeyka IM, Ross DB, Light PE, Dyck JR, Michelakis ED. Phosphodiesterase type 5 is highly expressed in the hypertrophied human right ventricle, and acute inhibition of phosphodiesterase type 5 improves contractility. *Circulation* 2007; 116: 238-248.

30. Seimetz M, Parajuli N, Pichl A, Veit F, Kwapiszewska G, Weisel FC, Milger K, Egemnazarov B, Turowska A, Fuchs B, Nikam S, Roth M, Sydykov A, Medebach T, Klepetko W, Jaksch P, Dumitrascu R, Garn H, Voswinckel R, Kostin S, Seeger W, Schermuly RT, Grimminger F, Ghofrani HA, Weissmann N. Inducible NOS inhibition reverses tobacco-smoke-induced emphysema and pulmonary hypertension in mice. *Cell* 2011; 147: 293-305.

TABLE 1. Assessment of *in vivo* pulmonary artery pressure and *in vitro* reactivity

		Vehicle		Sildenafil 1mg/kg		Two-way ANOVA main effects (p-value)		
		Sham-exposed (n=8)	**CS-exposed** (n=10)	**Sham-exposed** (n=8)	**CS-exposed** (n=10)	CS exposure	Sildenafil	Interaction
Pulmonary artery pressure (mmHg)	**Systolic**	9.0±4.3	14.3±8.0*	6.6±2.0	8.2±2.7†	0.082	0.038	0.346
	Diastolic	3.8±2.5	10.5±7.5	5.0±1.2	4.9±1.6	0.059	0.202	0.050
	Mean	5.7±1.6	12.4±7.7*	5.7±1.5	6.3±1.8†	0.036	0.081	0.081
Contraction (mg)	**KCl** (60 mM)	1828.4±489.2	2560.9±711.1*	1660.7±530.1	2604.9±605.7*	≤0.001	0.771	0.619
	NE (10^{-6} M)	574.6±163.1	573.5±200.2	538.1±105.7	717.0±172.0	0.141	0.370	0.136
Relaxation to ADP	**Change in tension** (AUC[a])	203.8±20.1	231.8±43.3	200.6±57.4	226.3±27.2	0.058	0.753	0.935
	EC_{50} (-log [M] ADP)	7.18±0.86	6.61±0.40	6.79±0.60	6.72±0.27	0.096	0.479	0.191

Values are mean±SD. [a]Arbitrary units of area under the curve (AUC).

* p <0.05 compared with its sham-exposed group.

† p <0.05 compared with vehicle CS-exposed group.

TABLE 2. Morphologic assessments and quantification of eNOS expression

	Vehicle		Sildenafil		Two-way ANOVA main effects (p-value)		
	Sham-exposed (n=8)	**CS-exposed** (n=10)	**Sham-exposed** (n=8)	**CS-exposed** (n=11)	CS exposure	Sildenafil	Interaction
Pulmonary artery wall thickness (μm)	57.7±23.3	77.8±9.0*	54.8±4.7	75.4±9.8*	≤0.001	0.565	0.963
SM α-actin-positive arteries (%)	25.1±5.5	40.3±13.1*	26.4±4.6	39.8±7.1*	≤0.001	0.877	0.760
Arteries with double elastic lamina (%)	1.3±2.5	4.1±6.6	0.7±2.0	2.8±1.2	0.101	0.512	0.833
Vessels <50μm/mm^2	23.5±4.2	19.0±5.6	27.3±5.0	25.4±5.7†	0.077	0.006	0.476
Interseptal distance (μm)	69.1±12.8	78.0±11.8	64.7±7.6	71.3±7.9	0.028	0.114	0.749
Relative eNOS expression (eNOS/β-actin)	1.07±0.14	1.08±0.13	1.10±0.14	0.96±0.12	0.632	0.699	0.586

Values are mean±SD.

* p <0.05 compared with its sham-exposed group.

† p <0.01 compared with vehicle CS-exposed group.

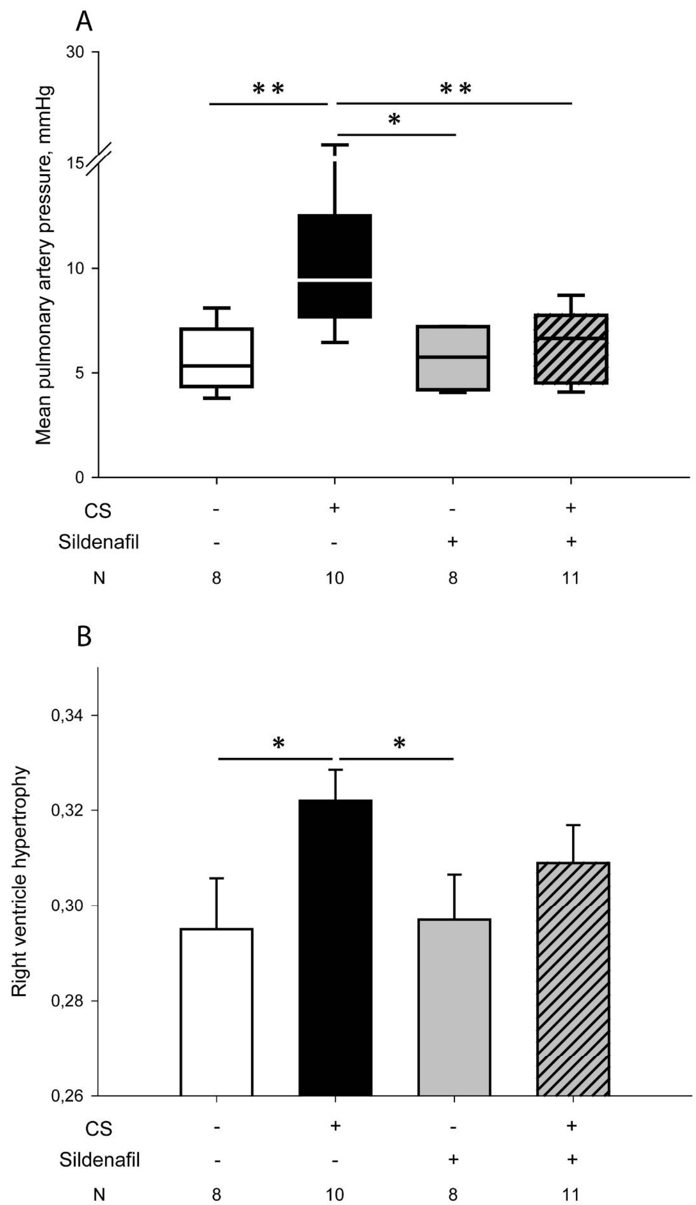

Figure 1. Pulmonary artery pressure and right ventricle hypertrophy. A) Mean pulmonary artery pressure (mPAP). Data represent the median in each group as the middle line in the box. The box stretches from the 25th percentile (lower hinge) to the 75th percentile (upper hinge). The whiskers extend from the box to the 90th and 10th percentiles. B) Right ventricle hypertrophy assessed as the weight ratio between the RV and the left ventricle (LV) plus septum (S). Data are presented as mean±SEM. Treatment with sildenafil in cigarette smoke (CS)-exposed animals prevented the increase in mPAP and attenuated RV hypertrophy. *$p<0.05$; **$p<0.01$.
165x290mm (300 x 300 DPI)

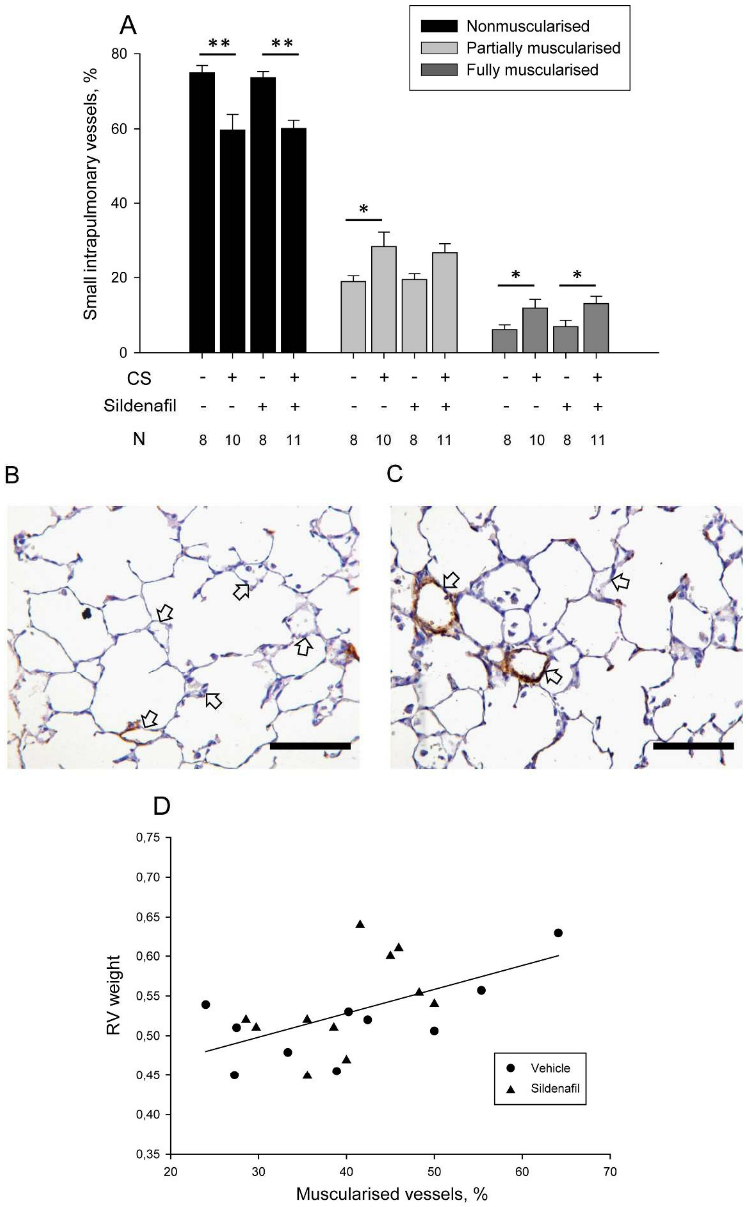

Figure 2. Muscularisation of small intrapulmonary arteries (<50 μm) (A). Bar charts show the percentage of small arteries according to their degree of muscularisation. Data are presented as mean±SEM. Animals exposed to cigarette smoke (CS), irrespective of sildenafil administration, showed a lower number of non-muscularised arteries and developed a greater number of partially and fully muscularised arteries. *$p<0.05$; **$p<0.01$. Microphotographs of α-actin immunostained small pulmonary vessels (<50 μm) in a control guinea pig (B) and an animal exposed to CS (C). In the exposed animal fully muscularised arteries are present. Arrows indicate small intrapulmonary vessels. Scale bar, 100 μm. (D) Correlation between the percentage of muscularised small intrapulmonary vessels and the weight of the right ventricle (RV) in guinea pigs exposed to CS treated with vehicle (solid circles) or sildenafil (solid triangles), $r=0.55$, $p=0.01$.
178x289mm (300 x 300 DPI)

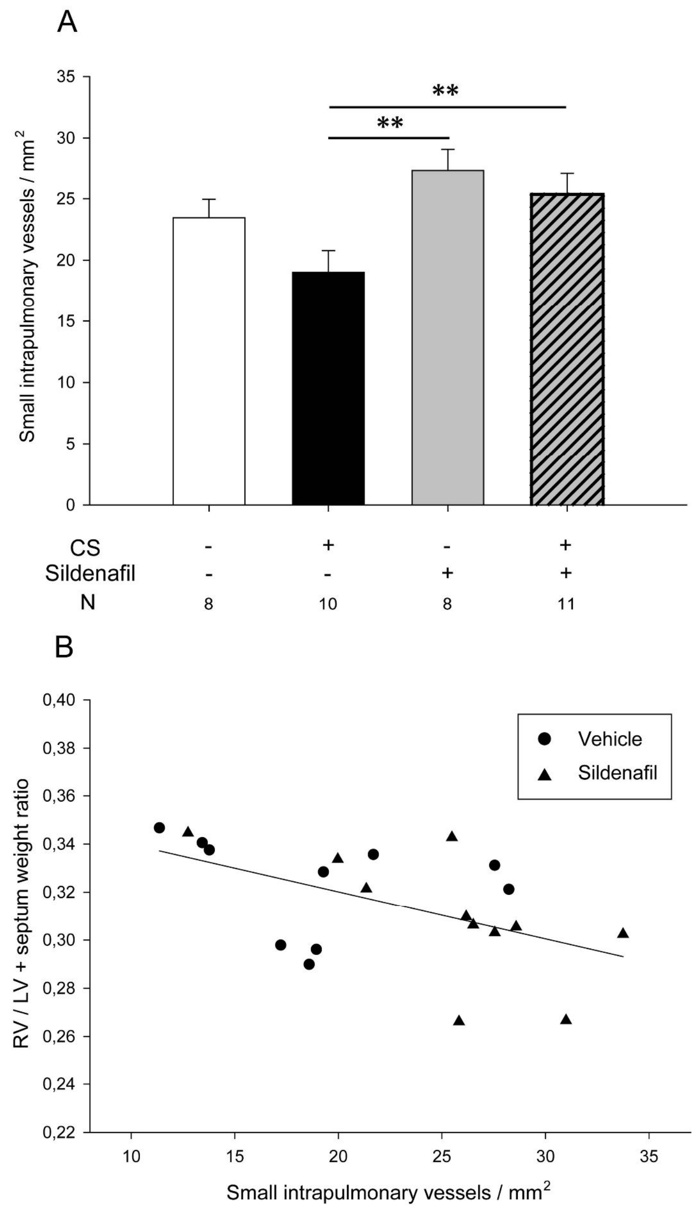

Figure 3. Density of small intrapulmonary vessels (<50 µm) (A). Cigarette smoke (CS)-exposed animals treated with sildenafil showed a greater density of small intrapulmonary vessels than CS-exposed only. Data are presented as mean±SEM. **p<0.01. (B) Correlation between the density of small intrapulmonary vessels and the right ventricular hypertrophy (RV/LV+septum weight ratio) in guinea pigs exposed to CS treated with vehicle (solid circles) or sildenafil (solid triangles), r=-0.52, p=0.01.
164x289mm (300 x 300 DPI)

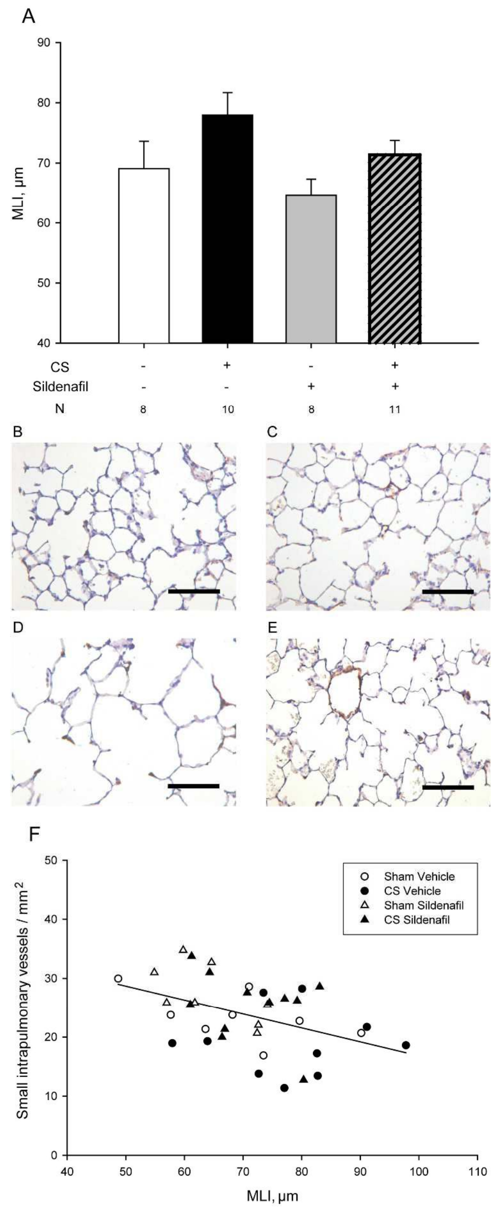

Figure 4. A) Airspace size, evaluated by the mean linear intercept (MLI). Bars show mean±SEM. Main effects in the two-way ANOVA: CS, p=0.028 and SIL, p=0.114. Photomicrographs of lung parenchyma sections stained with hematoxylin in sham-exposed guinea pigs treated with vehicle (B), or sildenafil (C); and cigarette smoke (CS)-exposed guinea pigs treated with vehicle (D), or sildenafil (E). Scale bar, 100 µm. (F) Correlation between the MLI and the pulmonary vascular density (number of vessels <50µm per square millimeter), r= 0.44, p=0.01.
117x292mm (300 x 300 DPI)

ONLINE SUPPLEMENTARY MATERIAL

Sildenafil in a cigarette smoke-induced model of COPD in the guinea pig

David Domínguez-Fandos, César Valdés, Elisabet Ferrer, Raquel Puig-Pey, Isabel Blanco, Olga Tura-Ceide, Tanja Paul, Víctor I. Peinado and Joan A. Barberà

SUPPLEMENTARY MATERIALS AND METHODS

Animals and cigarette smoke exposure

Forty-two male guinea pigs (~300g in weight) were divided into two groups at random: sham-exposed (room air, n=16) and exposed to the smoke of 7 non-filtered research cigarettes/day (3R4F; Kentucky University Research; Lexington, KY, USA), 5 days/week, for 12 weeks (n=26), using a nose-only system [1, 2] (Protowerx Design Inc; Langley, British Columbia, Canada). Guinea pigs were weighed weekly throughout the experimental protocol. All animal procedures were approved by the ethical review board on animal research of the University of Barcelona and complied with national and international guidelines.

Sildenafil administration

Animals were daily treated by gavage 1h after the exposure to CS or air (Sham) for five days a week along the study with either distilled water (Vehicle, n=18), or 1mg/kg of sildenafil (UK-92,480-10) citrate solution (Sildenafil, n=24) synthesized and provided by Pfizer (Sandwich, Kent, UK).

Four final groups were used: Sham Vehicle, CS Vehicle, Sham Sildenafil, and CS Sildenafil.

Unrestrained whole-body plethysmography

Respiratory function was measured weekly in conscious guinea pigs by unrestrained whole-body plethysmography (Buxco Research Systems, Wilmington, NC, USA). Guinea pigs breathing spontaneously were placed in plethysmographic chambers. The recording period started when animals were adapted (not scratching, sniffing or chewing) and data was collected and averaged for 3 min. Pressure signals were fed into a computer for visualization, storage and offline analysis with specific software. Data was recorded at the following time-points: 10 min before (baseline) and 10 min after the exposure to CS or sham exposure. At each time-point we recorded the breathing frequency (Bf), the tidal volume (TV), the minute ventilation (MV) and the respiratory resistance (enhanced pause (Penh)) [3, 4]. Penh is a unit-less index described as:

$$\text{Penh} = \text{PEF}/\text{PIF} \times (\text{Te}/\text{Rt}-1)$$

Where PEF is the peak of expiratory height, PIF is the peak of inspiratory height, Te is the expiratory time, and Rt is the time to expire 65% of the volume.

At the end of the study the area under the curve (AUC) for each parameter (Penh, Bf, TV and MV) assessed along the 3 months of study was calculated using a logistic curve-fitting equation for each animal.

Pulmonary haemodynamics measurements

Systolic (sPAP), diastolic (dPAP) and mPAP were measured under anaesthesia with ketamine and xylazine (50 and 7 mg/Kg respectively) in open-chest guinea pigs using a 20 GA catheter connected to a pressure transducer (Buxco Research Systems, Wilmington, NC, USA). The catheter was placed in the main pulmonary artery through the right ventricle (RV). Measurements were performed in normoxic conditions by pumping in fresh air.

Right ventricular hypertrophy

Immediately after the hemodynamic measurements were completed, the cardiopulmonary block was isolated and weighed. The heart was removed and the RV was dissected from the left ventricle and septum (LV+S), under a stereomicroscope (Leica Microsystems Imaging Solutions Ltd, Cambridge, UK), and these were weighed separately. RV hypertrophy was measured as the ratio between the RV weight and the weight of the LV+S ([RV/LV+S], Fulton index).

Arterial oxygenation

Blood gas analyses (CIBA-Corning 860, CIBA-Corning Diagnostics Corporation, Medfield, MA, USA) were performed in blood sampled from the carotid artery immediately after the hemodynamic measurements.

Endothelial function

The main pulmonary artery was isolated from the cardiopulmonary block. The artery was cleaned of fat and connective tissue, measured in length and weighed and cut into rings of 3 mm in length. The left and right branches of the main pulmonary artery were obtained and the left branch was placed in an organ bath chamber and was attached to an isometric transducer (Panlab, Barcelona, Spain). After a period of stabilization, arteries were contracted with KCl (60 mM) to determine their viability and contractile capacity. All rings were pre-incubated with indomethacin (1×10^{-5} M) in order to inhibit the synthesis of cyclo-oxygenase products. The rings were then contracted with norepinephrine (NE; 1×10^{-7} to 0.2×10^{-6} M) to obtain a stable plateau of tension. Endothelial function was assessed as the change in wall tension in response to cumulative doses of adenosine diphosphate (ADP; 10^{-9} to 10^{-5} M), an endothelial nitric oxide (NO)-dependent vasodilator, as previously described[1]. Endothelium-dependent vasodilator responses were assessed by the maximal relaxation induced by ADP, the dose that caused 50% relaxation (EC_{50}), and the area under the curve (AUC). Whereas EC_{50} is a single-point estimated value, the AUC is a summary measure obtained from all experimental points in the dose-response curve, providing a complete profile of vessel responsiveness.

Morphometric and histological assessments

After the hemodynamic measurements were completed, the lungs were removed, inflated and fixed during 24h with formalin by airway instillation under constant pressure of 30 cmH_2O. After sampling, tissue blocks were dehydrated and lung sections were embedded in paraffin or frozen by using optimal cutting temperature (O.C.T; Tissue-Tek, Sakura Finetek, Zoeterwoude, NL). Lung tissue was prepared and tissue sections were used for morphometric and histological analysis of the vasculature. Histological examination was performed in 4-µm sections.

After the organ bath studies, main pulmonary artery rings were fixed in 4% formaldehyde and cryo-embedded in O.C.T. Morphometric studies were performed in 4-µm slices sections. The thickness of the muscular layer of the main pulmonary artery wall was measured by planimetry in sections stained with elastin-Van Gienson. The distance between the external and internal elastic laminas was measured 10 times in two different rings of the artery using an image analysis system [5] (Leica Qwin).

Vascular remodelling was evaluated by assessing the number of intrapulmonary vessels (external diameter <50µm) showing positive immunostaining for smooth muscle (SM) α-actin antibody (Dako, Glostrup, Denmark) and by the number of vessels with double elastic laminas in orcein-stained sections, expressed as a percentage of the total number of small intrapulmonary vessels. Intrapulmonary vessels immunostained for α-actin were further semi-quantitatively classified in a scale depending on the proportion of the vessel wall positive for α-actin [6]: non-muscularised, ≤1/4 of the vessel wall; partially muscularised, >1/4 - ≤3/4; or fully muscularised, >3/4.

Real Time-PCR

Total RNA was extracted from lung tissue homogenates using RNeasy Micro Kit (Qiagen GmbH, Hilden, Germany). RNA concentration (A260) and sample purity (260/280 ratio) were measured in the NanoDrop 2000c spectrophotometer (Thermo Scientific, Wilmington, DE, USA). The quantification and quality of RNA was also measured in a Bioanalyser platform (Agilent Technologies, Inc., Santa Clara, CA, USA). Total RNA was retrotranscribed and quantification of eNOS was performed with real-time PCR as previously described[1]. Expression of eNOS was normalized to β-actin expression as endogenous housekeeping gene and relative gene expression was analysed using the $2^{-\Delta\Delta Ct}$ method [7]. Primers were designed based on guinea pig eNOS sequence from GeneBank using specific software (Primer Express, Applied Biosystems, Foster City, CA, USA). Amplification was performed on PTC-200 Peltier thermal cycler equipped with a Chromo4 real-time PCR detector module (MJ Research, BioRad, Hercules, CA, USA). The identities of the amplified products were examined using melt curve analysis. The primer sequences for eNOS were 3'-AGCCAACGCGGTGAAGATC-5' and 5'-TTAGCCATCACCGTGCCC-3' and for β-actin 3'-ATATCGCTGCGCTCGTTGTC-5' and 5'-AACGATGCCGTGCTCAATG-3'.

Data analysis

Results in tables are expressed as mean±standard deviation (SD) or as median and interquartile range (IQR), depending on whether or not the variables followed a normal distribution. Results in figures are showed as mean±standard error of the mean (SEM) or as box plots with median and 10th, 25th, 75th and 90th percentiles.

To analyse the evolution of plethysmographic respiratory parameters (Bf, TV, MV and Penh), assessed weekly through the 3 months study period, we calculated the AUC of all measurements performed in each animal as a summary measure.

Comparisons between groups were carried out using a two-way analysis of variance (ANOVA), considering exposure to CS and sildenafil treatment as main factors and their interaction. When significant, *post-hoc* pairwise comparisons were performed using the Student-Newman-Keuls test.

Relationships between variables were assessed using the Pearson's correlation test. A p-value < 0.05 was considered significant.

SUPPLEMENTARY RESULTS

Body weight and body mass index

Animals treated with sildenafil gained more weight than vehicle-treated animals irrespective of the exposure to CS ($p \leq 0.001$) (Supplementary Figure 4A). Additionally, sildenafil administration was significantly associated with higher body mass index (BMI) in animals exposed to CS (CS Vehicle vs. CS Sildenafil: 9.7±0.5 vs 10.8±0.7 kg/m^2, $p<0.001$) (Supplementary Figure 4B).

Pulmonary function

At baseline, animals exposed to CS showed a reduction in MV. Ten min after CS exposure the TV increased and the MV increased. Treatment with sildenafil did not modify any of the lung function measurements (Supplementary Table 1).

SUPPLEMENTARY REFERENCES

1. Ferrer E, Peinado VI, Diez M, Carrasco JL, Musri MM, Martinez A, Rodriguez-Roisin R, Barbera JA. Effects of cigarette smoke on endothelial function of pulmonary arteries in the guinea pig. *Respir Res* 2009; 10: 76.

2. Ardite E, Peinado VI, Rabinovich RA, Fernandez-Checa JC, Roca J, Barbera JA. Systemic effects of cigarette smoke exposure in the guinea pig. *Respir Med* 2006; 100: 1186-1194.

3. Lomask M. Further exploration of the Penh parameter. *Exp Toxicol Pathol* 2006; 57 Suppl 2: 13-20.

4. Hamelmann E, Schwarze J, Takeda K, Oshiba A, Larsen GL, Irvin CG, Gelfand EW. Noninvasive measurement of airway responsiveness in allergic mice using barometric plethysmography. *Am J Respir Crit Care Med* 1997; 156: 766-775.

5. Peinado VI, Barbera JA, Ramirez J, Gomez FP, Roca J, Jover L, Gimferrer JM, Rodriguez-Roisin R. Endothelial dysfunction in pulmonary arteries of patients with mild COPD. *Am J Physiol* 1998; 274: L908-L913.

6. Crosby A, Jones FM, Southwood M, Stewart S, Schermuly R, Butrous G, Dunne DW, Morrell NW. Pulmonary vascular remodeling correlates with lung eggs and cytokines in murine schistosomiasis. *Am J Respir Crit Care Med* 2010; 181: 279-288.

7. Livak KJ, Schmittgen TD. Analysis of relative gene expression data using real-time quantitative PCR and the 2(-Delta Delta C(T)) Method. *Methods* 2001; 25: 402-408.

SUPPLEMENTARY TABLE

Supplementary Table 1. Effects of sildenafil on respiratory function and arterial oxygen tension

AUC		Vehicle		Sildenafil 1mg/kg		Two-way ANOVA main effects (p-value)		
		Sham-exposed (n=8)	**CS-exposed** (n=10)	**Sham-exposed** (n=8)	**CS-exposed** (n=5)	CS exposure	Sildenafil	Interaction
Breathing Frequency[a]	**Baseline**	950.0±102.1	923.7±90.2	967.5±65.3	909.9±73.4	0.197	0.954	0.624
	After exposure	894.5±105.5	823.9±75.0	933.8±91.7	876.2±128.4	0.085	0.213	0.857
Tidal Volume[a]	**Baseline**	55.0±6.0	50.8±3.4	52.6±3.8	51.2±1.9	0.081	0.534	0.385
	After exposure	54.7±5.2	101.3±25.9*	54.3±4.2	106.8±4.7*	≤0.001	0.666	0.611
Minute Ventilation[a]	**Baseline**	5650.8±815.5	5191.5±506.0	5552.4±662.5	5070.7±320.9	0.051	0.638	0.962
	After exposure	5196.8±688.8	9358.9±2751.9*	5467.3±631.4	10156.3±1150.6*	≤0.001	0.409	0.682
PaO_2 (mmHg)		70.7±17.1	55.0±19.9	62.3±30.6	55.3±13.6	0.138	0.593	0.564

Values are mean±SD. Area under the curve. [a]Arbitrary Units.

* p < 0.001 compared with its sham-exposed group.

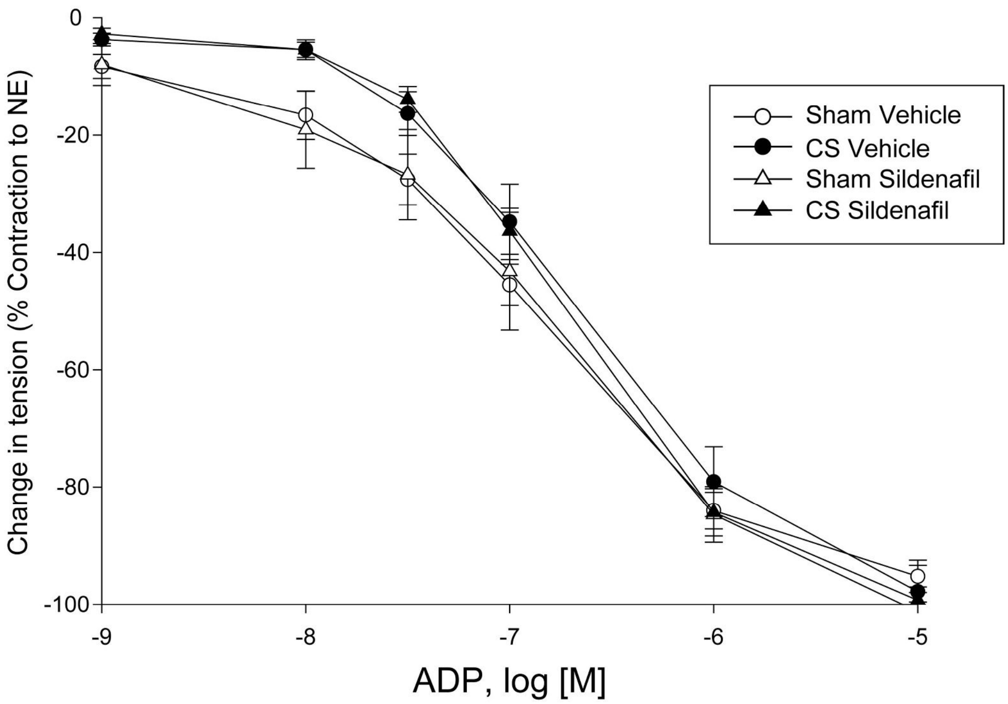

Supplementary Figure 1. Endothelium-dependent relaxation in pulmonary arteries. Relaxation of main pulmonary artery rings in response to cumulative doses of adenosine-5'-diphosphate (ADP), after pre-contraction with norepinephrine (NE). Values are expressed as % change in tension in NE pre-contracted artery rings . Panel shows dose-response curves of the 4 experimental groups (n=8-11, each). Data are presented as mean±SEM. Main effects in the two-way ANOVA for the area under the curve: cigarette smoke (CS), p=0.058; sildenafil, p=0.753.
202x141mm (300 x 300 DPI)

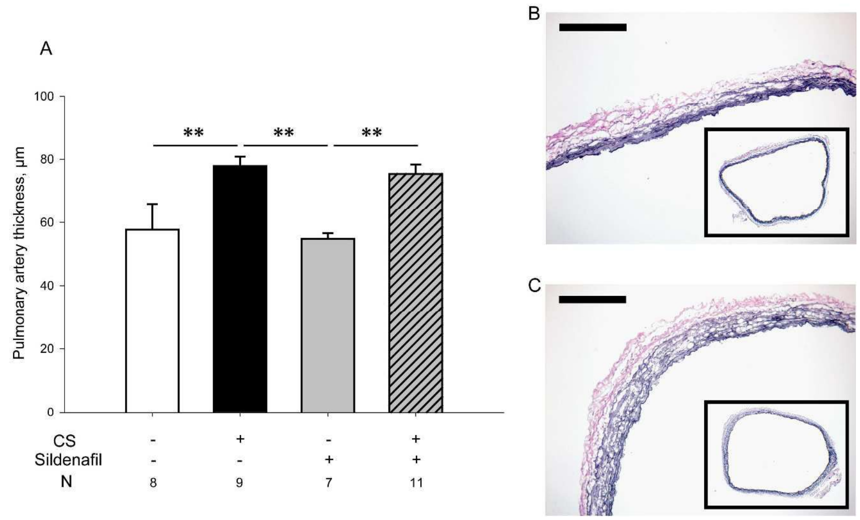

Supplementary Figure 2. Pulmonary artery wall thickness (A). Wall thickness of the main pulmonary artery was increased in animals exposed to cigarette smoke (CS) and unaffected by the administration of sildenafil. Data are presented as mean±SEM. **p<0.01. Microphotographs of elastin-Van Gienson stained main pulmonary artery in a control guinea pig (B) and an animal exposed to CS (C). Sildenafil treatment did not modify thickening of the main pulmonary artery induced by CS exposure. Scale bar, 300 µm.
324x166mm (300 x 300 DPI)

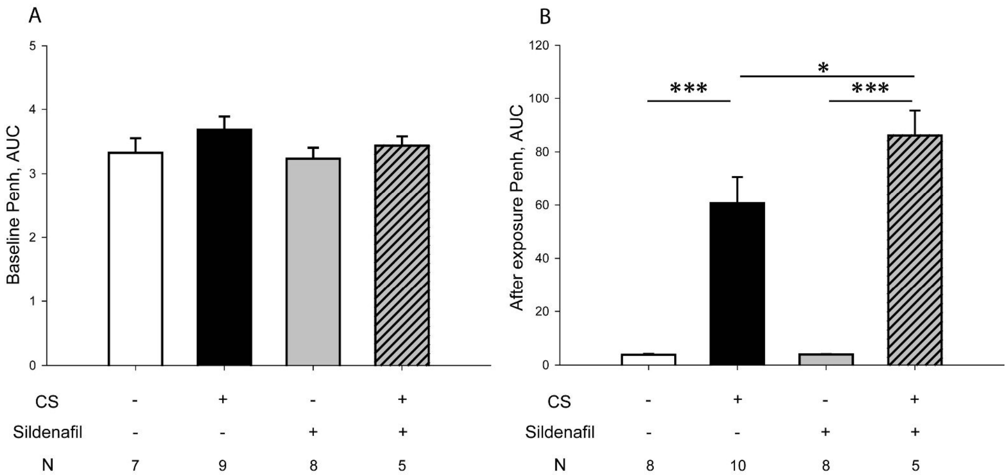

Supplementary Figure 3. Respiratory resistance. A) Area under the curve (AUC) of 12 weekly measurements of the enhanced pause (Penh) at baseline B) AUC of 12 weekly measurements of Penh obtained 10 min after cigarette smoke (CS) exposure. Graphs show mean±SEM. The AUC has arbitrary units. Main effects in the two-way ANOVA for Penh at baseline and after CS exposure: CS, $p=0.187$; SIL, $p=0.417$ and CS, $p<0.001$; SIL, $p=0.095$, respectively. Comparison between groups: *$p<0.05$; ***$p<0.001$.
281x133mm (300 x 300 DPI)

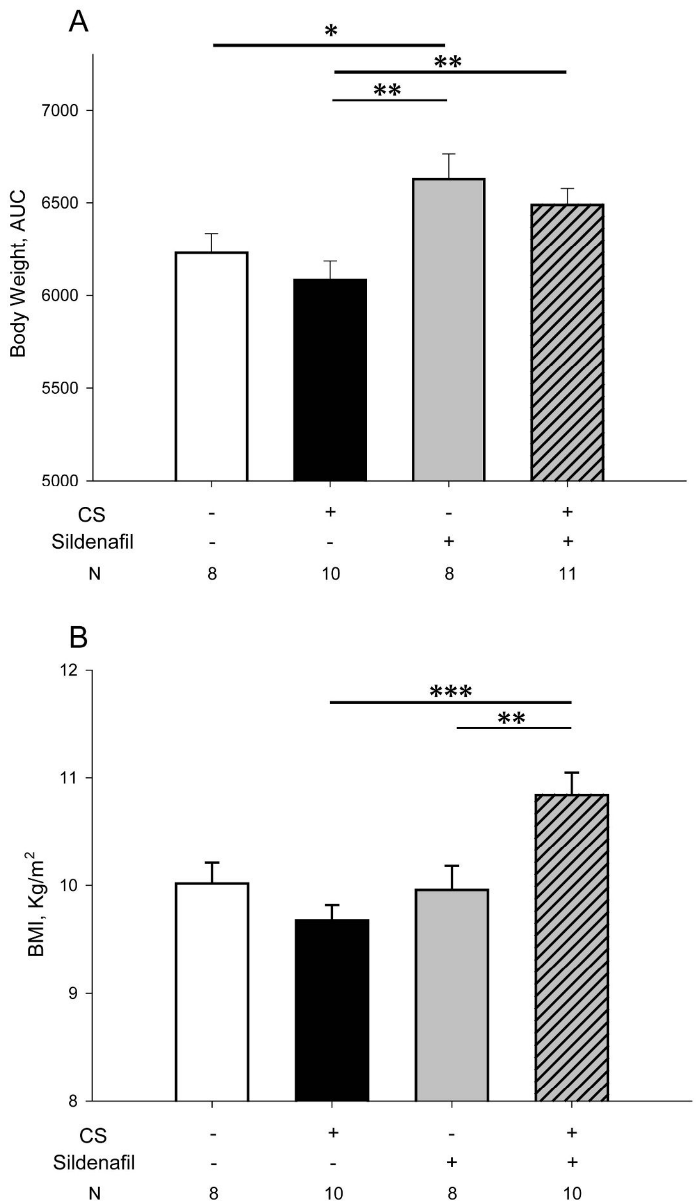

Supplementary Figure 4. Body weight. Area under the curve (AUC) of 12 weekly measurements of body weight (A) and body mass index (BMI) (B). Values are mean±SEM. Sildenafil treatment induced greater weight gain in both cigarette smoke (CS)-exposed and unexposed animals. Main effects in the two-way ANOVA for body weight and BMI: CS, $p=0.193$ and 0.172; SIL, $p<0.001$ and 0.007, respectively. Comparisons between groups *$p<0.05$; **$p<0.01$; ***$p<0.001$.
205x286mm (300 x 300 DPI)

3.1.- Resultados principales

Hemodinámica pulmonar e hipertrofia del ventrículo derecho

Los animales expuestos al HC mostraron mayor PAP que los no expuestos y el tratamiento con sildenafilo previno este incremento de PAP, manteniéndose los valores próximos a los de animales no expuestos.

Los animales expuestos a HC no tratados con sildenafilo mostraron hipertrofia del VD. Hubo una tendencia a la prevención de la hipertrofia de VD en los animales tratados con sildenafilo, ya que no se observaron diferencias en el índice de pesos VD/VI+S entre los cobayos expuestos al HC tratados con sildenafilo y los animales no expuestos.

Función endotelial y contractilidad vascular

La contracción máxima inducida por KCl en arterias pulmonares fue mayor en animales expuestos al HC y el tratamiento con sildenafilo no modificó esta respuesta contráctil. La relajación dependiente de endotelio inducida por dosis acumulativas de ADP se atenuó ligeramente en los animales expuestos al HC, como sugiere la tendencia a desplazarse a la derecha (EC_{50}) y el aumento de AUC de la curva dosis-respuesta. El tratamiento con sildenafilo no modificó esta respuesta vasodilatadora dependiente de endotelio.

Análisis morfométrico e histológico

El grosor de la pared de la arteria pulmonar principal fue mayor en los animales expuestos al HC y no se observaron diferencias en los animales expuestos tratados con sildenafilo.

La proporción de vasos pequeños α-actina+ fue mayor en los animales expuestos al HC, con una disminución en la proporción de vasos no muscularizados y un aumento en la de vasos intrapulmonares parcial y completamente muscularizados. El tratamiento con sildenafilo no modificó los cambios inducidos con HC.

No se observaron diferencias significativas entre grupos en la proporción de arterias con lámina elástica doble.

La exposición al HC mostró una tendencia a reducir la densidad de vasos pequeños intrapulmonares y los animales tratados con sildenafilo mostraron una mayor densidad de vasos pequeños, previniendo la reducción inducida por la exposición al HC.

Se observó desarrollo de enfisema pulmonar en los animales expuestos al HC y los cobayos expuestos al HC tratados con sildenafilo mostraron valores intermedios de distancia media interseptal (*mean linear intercept*, MLI) que no difirieron de los animales expuestos al HC ni de los animales no expuestos.

Expresión génica de eNOS

No se observaron diferencias entre grupos en la expresión génica de eNOS en homogeneizado de pulmón.

Mediciones de función pulmonar y gasometría en sangre

Las mediciones basales de pletimosgrafía mostraron una tendencia a menor ventilación minuto (VM) en los grupos expuestos a HC. Tras la exposición al HC tuvo lugar un incremento drástico en el VC, VM y Penh. La administración concomitante de sildenafilo no modificó la función pulmonar basal ni tras la exposición a HC.

Los cobayos expuestos al HC mostraron una tendencia a menor PO_2 arterial y sildenafilo no modificó el valor de PaO_2, ni en cobayos expuestos al HC ni en los no expuestos.

Correlaciones

En los animales expuestos al HC, la muscularización de vasos pulmonares pequeños correlacionó con el peso del VD y la densidad de vasos intrapulmonares pequeños se relacionó inversamente con la hipertrofia del VD. Además, el MLI correlacionó con la PAPm y con el número total de vasos pulmonares pequeños.

DISCUSIÓN DE RESULTADOS

Respuesta inflamatoria en el modelo experimental de EPOC

La exposición al HC induce un proceso inflamatorio en el pulmón que puede llevar al desarrollo de la EPOC. En el cobayo, la exposición al HC durante 6 meses induce infiltración por células inflamatorias y cambios morfológicos en las diferentes estructuras pulmonares. La intensidad de la reacción inflamatoria correlaciona con el remodelado de la vía aérea. Estos cambios se asemejan a los que se observan en los pacientes con EPOC (3, 28, 29, 37, 46). Los cambios estructurales son especialmente pronunciados en la vía aérea de menor calibre y correlacionan con la infiltración por neutrófilos y macrófagos. Sin embargo, el remodelado de los vasos pulmonares más pequeños con la exposición al HC no correlaciona con el infiltrado por neutrófilos o macrófagos. La severidad del proceso inflamatorio también va en paralelo con el depósito de colágeno en el septo alveolar que presentan los animales expuestos al HC. De hecho, tras los 6 meses de exposición, el enfisema inducido se asocia con el depósito de colágeno y el aumento del infiltrado de neutrófilos y macrófagos en la pared bronquial y el septo alveolar.

En los animales control, los neutrófilos se localizan preferentemente en el septo alveolar, mientras que en vía aérea infiltran progresivamente con la exposición al HC. Alrededor de los vasos pulmonares también se observa un infiltrado de neutrófilos con la exposición. Estos hallazgos son consistentes con estudios en humanos que correlacionan el número de neutrófilos con el consumo acumulado de cigarrillos (33). Además, la acumulación de neutrófilos se considera uno de los eventos importantes en la patogénesis del enfisema pulmonar en individuos fumadores, al inducir un desequilibrio proteasa-antiproteasa (30). En este sentido, la reacción inflamatoria por neutrófilos correlaciona particularmente con el engrosamiento de la pared de la vía aérea de pequeño tamaño, y con la distancia interseptal, identificando a los neutrófilos como un componente que participaría en el remodelado de la vía aérea y el enfisema.

Por otro lado, el incremento de macrófagos en el árbol bronquial de sujetos con EPOC (40) también se ha relacionado con el enfisema, sugiriendo que también podrían colaborar en la respuesta inflamatoria elastolítica (39). En los animales expuestos al HC, observamos un aumento de macrófagos en el septo alveolar que se relaciona con el tamaño alveolar. En humanos, los macrófagos se encuentran en lugares de destrucción de la pared alveolar y en bronquios, correlacionando con la severidad de la EPOC (38, 175). Nuestros hallazgos son similares a las observaciones hechas en humanos, enfatizando el papel del HC sobre los macrófagos (37).

Aunque clásicamente la inflamación de la vía aérea por eosinófilos está considerada una característica del asma, la inflamación eosinofílica podría jugar un papel en la EPOC y estos pacientes podrían representar un fenotipo distinto de la enfermedad. Su presencia en la vía aérea y en el esputo se ha demostrado en pacientes con EPOC estable y aumenta durante las exacerbaciones (46, 47). En los cobayos, los eosinófilos son las células inflamatorias predominantes y se distribuyen homogéneamente en vía aérea, vasos pulmonares y septo alveolar, pero su correlación con los cambios morfológicos en la vía aérea y los vasos intrapulmonares de pequeño calibre es débil. Por eso, la reacción eosinofílica inducida por el HC podría ser especifica del cobayo, junto con la hiperreactividad bronquial, aunque la bronquitis eosinofílica en fumadores no asmáticos sugieren un papel del HC en el reclutamiento de eosinófilos en el pulmón (48).

La inflamación en el pulmón mediada por linfocitos (50, 176) podría jugar un papel destacado en la EPOC. Las células T y B pueden organizarse en folículos linfoides (3, 27) y su número en el pulmón es mayor en los estadios EPOC grave-muy grave (3). En nuestro estudio, hay un aumento de folículos linfoides en los pulmones de cobayos expuestos al HC que tiende a correlacionar con el remodelado de la vía aérea pequeña.

Algunos estudios han demostrado fibrosis pulmonar en fumadores y su asociación con el enfisema ha sido reconocida como una entidad específica, con malas consecuencias (62, 64-66). Los mecanismos de fibrosis probablemente suponen un intento de reparar la inflamación. En los cobayos expuestos al HC, el depósito de colágeno en la vía aérea y los septos alveolares encaja con un incremento del enfisema. También observamos un aumento de fibras de colágeno gruesas, que se ha asociado con la formación de cicatrices de reparación y podrían modular la rigidez de los tejidos (63).

Nuestro estudio en cobayos expuestos al HC sugiere que este modelo experimental reproduce las alteraciones inflamatorias que se observan en la EPOC, reforzando su validez como modelo experimental de EPOC y nuestra hipótesis de que a partir de la reacción inflamatoria producida por el HC se desencadenaría el remodelado de la vía aérea, el parénquima pulmonar y los vasos intrapulmonares. Por lo tanto, es un modelo apropiado para diseñar estudios de intervención terapéutica en la EPOC como son el segundo y tercer estudio de esta tesis doctoral.

Efectos de bromuro de aclidinio en el modelo experimental de EPOC

En los cobayos crónicamente expuestos al HC, la administración de aclidinio tiene un efecto antirremodelado en la vía aérea que se asocia con una disminución de la resistencia respiratoria. Además, aclidinio atenúa ligeramente el infiltrado de neutrófilos en el septo alveolar inducido por la exposición al HC. El incremento de la resistencia respiratoria con la exposición crónica al HC podría atribuirse a los cambios histopatológicos que tienen lugar en el pulmón (131), ya que el Penh basal correlaciona con el remodelado de la vía aérea y el enfisema; como ocurre en los pacientes con EPOC. Por lo tanto, la reducción de la resistencia respiratoria y la atenuación de la hiperreactividad aguda inducida por el HC con el tratamiento con aclidinio podría deberse, en parte, al comentado efecto antirremodelado del fármaco a nivel de las vías aéreas. Estos hallazgos sugieren la implicación de la activación muscarínica en el remodelado del músculo liso de la vía aérea (146, 150, 151), ampliando la observación previa sobre la inhibición de la cantidad de músculo liso en vía aérea con antagonistas muscarínicos en un modelo de asma alérgico (177). En otro estudio, aclidinio atenuó la proliferación y migración de fibroblastos, y la transición de fibroblastos a miofibroblastos en fumadores y pacientes con EPOC (174) evidenciando que la vía colinérgica estaría implicada en el remodelado de la vía aérea causado por la exposición crónica al HC. Estos hallazgos indican que además de su efecto broncodilatador mantenido, los antagonistas muscarínicos pueden tener un impacto importante en el remodelado de la vía aérea. En nuestro estudio, el efecto antirremodelado no difiere entre las dos dosis de aclidinio administradas, en cambio, la dosis más elevada de 30 µg/mL tuvo algo más de efecto sobre el Penh y los episodios de tos. En cualquier caso, la demostración de actividad antirremodelado con aclidinio en el modelo animal de EPOC refuerza los resultados de ensayos clínicos que muestran la eficacia de aclidinio en los pacientes con EPOC (155-157).

Por otro lado, el sistema colinérgico participa en la respuesta inflamatoria y los receptores muscarínicos se expresan en el sistema nervioso parasimpático y en casi todos los tipos celulares localizados en la vía aérea (150, 178). El receptor muscarínico M3, que está involucrado en la contracción del músculo liso de la vía aérea y la proliferación celular (151, 179), puede estimularse por el HC induciendo la secreción de IL-8 por las CML humanas de la vía aérea (149). Además, la ACh también es liberada por las células inflamatorias (150, 180) y se ha observado que aclidinio disminuye el número de eosinófilos en el LBA en un modelo murino de asma (159) y que el antagonista muscarínico, triotropio, inhibe la inflamación neutrofílica inducida por HC en LBA en ratón (158). Esto sugiere que los anticolinérgicos podrían atenuar el componente inflamatorio inducido por el daño en el pulmón. En nuestro estudio, el tratamiento con aclidinio se asocia a un menor número de neutrófilos en el septo alveolar pero no a una disminución del influjo inflamatorio inducido por el HC en la vía aérea. Estos hallazgos son consistentes con los mostrados con triotropio, que disminuyó los neutrófilos en el LBA de ratones (158) y sin embargo, no logró reducir el número de células inflamatorias en el esputo inducido en pacientes con EPOC (181). El efecto antiinflamatorio limitado de aclidinio en la vía aérea podría ser consecuencia de la intensa reacción inflamatoria inducida por el HC, o de que los neutrófilos en la pared bronquial de la vía aérea pueden suponer un perfil inflamatorio diferente que el esputo o BAL (182). En nuestro estudio, el grosor de la pared correlaciona con la intensidad del infiltrado inflamatorio en las vías aéreas, sin embargo, los efectos contrapuestos de aclidinio sobre el remodelado de la vía aérea y el infiltrado inflamatorio sugieren que el efecto antirremodelado fue más probablemente debido al efecto sobre las vías de señalización reguladas por los agonistas muscarínicos, que al efecto directo en el reclutamiento de células inflamatorias en la vía aérea.

El tamaño del espacio alveolar no difiere entre los animales expuestos al HC tratados con aclidinio y los animales control. Asimismo, al hacer el análisis juntando las dos dosis de aclidinio, la distancia media entre septo alveolar es mayor en los cobayos expuestos al HC no tratados que en los expuestos al HC tratados con aclidinio, sugiriendo que el fármaco podría tener un potencial efecto en la prevención de desarrollar enfisema. Una hipótesis que explicara esta observación sería que aclidinio reduce el influjo de neutrófilos inducido por el HC en el septo alveolar, previniendo en parte la destrucción del septo alveolar. Hipotetizamos que aclidinio podría prevenir el agrandamiento del espacio aéreo al bloquear en células epiteliales la activación de la cascada RhoA/Rho-quinasa asociada a receptores muscarínicos, mejorando el aclaramiento de células apoptóticas (150, 183).

En el presente estudio, los cobayos expuestos a HC muestran una prominente metaplasia de células caliciformes en las vías aéreas, que junto con la hipersecreción mucosa es una característica de los fumadores y pacientes con EPOC (7, 184). La administración de aclidinio no modifica el número de células caliciformes, a pesar de que aclidinio y otros LAMAs inhiben la expresión de la mucina MUC5AC inducida por HC en las vías aéreas (164, 185). Sin embargo, el análisis histoquímico de las células caliciformes puede no correlacionar con la expresión de MUC5AC (186), y en nuestro modelo animal, aclidinio también podría haber tenido efecto inhibitorio sobre MUC5AC.

Efectos de sildenafilo en el modelo experimental de EPOC

En el modelo experimental de EPOC en cobayos crónicamente expuestos al HC, sildenafilo previene el incremento de PAP y la subsiguiente hipertrofia del VD, pero no modifica el remodelado vascular pulmonar inducido por el HC. Aunque sí que se observa que sildenafilo preserva la densidad de vasos intrapulmonares y muestra una tendencia a disminuir el aumento de los espacios alveolares inducido por la exposición al HC.

El efecto principal observado en este estudio fue la prevención de HP en los animales expuestos al HC tratados con sildenafilo. Mientras que los cobayos expuestos al HC muestran un incremento de PAPm e hipertrofia del VD; los animales expuestos al HC, tratados con sildenafilo muestran valores de PAPm y un índice de pesos VD/VI+S similar a los animales no expuestos, confirmando la acción vasodilatadora que ejerce sildenafilo en este modelo experimental (169, 171). La falta de incremento en la PAP no se acompaña de cambios en la estructura de los vasos pulmonares, ya que los cobayos expuestos al HC tratados con sildenafilo muestran engrosamiento de la pared de la arteria pulmonar y muscularización de vasos pequeños similares a los cobayos expuestos al HC, no tratados. Por lo tanto, sildenafilo produce un efecto vasodilatador pero no antirremodelado en las arterias pulmonares. En algunos estudios en modelos experimentales de HP inducida por hipoxia sildenafilo previno el remodelado vascular pulmonar, junto con la reducción de PAP (169, 187) y en otros no produjo efecto antirremodelado (143), aunque redujera la PAP, similar a lo que sucede en nuestro estudio. Esto podría deberse a que usamos una dosis de sildenafilo similar a la aprobada en humanos con HAP (188), que es baja en comparación con otros estudios en animales (143, 169, 187, 189). Sin embargo, estudios previos en HP experimental, han demostrado efecto antirremodelado con dosis acumulativas de sildenafilo de 180 mg/kg (187), mientras que dosis acumulativas de 525 mg/kg no produjeron tal efecto (143).

No hay estudios previos realizados con sildenafilo en cobayos o utilizando la exposición al HC como mecanismo de daño vascular pulmonar para comparar nuestros resultados. En cambio, las observaciones con sildenafilo en el cobayo crónicamente expuesto al HC contrastan con los efectos que hemos mostrado en este modelo experimental utilizando un estimulador de sGC (BAY 41-2272) (60), con el que se consigue una disminución de la RVP pero también un menor remodelado vascular pulmonar. Una hipótesis que explicara este hecho es que la estimulación de sGC podría ser más efectiva en incrementar los niveles de cGMP que la inhibición de PDE5 (190), y de ese modo producir mayor efecto antirremodelado.

Es de interés destacar que el tamaño de los espacios aéreos es menor y la densidad de vasos pequeños mayor en los animales expuestos al HC tratados con sildenafilo, que en los animales expuestos al HC no tratados, y no difiere de los cobayos no expuestos. También se observa una correlación entre el tamaño de los espacios aéreos y la densidad de vasos intrapulmonares de pequeño tamaño que sugeriría que sildenafilo contribuiría a preservar la integridad estructural del pulmón. Además, la preservación de la superficie vascular intrapulmonar, que conllevaría una menor RVP, podría explicar la reducción de PAP con sildenafilo a pesar de no mejorar el remodelado vascular. La relación inversa entre la densidad de vasos pequeños y la hipertrofia del VD también apuntaría en esa dirección, aunque sildenafilo también podría ejercer un efecto directo sobre el VD que disminuyera su hipertrofia (187, 191). En conjunto, estos hallazgos sugieren que cGMP juega un papel crucial en la preservación de la estructura pulmonar. Aunque los mecanismos que subyacen a estos efectos de sildenafilo no se exploraron, estudios de nuestro grupo muestran que la producción aumentada de cGMP por la estimulación de sGC incrementa mediadores de integridad vascular y mantenimiento pulmonar, como VEFGA y FGF10, y enzimas antioxidantes, como SOD1; además de reducir la inflamación (60). El hecho de que la estimulación de sGC ejerza un mayor efecto sobre los niveles intracelulares de cGMP que prevenir su degradación inhibiendo la PDE5 con sildenafilo (190) también podría explicar que los efectos de sildenafilo sobre el tamaño del espacio alveolar sean menos pronunciados (60). Por otra parte, hay evidencia de que la sintasa inducible de NO (iNOS) y peroxinitrito (ONOO-), que actúa en parte a través de la oxidación de sGC, participarían en el desarrollo de enfisema y remodelado vascular inducido por HC (61) y podría prevenirse incrementando los niveles de cGMP (60).

CONCLUSIONES

A partir de los resultados obtenidos en los estudios realizados en esta tesis doctoral se extraen las siguientes conclusiones:

1. En el cobayo, la exposición crónica al HC induce una reacción inflamatoria pleiotrópica en la vía aérea, los vasos pulmonares y los septos alveolares del pulmón que se compone de neutrófilos, macrófagos y eosinófilos y persiste en el tiempo, especialmente en la vía aérea y vasos pulmonares de menor calibre.

2. La intensidad del infiltrado neutrofílico y macrofágico correlaciona con el remodelado de la vía aérea periférica y el enfisema. Asimismo, con la exposición al HC, aparecen áreas de depósito de colágeno en el septo alveolar y vía aérea periférica que se asocia con el agrandamiento del espacio alveolar. Por lo tanto, la reacción inflamatoria inducida por el HC no sólo comporta daño sobre las estructuras pulmonares sino también un proceso de reparación.

3. Estas alteraciones se asemejan a las que se observan en los pacientes con EPOC, avalando el papel patogénico del HC y se refuerza el uso del cobayo expuesto crónicamente al HC como modelo experimental válido de EPOC para su uso en estudios de progresión clínica e intervenciones terapéuticas.

4. En este modelo experimental de EPOC, aclidinio mejora la función respiratoria, previene el remodelado de la vía aérea pequeña, atenúa el infiltrado neutrofílico en el septo alveolar y contribuye parcialmente a evitar el desarrollo de enfisema. De ello se deduce que además de ejercer acción broncodilatadora, bromuro de aclidinio tiene efectos beneficiosos sobre la estructura pulmonar, que contribuirían a explicar los efectos del fármaco en los pacientes con EPOC.

5. En el modelo de EPOC en cobayos expuestos crónicamente al HC, sildenafilo previene el incremento de la PAP y la subsiguiente hipertrofia del VD, preserva la densidad vascular y contribuye parcialmente a evitar el desarrollo de enfisema. Estos hallazgos refuerzan la

idea de que el eje NO-cGMP se altera con la exposición al HC y que la intervención farmacológica sobre dicha vía de señalización no sólo tiene efecto vasodilatador sino que también contribuye a preservar la integridad de la estructura pulmonar.

BIBLIOGRAFÍA

1. Cosio, M. G., M. Saetta, and A. Agusti. 2009. Immunologic aspects of chronic obstructive pulmonary disease. *N.Engl.J.Med.* 360:2445-2454.

2. Rivera, R. M., M. G. Cosio, H. Ghezzo, M. Salazar, and R. Perez-Padilla. 2008. Comparison of lung morphology in COPD secondary to cigarette and biomass smoke. *Int.J.Tuberc.Lung Dis.* 12:972-977.

3. Hogg, J. C., F. Chu, S. Utokaparch, R. Woods, W. M. Elliott, L. Buzatu, R. M. Cherniack, R. M. Rogers, F. C. Sciurba, H. O. Coxson, and P. D. Pare. 2004. The nature of small-airway obstruction in chronic obstructive pulmonary disease. *N.Engl.J.Med.* 350:2645-2653.

4. Hogg, J. C. 2004. Pathophysiology of airflow limitation in chronic obstructive pulmonary disease. *Lancet* 364:709-721.

5. Rodriguez-Roisin, R., M. Drakulovic, D. A. Rodriguez, J. Roca, J. A. Barbera, and P. D. Wagner. 2009. Ventilation-perfusion imbalance and chronic obstructive pulmonary disease staging severity. *J.Appl.Physiol (1985.)* 106:1902-1908.

6. Vestbo, J., E. Prescott, and P. Lange. 1996. Association of chronic mucus hypersecretion with FEV1 decline and chronic obstructive pulmonary disease morbidity. Copenhagen City Heart Study Group. *Am.J.Respir.Crit Care Med.* 153:1530-1535.

7. Innes, A. L., P. G. Woodruff, R. E. Ferrando, S. Donnelly, G. M. Dolganov, S. C. Lazarus, and J. V. Fahy. 2006. Epithelial mucin stores are increased in the large airways of smokers with airflow obstruction. *Chest* 130:1102-1108.

8. Peinado, V. I., S. Pizarro, and J. A. Barbera. 2008. Pulmonary vascular involvement in COPD. *Chest* 134:808-814.

9. Peinado, V. I., F. P. Gomez, J. A. Barbera, A. Roman, M. M. Angels, J. Ramirez, J. Roca, and R. Rodriguez-Roisin. 2013. Pulmonary vascular abnormalities in chronic obstructive pulmonary disease undergoing lung transplant. *J.Heart Lung Transplant.* 32:1262-1269.

10. Adir, Y., R. Shachner, O. Amir, and M. Humbert. 2012. Severe pulmonary hypertension associated with emphysema: a new phenotype? *Chest* 142:1654-1658.

11. Peinado, V. I., J. A. Barbera, P. Abate, J. Ramirez, J. Roca, S. Santos, and R. Rodriguez-Roisin. 1999. Inflammatory reaction in pulmonary muscular arteries of patients with mild chronic obstructive pulmonary disease. *Am.J.Respir.Crit Care Med.* 159:1605-1611.

12. nh-Xuan, A. T., T. W. Higenbottam, C. A. Clelland, J. Pepke-Zaba, G. Cremona, A. Y. Butt, S. R. Large, F. C. Wells, and J. Wallwork. 1991. Impairment of endothelium-dependent pulmonary-artery relaxation in chronic obstructive lung disease. *N.Engl.J.Med.* 324:1539-1547.

13. Barnes, P. J. and B. R. Celli. 2009. Systemic manifestations and comorbidities of COPD. *Eur.Respir.J.* 33:1165-1185.

14. Barr, R. G., D. A. Bluemke, F. S. Ahmed, J. J. Carr, P. L. Enright, E. A. Hoffman, R. Jiang, S. M. Kawut, R. A. Kronmal, J. A. Lima, E. Shahar, L. J. Smith, and K. E. Watson. 2010. Percent emphysema, airflow obstruction, and impaired left ventricular filling. *N.Engl.J.Med.* 362:217-227.

15. Eisner, M. D., N. Anthonisen, D. Coultas, N. Kuenzli, R. Perez-Padilla, D. Postma, I. Romieu, E. K. Silverman, and J. R. Balmes. 2010. An official American Thoracic Society public policy statement: Novel risk factors and the global burden of chronic obstructive pulmonary disease. *Am.J.Respir.Crit Care Med.* 182:693-718.

16. Lamprecht, B., M. A. McBurnie, W. M. Vollmer, G. Gudmundsson, T. Welte, E. Nizankowska-Mogilnicka, M. Studnicka, E. Bateman, J. M. Anto, P. Burney, D. M. Mannino, and S. A. Buist. 2011. COPD in never smokers: results from the population-based burden of obstructive lung disease study. *Chest* 139:752-763.

17. Raad, D., S. Gaddam, H. J. Schunemann, J. Irani, J. P. Abou, R. Honeine, and E. A. Akl. 2011. Effects of water-pipe smoking on lung function: a systematic review and meta-analysis. *Chest* 139:764-774.

18. Tan, W. C., C. Lo, A. Jong, L. Xing, M. J. Fitzgerald, W. M. Vollmer, S. A. Buist, and D. D. Sin. 2009. Marijuana and chronic obstructive lung disease: a population-based study. *CMAJ.* 180:814-820.

19. Burrows, B., R. J. Knudson, M. G. Cline, and M. D. Lebowitz. 1977. Quantitative relationships between cigarette smoking and ventilatory function. *Am.Rev.Respir.Dis.* 115:195-205.

20. Eisner, M. D., J. Balmes, P. P. Katz, L. Trupin, E. H. Yelin, and P. D. Blanc. 2005. Lifetime environmental tobacco smoke exposure and the risk of chronic obstructive pulmonary disease. *Environ.Health* 4:7.

21. Matheson, M. C., G. Benke, J. Raven, M. R. Sim, H. Kromhout, R. Vermeulen, D. P. Johns, E. H. Walters, and M. J. Abramson. 2005. Biological dust exposure in the workplace is a risk factor for chronic obstructive pulmonary disease. *Thorax* 60:645-651.

22. Torres-Duque, C., D. Maldonado, R. Perez-Padilla, M. Ezzati, and G. Viegi. 2008. Biomass fuels and respiratory diseases: a review of the evidence. *Proc.Am.Thorac.Soc.* 5:577-590.

23. Stoller, J. K. and L. S. Aboussouan. 2005. Alpha1-antitrypsin deficiency. *Lancet* 365:2225-2236.

24. Vestbo, J., S. S. Hurd, A. G. Agusti, P. W. Jones, C. Vogelmeier, A. Anzueto, P. J. Barnes, L. M. Fabbri, F. J. Martinez, M. Nishimura, R. A. Stockley, D. D. Sin, and R. Rodriguez-Roisin. 2013. Global Strategy for the Diagnosis, Management, and Prevention of Chronic Obstructive Pulmonary Disease: GOLD Executive Summary. *Am.J.Respir.Crit Care Med.* 187:347-365.

25. Mathers, C. D. and D. Loncar. 2006. Projections of global mortality and burden of disease from 2002 to 2030. *PLoS.Med.* 3:e442.

26. van den, B. G., C. P. van Schayck, M. P. van Mollen, P. R. Tirimanna, J. J. den Otter, P. M. van Grunsven, M. J. Buitendijk, C. L. van Herwaarden, and W. C. van. 1998. Active detection of chronic obstructive pulmonary disease and asthma in the general population. Results and economic consequences of the DIMCA program. *Am.J.Respir.Crit Care Med.* 158:1730-1738.

27. van der Strate, B. W., D. S. Postma, C. A. Brandsma, B. N. Melgert, M. A. Luinge, M. Geerlings, M. N. Hylkema, B. A. van den, W. Timens, and H. A. Kerstjens. 2006. Cigarette smoke-induced emphysema: A role for the B cell? *Am.J.Respir.Crit Care Med.* 173:751-758.

28. Turato, G., R. Zuin, M. Miniati, S. Baraldo, F. Rea, B. Beghe, S. Monti, B. Formichi, P. Boschetto, S. Harari, A. Papi, P. Maestrelli, L. M. Fabbri, and M. Saetta. 2002. Airway inflammation in severe chronic obstructive pulmonary disease: relationship with lung function and radiologic emphysema. *Am.J.Respir.Crit Care Med.* 166:105-110.

29. Cosio, M. G., J. Majo, and M. G. Cosio. 2002. Inflammation of the airways and lung parenchyma in COPD: role of T cells. *Chest* 121:160S-165S.

30. Janoff, A. 1985. Elastases and emphysema. Current assessment of the protease-antiprotease hypothesis. *Am.Rev.Respir.Dis.* 132:417-433.

31. Saetta, M., G. Turato, F. M. Facchini, L. Corbino, R. E. Lucchini, G. Casoni, P. Maestrelli, C. E. Mapp, A. Ciaccia, and L. M. Fabbri. 1997. Inflammatory cells in the bronchial glands of smokers with chronic bronchitis. *Am.J.Respir.Crit Care Med.* 156:1633-1639.

32. Baraldo, S., G. Turato, C. Badin, E. Bazzan, B. Beghe, R. Zuin, F. Calabrese, G. Casoni, P. Maestrelli, A. Papi, L. M. Fabbri, and M. Saetta. 2004. Neutrophilic infiltration within the airway smooth muscle in patients with COPD. *Thorax* 59:308-312.

33. Turato, G., R. Zuin, and M. Saetta. 2001. Pathogenesis and pathology of COPD. *Respiration* 68:117-128.

34. Nadel, J. A. 1991. Role of mast cell and neutrophil proteases in airway secretion. *Am.Rev.Respir.Dis.* 144:S48-S51.

35. Churg, A., R. Wang, X. Wang, P. O. Onnervik, K. Thim, and J. L. Wright. 2007. Effect of an MMP-9/MMP-12 inhibitor on smoke-induced emphysema and airway remodelling in guinea pigs. *Thorax* 62:706-713.

36. Stringer, K. A., M. Tobias, H. C. O'Neill, and C. C. Franklin. 2007. Cigarette smoke extract-induced suppression of caspase-3-like activity impairs human neutrophil phagocytosis. *Am.J.Physiol Lung Cell Mol.Physiol* 292:L1572-L1579.

37. Shapiro, S. D. 1999. The macrophage in chronic obstructive pulmonary disease. *Am.J.Respir.Crit Care Med.* 160:S29-S32.

38. Di, S. A., A. Capelli, M. Lusuardi, P. Balbo, C. Vecchio, P. Maestrelli, C. E. Mapp, L. M. Fabbri, C. F. Donner, and M. Saetta. 1998. Severity of airflow limitation is associated with severity of airway inflammation in smokers. *Am.J.Respir.Crit Care Med.* 158:1277-1285.

39. Churg, A., R. D. Wang, H. Tai, X. Wang, C. Xie, J. Dai, S. D. Shapiro, and J. L. Wright. 2003. Macrophage metalloelastase mediates acute cigarette smoke-induced inflammation via tumor necrosis factor-alpha release. *Am.J.Respir.Crit Care Med.* 167:1083-1089.

40. Di, S. A., G. Turato, P. Maestrelli, C. E. Mapp, M. P. Ruggieri, A. Roggeri, P. Boschetto, L. M. Fabbri, and M. Saetta. 1996. Airflow limitation in chronic bronchitis is associated with T-lymphocyte and macrophage infiltration of the bronchial mucosa. *Am.J.Respir.Crit Care Med.* 153:629-632.

41. Barnes, P. J. 2004. Alveolar macrophages in chronic obstructive pulmonary disease (COPD). *Cell Mol.Biol.(Noisy.-le-grand)* 50 Online Pub:OL627-OL637.

42. Hodge, S., G. Hodge, J. Ahern, H. Jersmann, M. Holmes, and P. N. Reynolds. 2007. Smoking alters alveolar macrophage recognition and phagocytic ability: implications in chronic obstructive pulmonary disease. *Am.J.Respir.Cell Mol.Biol.* 37:748-755.

43. Hodge, S., G. Hodge, R. Scicchitano, P. N. Reynolds, and M. Holmes. 2003. Alveolar macrophages from subjects with chronic obstructive pulmonary disease are deficient in their ability to phagocytose apoptotic airway epithelial cells. *Immunol.Cell Biol.* 81:289-296.

44. Fujimoto, K., K. Kubo, H. Yamamoto, S. Yamaguchi, and Y. Matsuzawa. 1999. Eosinophilic inflammation in the airway is related to glucocorticoid reversibility in patients with pulmonary emphysema. *Chest* 115:697-702.

45. Pizzichini, E., M. M. Pizzichini, P. Gibson, K. Parameswaran, G. J. Gleich, L. Berman, J. Dolovich, and F. E. Hargreave. 1998. Sputum eosinophilia predicts benefit from prednisone in smokers with chronic obstructive bronchitis. *Am.J.Respir.Crit Care Med.* 158:1511-1517.

46. Gorska, K., R. Krenke, P. Korczynski, J. Kosciuch, J. Domagala-Kulawik, and R. Chazan. 2008. Eosinophilic airway inflammation in chronic obstructive pulmonary disease and asthma. *J.Physiol Pharmacol.* 59 Suppl 6:261-270.

47. Snoeck-Stroband, J. B., T. S. Lapperre, M. M. Gosman, H. M. Boezen, W. Timens, N. H. ten Hacken, J. K. Sont, P. J. Sterk, and P. S. Hiemstra. 2008. Chronic bronchitis sub-phenotype within COPD: inflammation in sputum and biopsies. *Eur.Respir.J.* 31:70-77.

48. Papi, A., M. Romagnoli, S. Baraldo, F. Braccioni, I. Guzzinati, M. Saetta, A. Ciaccia, and L. M. Fabbri. 2000. Partial reversibility of airflow limitation and increased exhaled NO and sputum eosinophilia in chronic obstructive pulmonary disease. *Am.J.Respir.Crit Care Med.* 162:1773-1777.

49. Barrecheguren, M., C. Esquinas, and M. Miravitlles. 2015. The asthma-chronic obstructive pulmonary disease overlap syndrome (ACOS): opportunities and challenges. *Curr.Opin.Pulm.Med.* 21:74-79.

50. Cosio, M. G. 2004. Autoimmunity, T-cells and STAT-4 in the pathogenesis of chronic obstructive pulmonary disease. *Eur.Respir.J.* 24:3-5.

51. Gamble, E., D. C. Grootendorst, K. Hattotuwa, T. O'Shaughnessy, F. S. Ram, Y. Qiu, J. Zhu, A. M. Vignola, C. Kroegel, F. Morell, I. D. Pavord, K. F. Rabe, P. K. Jeffery, and N. C. Barnes. 2007. Airway mucosal inflammation in COPD is similar in smokers and ex-smokers: a pooled analysis. *Eur.Respir.J.* 30:467-471.

52. O'Shaughnessy, T. C., T. W. Ansari, N. C. Barnes, and P. K. Jeffery. 1997. Inflammation in bronchial biopsies of subjects with chronic bronchitis: inverse relationship of CD8+ T lymphocytes with FEV1. *Am.J.Respir.Crit Care Med.* 155:852-857.

53. Majo, J., H. Ghezzo, and M. G. Cosio. 2001. Lymphocyte population and apoptosis in the lungs of smokers and their relation to emphysema. *Eur.Respir.J.* 17:946-953.

54. Rennard, S. I., S. Togo, and O. Holz. 2006. Cigarette smoke inhibits alveolar repair: a mechanism for the development of emphysema. *Proc.Am.Thorac.Soc.* 3:703-708.

55. 1997. Alpha 1-antitrypsin deficiency: memorandum from a WHO meeting. *Bull.World Health Organ* 75:397-415.

56. McDonough, J. E., R. Yuan, M. Suzuki, N. Seyednejad, W. M. Elliott, P. G. Sanchez, A. C. Wright, W. B. Gefter, L. Litzky, H. O. Coxson, P. D. Pare, D. D. Sin, R. A. Pierce, J. C. Woods, A. M. McWilliams, J. R. Mayo, S. C. Lam, J. D. Cooper, and J. C. Hogg. 2011. Small-airway obstruction and emphysema in chronic obstructive pulmonary disease. *N.Engl.J.Med.* 365:1567-1575.

57. Matsuoka, S., G. R. Washko, T. Yamashiro, R. S. Estepar, A. Diaz, E. K. Silverman, E. Hoffman, H. E. Fessler, G. J. Criner, N. Marchetti, S. M. Scharf, F. J. Martinez, J. J. Reilly, and H. Hatabu. 2010. Pulmonary hypertension and computed tomography measurement of small pulmonary vessels in severe emphysema. *Am.J.Respir.Crit Care Med.* 181:218-225.

58. Matsuoka, S., G. R. Washko, M. T. Dransfield, T. Yamashiro, E. R. San Jose, A. Diaz, E. K. Silverman, S. Patz, and H. Hatabu. 2010. Quantitative CT measurement of cross-sectional area of small pulmonary vessel in COPD: correlations with emphysema and airflow limitation. *Acad.Radiol.* 17:93-99.

59. Coxson, H. O., I. H. Chan, J. R. Mayo, J. Hlynsky, Y. Nakano, and C. L. Birmingham. 2004. Early emphysema in patients with anorexia nervosa. *Am.J.Respir.Crit Care Med.* 170:748-752.

60. Weissmann, N., B. Lobo, A. Pichl, N. Parajuli, M. Seimetz, R. Puig-Pey, E. Ferrer, V. I. Peinado, D. Dominguez-Fandos, A. Fysikopoulos, J. P. Stasch, H. A. Ghofrani, N. Coll-Bonfill, R. Frey, R. T. Schermuly, J. Garcia-Lucio, I. Blanco, M. Bednorz, O. Tura-Ceide, E. Tadele, R. P. Brandes, J. Grimminger, W. Klepetko, P. Jaksch, R. Rodriguez-Roisin, W. Seeger, F. Grimminger, and J. A. Barbera. 2014. Stimulation of soluble guanylate cyclase prevents cigarette smoke-induced pulmonary hypertension and emphysema. *Am.J.Respir.Crit Care Med.* 189:1359-1373.

61. Seimetz, M., N. Parajuli, A. Pichl, F. Veit, G. Kwapiszewska, F. C. Weisel, K. Milger, B. Egemnazarov, A. Turowska, B. Fuchs, S. Nikam, M. Roth, A. Sydykov, T. Medebach, W. Klepetko, P. Jaksch, R. Dumitrascu, H. Garn, R. Voswinckel, S. Kostin, W. Seeger, R. T. Schermuly, F. Grimminger, H. A. Ghofrani, and N. Weissmann. 2011. Inducible NOS inhibition reverses tobacco-smoke-induced emphysema and pulmonary hypertension in mice. *Cell* 147:293-305.

62. Kranenburg, A. R., A. Willems-Widyastuti, W. J. Moori, P. J. Sterk, V. K. Alagappan, W. I. de Boer, and H. S. Sharma. 2006. Enhanced bronchial expression of extracellular matrix proteins in chronic obstructive pulmonary disease. *Am.J.Clin.Pathol.* 126:725-735.

63. Suki, B., S. Ito, D. Stamenovic, K. R. Lutchen, and E. P. Ingenito. 2005. Biomechanics of the lung parenchyma: critical roles of collagen and mechanical forces. *J.Appl.Physiol* 98:1892-1899.

64. Cottin, V., H. Nunes, P. Y. Brillet, P. Delaval, G. Devouassoux, I. Tillie-Leblond, D. Israel-Biet, Court-Fortune, D. Valeyre, and J. F. Cordier. 2005. Combined pulmonary fibrosis and emphysema: a distinct underrecognised entity. *Eur.Respir.J.* 26:586-593.

65. Katzenstein, A. L., S. Mukhopadhyay, C. Zanardi, and E. Dexter. 2010. Clinically occult interstitial fibrosis in smokers: classification and significance of a surprisingly common finding in lobectomy specimens. *Hum.Pathol.* 41:316-325.

66. Washko, G. R., G. M. Hunninghake, I. E. Fernandez, M. Nishino, Y. Okajima, T. Yamashiro, J. C. Ross, R. S. Estepar, D. A. Lynch, J. M. Brehm, K. P. Andriole, A. A. Diaz, R. Khorasani, K. D'Aco, F. C. Sciurba, E. K. Silverman, H. Hatabu, and I. O. Rosas. 2011. Lung volumes and emphysema in smokers with interstitial lung abnormalities. *N.Engl.J.Med.* 364:897-906.

67. Peinado, V. I., J. A. Barbera, J. Ramirez, F. P. Gomez, J. Roca, L. Jover, J. M. Gimferrer, and R. Rodriguez-Roisin. 1998. Endothelial dysfunction in pulmonary arteries of patients with mild COPD. *Am.J.Physiol* 274:L908-L913.

68. Santos, S., V. I. Peinado, J. Ramirez, J. Morales-Blanhir, R. Bastos, J. Roca, R. Rodriguez-Roisin, and J. A. Barbera. 2003. Enhanced expression of vascular endothelial growth factor

in pulmonary arteries of smokers and patients with moderate chronic obstructive pulmonary disease. *Am.J.Respir.Crit Care Med.* 167:1250-1256.

69. Barbera, J. A., A. Riverola, J. Roca, J. Ramirez, P. D. Wagner, D. Ros, B. R. Wiggs, and R. Rodriguez-Roisin. 1994. Pulmonary vascular abnormalities and ventilation-perfusion relationships in mild chronic obstructive pulmonary disease. *Am.J.Respir.Crit Care Med.* 149:423-429.

70. Barbera, J. A., V. I. Peinado, and S. Santos. 2003. Pulmonary hypertension in chronic obstructive pulmonary disease. *Eur.Respir.J.* 21:892-905.

71. Santos, S., V. I. Peinado, J. Ramirez, T. Melgosa, J. Roca, R. Rodriguez-Roisin, and J. A. Barbera. 2002. Characterization of pulmonary vascular remodelling in smokers and patients with mild COPD. *Eur.Respir.J.* 19:632-638.

72. Hislop, A. and L. Reid. 1976. New findings in pulmonary arteries of rats with hypoxia-induced pulmonary hypertension. *Br.J.Exp.Pathol.* 57:542-554.

73. Furchgott, R. F. and J. V. Zawadzki. 1980. The obligatory role of endothelial cells in the relaxation of arterial smooth muscle by acetylcholine. *Nature* 288:373-376.

74. Barbera, J. A., V. I. Peinado, S. Santos, J. Ramirez, J. Roca, and R. Rodriguez-Roisin. 2001. Reduced expression of endothelial nitric oxide synthase in pulmonary arteries of smokers. *Am.J.Respir.Crit Care Med.* 164:709-713.

75. Schermuly, R. T., J. P. Stasch, S. S. Pullamsetti, R. Middendorff, D. Muller, K. D. Schluter, A. Dingendorf, S. Hackemack, E. Kolosionek, C. Kaulen, R. Dumitrascu, N. Weissmann, J. Mittendorf, W. Klepetko, W. Seeger, H. A. Ghofrani, and F. Grimminger. 2008. Expression and function of soluble guanylate cyclase in pulmonary arterial hypertension. *Eur.Respir.J.* 32:881-891.

76. Garg, U. C. and A. Hassid. 1989. Nitric oxide-generating vasodilators and 8-bromo-cyclic guanosine monophosphate inhibit mitogenesis and proliferation of cultured rat vascular smooth muscle cells. *J.Clin.Invest* 83:1774-1777.

77. Christman, B. W., C. D. McPherson, J. H. Newman, G. A. King, G. R. Bernard, B. M. Groves, and J. E. Loyd. 1992. An imbalance between the excretion of thromboxane and prostacyclin metabolites in pulmonary hypertension. *N.Engl.J.Med.* 327:70-75.

78. Tuder, R. M., C. D. Cool, M. W. Geraci, J. Wang, S. H. Abman, L. Wright, D. Badesch, and N. F. Voelkel. 1999. Prostacyclin synthase expression is decreased in lungs from patients with severe pulmonary hypertension. *Am.J.Respir.Crit Care Med.* 159:1925-1932.

79. Thabut, G., G. Dauriat, J. B. Stern, D. Logeart, A. Levy, R. Marrash-Chahla, and H. Mal. 2005. Pulmonary hemodynamics in advanced COPD candidates for lung volume reduction surgery or lung transplantation. *Chest* 127:1531-1536.

80. Kessler, R., M. Faller, G. Fourgaut, B. Mennecier, and E. Weitzenblum. 1999. Predictive factors of hospitalization for acute exacerbation in a series of 64 patients with chronic obstructive pulmonary disease. *Am.J.Respir.Crit Care Med.* 159:158-164.

81. Weitzenblum, E., C. Hirth, A. Ducolone, R. Mirhom, J. Rasaholinjanahary, and M. Ehrhart. 1981. Prognostic value of pulmonary artery pressure in chronic obstructive pulmonary disease. *Thorax* 36:752-758.

82. Simonneau, G., M. A. Gatzoulis, I. Adatia, D. Celermajer, C. Denton, A. Ghofrani, M. A. Gomez Sanchez, K. R. Krishna, M. Landzberg, R. F. Machado, H. Olschewski, I. M. Robbins, and R. Souza. 2013. Updated clinical classification of pulmonary hypertension. *J.Am.Coll.Cardiol.* 62:D34-D41.

83. Badesch, D. B., H. C. Champion, M. A. Sanchez, M. M. Hoeper, J. E. Loyd, A. Manes, M. McGoon, R. Naeije, H. Olschewski, R. J. Oudiz, and A. Torbicki. 2009. Diagnosis and assessment of pulmonary arterial hypertension. *J.Am.Coll.Cardiol.* 54:S55-S66.

84. Burrows, B., L. J. Kettel, A. H. Niden, M. Rabinowitz, and C. F. Diener. 1972. Patterns of cardiovascular dysfunction in chronic obstructive lung disease. *N.Engl.J.Med.* 286:912-918.

85. Oswald-Mammosser, M., E. Weitzenblum, E. Quoix, G. Moser, A. Chaouat, C. Charpentier, and R. Kessler. 1995. Prognostic factors in COPD patients receiving long-term oxygen therapy. Importance of pulmonary artery pressure. *Chest* 107:1193-1198.

86. Church, D. F. and W. A. Pryor. 1985. Free-radical chemistry of cigarette smoke and its toxicological implications. *Environ.Health Perspect.* 64:111-126.

87. Pryor, W. A., M. M. Dooley, and D. F. Church. 1985. Mechanisms of cigarette smoke toxicity: the inactivation of human alpha-1-proteinase inhibitor by nitric oxide/isoprene mixtures in air. *Chem.Biol.Interact.* 54:171-183.

88. Pryor, W. A., D. F. Church, M. D. Evans, W. Y. Rice, Jr., and J. R. Hayes. 1990. A comparison of the free radical chemistry of tobacco-burning cigarettes and cigarettes that only heat tobacco. *Free Radic.Biol.Med.* 8:275-279.

89. Pinkerton, K. E. and J. P. Joad. 2006. Influence of air pollution on respiratory health during perinatal development. *Clin.Exp.Pharmacol.Physiol* 33:269-272.

90. Sethi, J. M. and C. L. Rochester. 2000. Smoking and chronic obstructive pulmonary disease. *Clin.Chest Med.* 21:67-86, viii.

91. Peinado, V. I., S. Santos, J. Ramirez, J. Roca, R. Rodriguez-Roisin, and J. A. Barbera. 2002. Response to hypoxia of pulmonary arteries in chronic obstructive pulmonary disease: an in vitro study. *Eur.Respir.J.* 20:332-338.

92. Omar, H. A. and M. S. Wolin. 1992. Endothelium-dependent and independent cGMP mechanisms appear to mediate O2 responses in calf pulmonary resistance arteries. *Am.J.Physiol* 262:L560-L565.

93. Voelkel, N. F. 1986. Mechanisms of hypoxic pulmonary vasoconstriction. *Am.Rev.Respir.Dis.* 133:1186-1195.

94. Michelakis, E. D., V. Hampl, A. Nsair, X. Wu, G. Harry, A. Haromy, R. Gurtu, and S. L. Archer. 2002. Diversity in mitochondrial function explains differences in vascular oxygen sensing. *Circ.Res.* 90:1307-1315.

95. Coggins, M. P. and K. D. Bloch. 2007. Nitric oxide in the pulmonary vasculature. *Arterioscler.Thromb.Vasc.Biol.* 27:1877-1885.

96. Le Cras, T. D. and I. F. McMurtry. 2001. Nitric oxide production in the hypoxic lung. *Am.J.Physiol Lung Cell Mol.Physiol* 280:L575-L582.

97. Giaid, A. and D. Saleh. 1995. Reduced expression of endothelial nitric oxide synthase in the lungs of patients with pulmonary hypertension. *N.Engl.J.Med.* 333:214-221.

98. Stewart, D. J., R. D. Levy, P. Cernacek, and D. Langleben. 1991. Increased plasma endothelin-1 in pulmonary hypertension: marker or mediator of disease? *Ann.Intern.Med.* 114:464-469.

99. Chaouat, A., L. Savale, C. Chouaid, L. Tu, B. Sztrymf, M. Canuet, B. Maitre, B. Housset, C. Brandt, C. P. Le, E. Weitzenblum, S. Eddahibi, and S. Adnot. 2009. Role for interleukin-6 in COPD-related pulmonary hypertension. *Chest* 136:678-687.

100. Joppa, P., D. Petrasova, B. Stancak, and R. Tkacova. 2006. Systemic inflammation in patients with COPD and pulmonary hypertension. *Chest* 130:326-333.

101. Ko, H. J., S. K. Oh, J. H. Jin, K. H. Son, and H. P. Kim. 2013. Inhibition of Experimental Systemic Inflammation (Septic Inflammation) and Chronic Bronchitis by New Phytoformula BL Containing Broussonetia papyrifera and Lonicera japonica. *Biomol.Ther.(Seoul.)* 21:66-71.

102. Wright, J. L., M. Cosio, and A. Churg. 2008. Animal models of chronic obstructive pulmonary disease. *Am.J.Physiol Lung Cell Mol.Physiol* 295:L1-15.

103. Aul, R., J. Armstrong, A. Duvoix, D. Lomas, B. Hayes, B. E. Miller, C. Jagger, and D. Singh. 2012. Inhaled LPS challenges in smokers: a study of pulmonary and systemic effects. *Br.J.Clin.Pharmacol.* 74:1023-1032.

104. Birrell, M. A., S. Wong, A. Dekkak, A. J. de, S. Haj-Yahia, and M. G. Belvisi. 2006. Role of matrix metalloproteinases in the inflammatory response in human airway cell-based assays and in rodent models of airway disease. *J.Pharmacol.Exp.Ther.* 318:741-750.

105. Chen, P., J. Hou, D. Ding, X. Hua, Z. Yang, and L. Cui. 2013. Lipopolysaccharide-induced inflammation of bronchi and emphysematous changes of pulmonary parenchyma in miniature pigs (Sus scrofa domestica). *Lab Anim (NY)* 42:86-91.

106. Lee, K. M., R. A. Renne, S. J. Harbo, M. L. Clark, R. E. Johnson, and K. M. Gideon. 2007. 3-week inhalation exposure to cigarette smoke and/or lipopolysaccharide in AKR/J mice. *Inhal.Toxicol.* 19:23-35.

107. Vernooy, J. H., M. A. Dentener, R. J. van Suylen, W. A. Buurman, and E. F. Wouters. 2002. Long-term intratracheal lipopolysaccharide exposure in mice results in chronic lung inflammation and persistent pathology. *Am.J.Respir.Cell Mol.Biol.* 26:152-159.

108. Brass, D. M., J. W. Hollingsworth, M. Cinque, Z. Li, E. Potts, E. Toloza, W. M. Foster, and D. A. Schwartz. 2008. Chronic LPS inhalation causes emphysema-like changes in mouse lung that are associated with apoptosis. *Am.J.Respir.Cell Mol.Biol.* 39:584-590.

109. Hakansson, H. F., A. Smailagic, C. Brunmark, A. Miller-Larsson, and H. Lal. 2012. Altered lung function relates to inflammation in an acute LPS mouse model. *Pulm.Pharmacol.Ther.* 25:399-406.

110. Birrell, M. A., K. McCluskie, S. Wong, L. E. Donnelly, P. J. Barnes, and M. G. Belvisi. 2005. Resveratrol, an extract of red wine, inhibits lipopolysaccharide induced airway neutrophilia and inflammatory mediators through an NF-kappaB-independent mechanism. *FASEB J.* 19:840-841.

111. Dusad, A., G. M. Thiele, L. W. Klassen, A. M. Gleason, C. Bauer, T. R. Mikuls, M. J. Duryee, W. W. West, D. J. Romberger, and J. A. Poole. 2013. Organic dust, lipopolysaccharide, and peptidoglycan inhalant exposures result in bone loss/disease. *Am.J.Respir.Cell Mol.Biol.* 49:829-836.

112. Lugade, A. A., P. N. Bogner, and Y. Thanavala. 2011. Murine model of chronic respiratory inflammation. *Adv.Exp.Med.Biol.* 780:125-141.

113. Luo, Y. L., C. C. Zhang, P. B. Li, Y. C. Nie, H. Wu, J. G. Shen, and W. W. Su. 2012. Naringin attenuates enhanced cough, airway hyperresponsiveness and airway inflammation in a

guinea pig model of chronic bronchitis induced by cigarette smoke. *Int.Immunopharmacol.* 13:301-307.

114. Gross, P., E. A. Pfitzer, E. Tolker, M. A. Babyak, and M. Kaschak. 1965. Experimental emphysema: its production with papain in normal and silicotic rats. *Arch.Environ.Health* 11:50-58.

115. Martin, J. G. and M. Tamaoka. 2006. Rat models of asthma and chronic obstructive lung disease. *Pulm.Pharmacol.Ther.* 19:377-385.

116. Lesser, M., M. L. Padilla, and C. Cardozo. 1992. Induction of emphysema in hamsters by intratracheal instillation of cathepsin B. *Am.Rev.Respir.Dis.* 145:661-668.

117. Gamze, K., H. M. Mehmet, F. Deveci, T. Turgut, F. Ilhan, and I. Ozercan. 2007. Effect of bosentan on the production of proinflammatory cytokines in a rat model of emphysema. *Exp.Mol.Med.* 39:614-620.

118. Birrell, M. A., S. Wong, D. J. Hele, K. McCluskie, E. Hardaker, and M. G. Belvisi. 2005. Steroid-resistant inflammation in a rat model of chronic obstructive pulmonary disease is associated with a lack of nuclear factor-kappaB pathway activation. *Am.J.Respir.Crit Care Med.* 172:74-84.

119. Massaro, D., E. Alexander, K. Reiland, E. P. Hoffman, G. D. Massaro, and L. B. Clerch. 2007. Rapid onset of gene expression in lung, supportive of formation of alveolar septa, induced by refeeding mice after calorie restriction. *Am.J.Physiol Lung Cell Mol.Physiol* 292:L1313-L1326.

120. Kasahara, Y., R. M. Tuder, L. Taraseviciene-Stewart, T. D. Le Cras, S. Abman, P. K. Hirth, J. Waltenberger, and N. F. Voelkel. 2000. Inhibition of VEGF receptors causes lung cell apoptosis and emphysema. *J.Clin.Invest* 106:1311-1319.

121. Marwick, J. A., C. S. Stevenson, J. Giddings, W. MacNee, K. Butler, I. Rahman, and P. A. Kirkham. 2006. Cigarette smoke disrupts VEGF165-VEGFR-2 receptor signaling complex in rat lungs and patients with COPD: morphological impact of VEGFR-2 inhibition. *Am.J.Physiol Lung Cell Mol.Physiol* 290:L897-L908.

122. Aoshiba, K., N. Yokohori, and A. Nagai. 2003. Alveolar wall apoptosis causes lung destruction and emphysematous changes. *Am.J.Respir.Cell Mol.Biol.* 28:555-562.

123. Stenmark, K. R., K. A. Fagan, and M. G. Frid. 2006. Hypoxia-induced pulmonary vascular remodeling: cellular and molecular mechanisms. *Circ.Res.* 99:675-691.

124. Steiner, M. K., O. L. Syrkina, N. Kolliputi, E. J. Mark, C. A. Hales, and A. B. Waxman. 2009. Interleukin-6 overexpression induces pulmonary hypertension. *Circ.Res.* 104:236-44, 28p.

125. Frank, D. B., J. Lowery, L. Anderson, M. Brink, J. Reese, and C. M. de. 2008. Increased susceptibility to hypoxic pulmonary hypertension in Bmpr2 mutant mice is associated with endothelial dysfunction in the pulmonary vasculature. *Am.J.Physiol Lung Cell Mol.Physiol* 294:L98-109.

126. Meyrick, B., W. Gamble, and L. Reid. 1980. Development of Crotalaria pulmonary hypertension: hemodynamic and structural study. *Am.J.Physiol* 239:H692-H702.

127. Jasmin, J. F., M. Lucas, P. Cernacek, and J. Dupuis. 2001. Effectiveness of a nonselective ET(A/B) and a selective ET(A) antagonist in rats with monocrotaline-induced pulmonary hypertension. *Circulation* 103:314-318.

128. Wilson, D. W., H. J. Segall, L. C. Pan, and S. K. Dunston. 1989. Progressive inflammatory and structural changes in the pulmonary vasculature of monocrotaline-treated rats. *Microvasc.Res.* 38:57-80.

129. Stevenson, C. S., C. Docx, R. Webster, C. Battram, D. Hynx, J. Giddings, P. R. Cooper, P. Chakravarty, I. Rahman, J. A. Marwick, P. A. Kirkham, C. Charman, D. L. Richardson, N. R. Nirmala, P. Whittaker, and K. Butler. 2007. Comprehensive gene expression profiling of rat lung reveals distinct acute and chronic responses to cigarette smoke inhalation. *Am.J.Physiol Lung Cell Mol.Physiol* 293:L1183-L1193.

130. Bartalesi, B., E. Cavarra, S. Fineschi, M. Lucattelli, B. Lunghi, P. A. Martorana, and G. Lungarella. 2005. Different lung responses to cigarette smoke in two strains of mice sensitive to oxidants. *Eur.Respir.J.* 25:15-22.

131. Wright, J. L., D. S. Postma, H. A. Kerstjens, W. Timens, P. Whittaker, and A. Churg. 2007. Airway remodeling in the smoke exposed guinea pig model. *Inhal.Toxicol.* 19:915-923.

132. Simani, A. S., S. Inoue, and J. C. Hogg. 1974. Penetration of the respiratory epithelium of guinea pigs following exposure to cigarette smoke. *Lab Invest* 31:75-81.

133. Wright, J. L. and A. Churg. 2002. A model of tobacco smoke-induced airflow obstruction in the guinea pig. *Chest* 121:188S-191S.

134. Ferrer, E., V. I. Peinado, M. Diez, J. L. Carrasco, M. M. Musri, A. Martinez, R. Rodriguez-Roisin, and J. A. Barbera. 2009. Effects of cigarette smoke on endothelial function of pulmonary arteries in the guinea pig. *Respir.Res.* 10:76.

135. Wright, J. L. and A. Churg. 2002. Animal models of cigarette smoke-induced COPD. *Chest* 122:301S-306S.

136. Yamato, H., J. P. Sun, A. Churg, and J. L. Wright. 1997. Guinea pig pulmonary hypertension caused by cigarette smoke cannot be explained by capillary bed destruction. *J.Appl.Physiol* 82:1644-1653.

137. Wright, J. L., H. Tai, and A. Churg. 2006. Vasoactive mediators and pulmonary hypertension after cigarette smoke exposure in the guinea pig. *J.Appl.Physiol (1985.)* 100:672-678.

138. Ferrer, E., V. I. Peinado, J. Castaneda, J. Prieto-Lloret, E. Olea, M. C. Gonzalez-Martin, M. V. Vega-Agapito, M. Diez, D. Dominguez-Fandos, A. Obeso, C. Gonzalez, and J. A. Barbera. 2011. Effects of cigarette smoke and hypoxia on pulmonary circulation in the guinea pig. *Eur.Respir.J.* 38:617-627.

139. Galie, N., M. M. Hoeper, M. Humbert, A. Torbicki, J. L. Vachiery, J. A. Barbera, M. Beghetti, P. Corris, S. Gaine, J. S. Gibbs, M. A. Gomez-Sanchez, G. Jondeau, W. Klepetko, C. Opitz, A. Peacock, L. Rubin, M. Zellweger, and G. Simonneau. 2009. Guidelines for the diagnosis and treatment of pulmonary hypertension. *Eur.Respir.J.* 34:1219-1263.

140. Barbera, J. A., N. Roger, J. Roca, I. Rovira, T. W. Higenbottam, and R. Rodriguez-Roisin. 1996. Worsening of pulmonary gas exchange with nitric oxide inhalation in chronic obstructive pulmonary disease. *Lancet* 347:436-440.

141. Jones, A. T. and T. W. Evans. 1997. NO: COPD and beyond. *Thorax* 52 Suppl 3:S16-S21.

142. Blanco, I., E. Gimeno, P. A. Munoz, S. Pizarro, C. Gistau, R. Rodriguez-Roisin, J. Roca, and J. A. Barbera. 2010. Hemodynamic and gas exchange effects of sildenafil in patients with chronic obstructive pulmonary disease and pulmonary hypertension. *Am.J.Respir.Crit Care Med.* 181:270-278.

143. Zhao, L., N. A. Mason, N. W. Morrell, B. Kojonazarov, A. Sadykov, A. Maripov, M. M. Mirrakhimov, A. Aldashev, and M. R. Wilkins. 2001. Sildenafil inhibits hypoxia-induced pulmonary hypertension. *Circulation* 104:424-428.

144. Karner, C., J. Chong, and P. Poole. 2012. Tiotropium versus placebo for chronic obstructive pulmonary disease. *Cochrane.Database.Syst.Rev.* 7:CD009285.

145. Decramer, M., B. Celli, S. Kesten, T. Lystig, S. Mehra, and D. P. Tashkin. 2009. Effect of tiotropium on outcomes in patients with moderate chronic obstructive pulmonary disease (UPLIFT): a prespecified subgroup analysis of a randomised controlled trial. *Lancet* 374:1171-1178.

146. Bateman, E. D., S. Rennard, P. J. Barnes, P. V. Dicpinigaitis, R. Gosens, N. J. Gross, J. A. Nadel, M. Pfeifer, K. Racke, K. F. Rabe, B. K. Rubin, T. Welte, and I. Wessler. 2009. Alternative mechanisms for tiotropium. *Pulm.Pharmacol.Ther.* 22:533-542.

147. Suzaki, I., K. Asano, Y. Shikama, T. Hamasaki, A. Kanei, and H. Suzaki. 2011. Suppression of IL-8 production from airway cells by tiotropium bromide in vitro. *Int.J.Chron.Obstruct.Pulmon.Dis.* 6:439-448.

148. Profita, M., A. Bonanno, A. M. Montalbano, M. Ferraro, L. Siena, A. Bruno, S. Girbino, G. D. Albano, P. Casarosa, M. P. Pieper, and M. Gjomarkaj. 2011. Cigarette smoke extract activates human bronchial epithelial cells affecting non-neuronal cholinergic system signalling in vitro. *Life Sci.* 89:36-43.

149. Gosens, R., D. Rieks, H. Meurs, D. K. Ninaber, K. F. Rabe, J. Nanninga, S. Kolahian, A. J. Halayko, P. S. Hiemstra, and S. Zuyderduyn. 2009. Muscarinic M3 receptor stimulation increases cigarette smoke-induced IL-8 secretion by human airway smooth muscle cells. *Eur.Respir.J.* 34:1436-1443.

150. Gosens, R., J. Zaagsma, H. Meurs, and A. J. Halayko. 2006. Muscarinic receptor signaling in the pathophysiology of asthma and COPD. *Respir.Res.* 7:73.

151. Gosens, R., S. A. Nelemans, M. M. Grootte Bromhaar, S. McKay, J. Zaagsma, and H. Meurs. 2003. Muscarinic M3-receptors mediate cholinergic synergism of mitogenesis in airway smooth muscle. *Am.J.Respir.Cell Mol.Biol.* 28:257-262.

152. Krymskaya, V. P., M. J. Orsini, A. J. Eszterhas, K. C. Brodbeck, J. L. Benovic, R. A. Panettieri, Jr., and R. B. Penn. 2000. Mechanisms of proliferation synergy by receptor tyrosine kinase and G protein-coupled receptor activation in human airway smooth muscle. *Am.J.Respir Cell Mol.Biol.* 23:546-554.

153. Gavalda, A., M. Miralpeix, I. Ramos, R. Otal, C. Carreno, M. Vinals, T. Domenech, C. Carcasona, B. Reyes, D. Vilella, J. Gras, J. Cortijo, E. Morcillo, J. Llenas, H. Ryder, and J. Beleta. 2009. Characterization of aclidinium bromide, a novel inhaled muscarinic antagonist, with long duration of action and a favorable pharmacological profile. *J.Pharmacol.Exp.Ther.* 331:740-751.

154. Maltais, F., B. Celli, R. Casaburi, J. Porszasz, D. Jarreta, B. Seoane, and C. Caracta. 2011. Aclidinium bromide improves exercise endurance and lung hyperinflation in patients with moderate to severe COPD. *Respir Med.* 105:580-587.

155. Fuhr, R., H. Magnussen, K. Sarem, A. R. Llovera, A. M. Kirsten, M. Falques, C. F. Caracta, and G. E. Garcia. 2012. Efficacy of aclidinium bromide 400 mug twice daily compared with placebo and tiotropium in patients with moderate to severe COPD. *Chest* 141:745-752.

156. Jones, P. W., D. Singh, E. D. Bateman, A. Agusti, R. Lamarca, M. G. de, R. Segarra, C. Caracta, and G. E. Garcia. 2012. Efficacy and safety of twice-daily aclidinium bromide in COPD patients: the ATTAIN study. *Eur.Respir.J.* 40:830-836.

157. Kerwin, E. M., A. D. D'Urzo, A. F. Gelb, H. Lakkis, G. E. Garcia, and C. F. Caracta. 2012. Efficacy and safety of a 12-week treatment with twice-daily aclidinium bromide in COPD patients (ACCORD COPD I). *COPD.* 9:90-101.

158. Wollin, L. and M. P. Pieper. 2010. Tiotropium bromide exerts anti-inflammatory activity in a cigarette smoke mouse model of COPD. *Pulm.Pharmacol.Ther.* 23:345-354.

159. Damera, G., M. Jiang, H. Zhao, H. W. Fogle, W. F. Jester, J. Freire, and R. A. Panettieri, Jr. 2010. Aclidinium bromide abrogates allergen-induced hyperresponsiveness and reduces eosinophilia in murine model of airway inflammation. *Eur.J.Pharmacol.* 649:349-353.

160. Bos, I. S., R. Gosens, A. B. Zuidhof, D. Schaafsma, A. J. Halayko, H. Meurs, and J. Zaagsma. 2007. Inhibition of allergen-induced airway remodelling by tiotropium and budesonide: a comparison. *Eur.Respir.J.* 30:653-661.

161. Alagha, K., A. Palot, T. Sofalvi, L. Pahus, M. Gouitaa, C. Tummino, S. Martinez, D. Charpin, A. Bourdin, and P. Chanez. 2014. Long-acting muscarinic receptor antagonists for the treatment of chronic airway diseases. *Ther.Adv.Chronic.Dis.* 5:85-98.

162. Buels, K. S., D. B. Jacoby, and A. D. Fryer. 2012. Non-bronchodilating mechanisms of tiotropium prevent airway hyperreactivity in a guinea-pig model of allergic asthma. *Br.J.Pharmacol.* 165:1501-1514.

163. Ohta, S., N. Oda, T. Yokoe, A. Tanaka, Y. Yamamoto, Y. Watanabe, K. Minoguchi, T. Ohnishi, T. Hirose, H. Nagase, K. Ohta, and M. Adachi. 2010. Effect of tiotropium bromide on airway inflammation and remodelling in a mouse model of asthma. *Clin.Exp.Allergy* 40:1266-1275.

164. Pera, T., A. Zuidhof, J. Valadas, M. Smit, R. G. Schoemaker, R. Gosens, H. Maarsingh, J. Zaagsma, and H. Meurs. 2011. Tiotropium inhibits pulmonary inflammation and remodelling in a guinea pig model of COPD. *Eur.Respir.J.* 38:789-796.

165. Klinger, J. R., S. H. Abman, and M. T. Gladwin. 2013. Nitric oxide deficiency and endothelial dysfunction in pulmonary arterial hypertension. *Am.J.Respir.Crit Care Med.* 188:639-646.

166. Jeremy, J. Y., D. Rowe, A. M. Emsley, and A. C. Newby. 1999. Nitric oxide and the proliferation of vascular smooth muscle cells. *Cardiovasc.Res.* 43:580-594.

167. Humbert, M., O. Sitbon, and G. Simonneau. 2004. Treatment of pulmonary arterial hypertension. *N.Engl.J.Med.* 351:1425-1436.

168. Ghofrani, H. A., R. Voswinckel, F. Reichenberger, H. Olschewski, P. Haredza, B. Karadas, R. T. Schermuly, N. Weissmann, W. Seeger, and F. Grimminger. 2004. Differences in hemodynamic and oxygenation responses to three different phosphodiesterase-5 inhibitors in patients with pulmonary arterial hypertension: a randomized prospective study. *J.Am.Coll.Cardiol.* 44:1488-1496.

169. Sebkhi, A., J. W. Strange, S. C. Phillips, J. Wharton, and M. R. Wilkins. 2003. Phosphodiesterase type 5 as a target for the treatment of hypoxia-induced pulmonary hypertension. *Circulation* 107:3230-3235.

170. Schafer, S., P. Ellinghaus, W. Janssen, F. Kramer, K. Lustig, H. Milting, R. Kast, and M. Klein. 2009. Chronic inhibition of phosphodiesterase 5 does not prevent pressure-overload-induced right-ventricular remodelling. *Cardiovasc.Res.* 82:30-39.

171. Schermuly, R. T., K. P. Kreisselmeier, H. A. Ghofrani, H. Yilmaz, G. Butrous, L. Ermert, M. Ermert, N. Weissmann, F. Rose, A. Guenther, D. Walmrath, W. Seeger, and F. Grimminger. 2004. Chronic sildenafil treatment inhibits monocrotaline-induced pulmonary hypertension in rats. *Am.J.Respir.Crit Care Med.* 169:39-45.

172. Galie, N., P. A. Corris, A. Frost, R. E. Girgis, J. Granton, Z. C. Jing, W. Klepetko, M. D. McGoon, V. V. McLaughlin, I. R. Preston, L. J. Rubin, J. Sandoval, W. Seeger, and A. Keogh. 2013. Updated treatment algorithm of pulmonary arterial hypertension. *J.Am.Coll.Cardiol.* 62:D60-D72.

173. Blanco, I., S. Santos, J. Gea, R. Guell, F. Torres, E. Gimeno-Santos, D. A. Rodriguez, J. Vilaro, B. Gomez, J. Roca, and J. A. Barbera. 2013. Sildenafil to improve respiratory rehabilitation outcomes in COPD: a controlled trial. *Eur.Respir.J.* 42:982-992.

174. Milara, J., A. Serrano, T. Peiro, A. Gavalda, M. Miralpeix, E. J. Morcillo, and J. Cortijo. 2012. Aclidinium inhibits human lung fibroblast to myofibroblast transition. *Thorax* 67:229-237.

175. Finkelstein, R., R. S. Fraser, H. Ghezzo, and M. G. Cosio. 1995. Alveolar inflammation and its relation to emphysema in smokers. *Am.J.Respir.Crit Care Med.* 152:1666-1672.

176. Saetta, M., A. Di Stefano, P. Maestrelli, A. Ferraresso, R. Drigo, A. Potena, A. Ciaccia, and L. M. Fabbri. 1993. Activated T-lymphocytes and macrophages in bronchial mucosa of subjects with chronic bronchitis. *Am.Rev.Respir.Dis.* 147:301-306.

177. Gosens, R., I. S. Bos, J. Zaagsma, and H. Meurs. 2005. Protective effects of tiotropium bromide in the progression of airway smooth muscle remodeling. *Am.J.Respir.Crit Care Med.* 171:1096-1102.

178. Gwilt, C. R., L. E. Donnelly, and D. F. Rogers. 2007. The non-neuronal cholinergic system in the airways: an unappreciated regulatory role in pulmonary inflammation? *Pharmacol.Ther.* 115:208-222.

179. Roffel, A. F., C. R. Elzinga, and J. Zaagsma. 1990. Muscarinic M3 receptors mediate contraction of human central and peripheral airway smooth muscle. *Pulm.Pharmacol.* 3:47-51.

180. Wessler, I. and C. J. Kirkpatrick. 2008. Acetylcholine beyond neurons: the non-neuronal cholinergic system in humans. *Br.J.Pharmacol.* 154:1558-1571.

181. Perng, D. W., C. W. Tao, K. C. Su, C. C. Tsai, L. Y. Liu, and Y. C. Lee. 2009. Anti-inflammatory effects of salmeterol/fluticasone, tiotropium/fluticasone or tiotropium in COPD. *Eur Respir J.* 33:778-784.

182. Wen, Y., D. W. Reid, D. Zhang, C. Ward, R. Wood-Baker, and E. H. Walters. 2010. Assessment of airway inflammation using sputum, BAL, and endobronchial biopsies in current and ex-smokers with established COPD. *Int.J.Chron.Obstruct.Pulmon.Dis.* 5:327-334.

183. Richens, T. R., D. J. Linderman, S. A. Horstmann, C. Lambert, Y. Q. Xiao, R. L. Keith, D. M. Boe, K. Morimoto, R. P. Bowler, B. J. Day, W. J. Janssen, P. M. Henson, and R. W. Vandivier. 2009. Cigarette smoke impairs clearance of apoptotic cells through oxidant-dependent activation of RhoA. *Am.J.Respir.Crit Care Med.* 179:1011-1021.

184. Saetta, M., G. Turato, S. Baraldo, A. Zanin, F. Braccioni, C. E. Mapp, P. Maestrelli, G. Cavallesco, A. Papi, and L. M. Fabbri. 2000. Goblet cell hyperplasia and epithelial inflammation in peripheral airways of smokers with both symptoms of chronic bronchitis and chronic airflow limitation. *Am.J.Respir Crit Care Med.* 161:1016-1021.

185. Cortijo, J., M. Mata, J. Milara, E. Donet, A. Gavalda, M. Miralpeix, and E. J. Morcillo. 2011. Aclidinium inhibits cholinergic and tobacco smoke-induced MUC5AC in human airways. *Eur Respir J.* 37:244-254.

186. Caramori, G., P. Casolari, G. C. Di, M. Saetta, S. Baraldo, P. Boschetto, K. Ito, L. M. Fabbri, P. J. Barnes, I. M. Adcock, G. Cavallesco, K. F. Chung, and A. Papi. 2009. MUC5AC expression is increased in bronchial submucosal glands of stable COPD patients. *Histopathology* 55:321-331.

187. Weissmann, N., B. Gerigk, O. Kocer, M. Nollen, S. Hackemack, H. A. Ghofrani, R. T. Schermuly, G. Butrous, A. Schulz, M. Roth, W. Seeger, and F. Grimminger. 2007. Hypoxia-induced pulmonary hypertension: different impact of iloprost, sildenafil, and nitric oxide. *Respir.Med.* 101:2125-2132.

188. Galie, N., L. J. Rubin, and G. Simonneau. 2010. Phosphodiesterase inhibitors for pulmonary hypertension. *N.Engl.J.Med.* 362:559-560.

189. Preston, I. R., N. S. Hill, L. S. Gambardella, R. R. Warburton, and J. R. Klinger. 2004. Synergistic effects of ANP and sildenafil on cGMP levels and amelioration of acute hypoxic pulmonary hypertension. *Exp.Biol.Med.(Maywood.)* 229:920-925.

190. Stasch, J. P. and O. V. Evgenov. 2013. Soluble guanylate cyclase stimulators in pulmonary hypertension. *Handb.Exp.Pharmacol.* 218:279-313.

191. Nagendran, J., S. L. Archer, D. Soliman, V. Gurtu, R. Moudgil, A. Haromy, A. C. St, L. Webster, I. M. Rebeyka, D. B. Ross, P. E. Light, J. R. Dyck, and E. D. Michelakis. 2007. Phosphodiesterase type 5 is highly expressed in the hypertrophied human right ventricle, and acute inhibition of phosphodiesterase type 5 improves contractility. *Circulation* 116:238-248.